

Supporting Information

Terfestatins B and C, New *p*-Terphenyl Glycosides Produced by *Streptomyces* sp. RM-5-8

Xiachang Wang,^{†,‡} Anna R. Reynolds,[§] Sherif I. Elshahawi,^{†,‡} Khaled A. Shaaban,^{†,‡} Larissa V. Ponomareva,^{†,‡} Meredith A. Saunders,[§] Ibrahim S. Elgumati,[§] Yinan Zhang,^{†,‡} Gregory C. Copley,[∇] James C. Hower,[∇] Manjula Sunkara,[⊥] Andrew J. Morris,[⊥] Madan K. Kharel,^{||} Steven G. Van Lanen,[‡] Mark A. Prendergast,[§] Jon S. Thorson^{*,†,‡}

[†]Center for Pharmaceutical Research and Innovation, College of Pharmacy, University of Kentucky, Lexington, Kentucky 40536, United States

[‡]Department of Pharmaceutical Sciences, College of Pharmacy, University of Kentucky, Lexington, Kentucky 40536, United States

[§]University of Kentucky Departments of Psychology and Spinal Cord and Brain Injury Research Center, 741 South Limestone Street, Lexington, KY 40536-0509, United States

[∇]Center for Applied Energy Research, University of Kentucky, Lexington, KY, 40511, United States

[⊥]Division of Cardiovascular Medicine, University of Kentucky, Lexington, KY 40536, United States

^{||}School of Pharmacy, University of Maryland Eastern Shore, Princess Anne, Maryland 21853, United States

*To whom correspondence should be addressed. Email: jsthorson@uky.edu

Contents	Page
Experimental Methods and Materials	S4
Supplemental References	S7
Figure S1. Structures of the compounds isolated from <i>Streptomyces</i> sp. RM-5-8	S8
Table S1. ¹ H and ¹³ C NMR data for terfestatins B (1) and C (2) in DMSO- <i>d</i> ₆ (<i>J</i> in Hz)	S9
Table S2. ¹ H and ¹³ C NMR data for 10- <i>O</i> -(4''-deoxy- α -L- <i>threo</i> -hex-4''-enopyranosid)-uronic acid-5-isoprenylindole-3-carboxylate (3), prehygromycin (4) and 4'- <i>epi</i> -prehygromycin (5), (<i>J</i> in Hz)	S10
Figure S2. ¹ H, ¹ H-COSY (—), selected HMBC (→) and key ROESY correlations of prehygromycin (4) and 4'- <i>epi</i> -prehygromycin (5)	S11
Figure S3. ¹ H NMR spectrum (DMSO- <i>d</i> ₆ , 400 MHz) of terfestatin B (1)	S12
Figure S4. ¹³ C NMR spectrum (DMSO- <i>d</i> ₆ , 100 MHz) of terfestatin B (1)	S13
Figure S5. HSQC spectrum (DMSO- <i>d</i> ₆ , 400 MHz) of terfestatin B (1)	S14
Figure S6. HMBC spectrum (DMSO- <i>d</i> ₆ , 400 MHz) of terfestatin B (1)	S15
Figure S7. ROESY spectrum (DMSO- <i>d</i> ₆ , 400 MHz) of terfestatin B (1)	S16
Figure S8. APCI-MS/UV of terfestatin B (1)	S17
Figure S9. (+)-HRESI-MS of terfestatin B (1)	S18
Figure S10. (–)-HRESI-MS of terfestatin B (1)	S19

Figure S11. ¹ H NMR spectrum (DMSO- <i>d</i> ₆ , 400 MHz) of terfestatin C (2)	S20
Figure S12. ¹³ C NMR spectrum (DMSO- <i>d</i> ₆ , 100 MHz) of terfestatin C (2)	S21
Figure S13. HSQC spectrum (DMSO- <i>d</i> ₆ , 400 MHz) of terfestatin C (2)	S22
Figure S14. HMBC spectrum (DMSO- <i>d</i> ₆ , 400 MHz) of terfestatin C (2)	S23
Figure S15. ROESY spectrum (DMSO- <i>d</i> ₆ , 400 MHz) of terfestatin C (2)	S24
Figure S16. APCI-MS/UV of terfestatin C (2)	S25
Figure S17. (-)-HRESI-MS of terfestatin C (2)	S26
Figure S18. ¹ H NMR spectrum (DMSO- <i>d</i> ₆ , 400 MHz) of 10- <i>O</i> -(4''-deoxy- α -L- <i>threo</i> -hex-4''-enopyranosid)-uronic acid-5-isoprenylindole-3-carboxylate (3)	S27
Figure S19. ¹³ C NMR spectrum (DMSO- <i>d</i> ₆ , 100 MHz) of 10- <i>O</i> -(4''-deoxy- α -L- <i>threo</i> -hex-4''-enopyranosid)-uronic acid-5-isoprenylindole-3-carboxylate (3)	S28
Figure S20. HSQC spectrum (DMSO- <i>d</i> ₆ , 400 MHz) of 10- <i>O</i> -(4''-deoxy- α -L- <i>threo</i> -hex-4''-enopyranosid)uronic acid-5-isoprenylindole-3-carboxylate (3)	S29
Figure S21. HMBC spectrum (DMSO- <i>d</i> ₆ , 400 MHz) of 10- <i>O</i> -(4''-deoxy- α -L- <i>threo</i> -hex-4''-enopyranosid)-uronic acid-5-isoprenylindole-3-carboxylate (3)	S30
Figure S22. ROESY spectrum (DMSO- <i>d</i> ₆ , 400 MHz) of 10- <i>O</i> -(4''-deoxy- α -L- <i>threo</i> -hex-4''-enopyranosid)-uronic acid-5-isoprenylindole-3-carboxylate (3)	S31
Figure S23. (+)-HRESI-MS of 10- <i>O</i> -(4''-deoxy- α -L- <i>threo</i> -hex-4''-enopyranosid)-uronic acid-5-isoprenylindole-3-carboxylate (3)	S32
Figure S24. ¹ H NMR spectrum (CD ₃ OD, 500 MHz) of prehygromycin (4)	S33
Figure S25. ¹ H NMR spectrum (DMSO- <i>d</i> ₆ , 400 MHz) of prehygromycin (4)	S34
Figure S26. ¹³ C NMR (DMSO- <i>d</i> ₆ , 100 MHz) of prehygromycin (4)	S35
Figure S27. HSQC spectrum (DMSO- <i>d</i> ₆ , 400 MHz) of prehygromycin (4)	S36
Figure S28. HMBC spectrum (DMSO- <i>d</i> ₆ , 400 MHz) of prehygromycin (4)	S37
Figure S29. ROESY spectrum (DMSO- <i>d</i> ₆ , 400 MHz) of prehygromycin (4)	S38
Figure S30. APCI-MS/UV of prehygromycin (4)	S39
Figure S31. (-)-HRESI-MS of prehygromycin (4)	S40
Figure S32. ¹ H NMR spectrum (CD ₃ OD, 400 MHz) of 4'- <i>epi</i> -prehygromycin (5)	S41
Figure S33. ¹³ C NMR spectrum (CD ₃ OD, 100 MHz) of 4'- <i>epi</i> -prehygromycin (5)	S42
Figure S34. HSQC spectrum (CD ₃ OD, 400 MHz) of 4'- <i>epi</i> -prehygromycin (5)	S43
Figure S35. HMBC spectrum (CD ₃ OD, 400 MHz) of 4'- <i>epi</i> -prehygromycin (5)	S44

Figure S36. ROESY spectrum (CD ₃ OD, 400 MHz) of 4'- <i>epi</i> -prehygromycin (5)	S45
Figure S37. APCI-MS/UV of 4'- <i>epi</i> -prehygromycin (5)	S46
Figure S38. (-)-HRESI-MS of 4'- <i>epi</i> -prehygromycin (5)	S47
Figure S39. ¹ H NMR spectrum (CD ₃ OD, 400 MHz) of echoside B	S48
Figure S40. ¹³ C NMR spectrum (CD ₃ OD, 100 MHz) of echoside B	S49
Figure S41. ESI-MS of echoside B	S50
Figure S42. ¹ H NMR spectrum (CD ₃ OD, 400 MHz) of hygromycin A	S51
Figure S43. ¹³ C NMR spectrum (CD ₃ OD, 100 MHz) of hygromycin A	S52
Figure S44. APCI-MS/UV of hygromycin A	S53
Figure S45. ¹ H NMR spectrum (CD ₃ OD, 400 MHz) of 4''- <i>epi</i> -hygromycin	S54
Figure S46. ¹³ C NMR spectrum (CD ₃ OD, 100 MHz) of 4''- <i>epi</i> -hygromycin	S55
Figure S47. APCI-MS of 4''- <i>epi</i> -hygromycin	S56
Figure S48. ¹ H NMR spectrum (CD ₃ OD, 400 MHz) of 5-methoxyhygromycin	S57
Figure S49. ¹³ C NMR spectrum (CD ₃ OD, 100 MHz) of 5-methoxyhygromycin	S58
Figure S50. APCI-MS/UV of 5-methoxyhygromycin	S59
Figure S51. ¹ H NMR spectrum (CD ₃ OD, 400 MHz) of 5-methoxy-4''- <i>epi</i> -hygromycin	S60
Figure S52. APCI-MS/UV of 5-methoxy-4''- <i>epi</i> -hygromycin	S61
Figure S53. ¹ H NMR spectrum (CDCl ₃ , 400 MHz) of geldanamycin	S62
Figure S54. ¹³ C NMR spectrum (CDCl ₃ , 100 MHz) of geldanamycin	S63
Figure S55. APCI-MS/UV of geldanamycin	S64
Figure S56. ¹ H NMR spectrum (CDCl ₃ , 500 MHz) of 17-O-demethyl-geldanamycin	S65
Figure S57. ¹³ C NMR spectrum (CDCl ₃ , 100 MHz) of 17-O-demethyl-geldanamycin	S66
Figure S58. APCI-MS/UV of 17-O-demethyl-geldanamycin	S67
Figure S59. Photograph of <i>Streptomyces</i> sp. RM-5-8 (7 day growth on M ₂ -agar)	S68

Experimental Methods and Materials

General Experimental Procedures. Optical rotation was recorded on a Jasco DIP-370 Digital Polarimeter (Jasco, Easton, MD, USA). UV spectra were recorded on an Ultrospec 8000 spectrometer (GE, Pittsburgh, PA, USA). All NMR data was recorded at 500 MHz or 400 MHz for ^1H and 100 MHz for ^{13}C with Varian Inova NMR spectrometers (Agilent, Santa Clara, CA). LC-MS was conducted with a Waters 2695 LC module (Waters, Milford, MA), equipped with a micromass ZQ and a Symmetry Anal C_{18} column (4.6 × 250 mm, 5 μm ; Waters). HR-ESI-MS spectra were recorded on an AB SCIEX Triple TOF 5600 System (AB Sciex, Framingham, MA, USA). HPLC analyses were performed on an Agilent 1260 system equipped with a photodiode array detector (PDA) detector and a Phenomenex C_{18} column (250 × 4.6 mm, 5 μm ; Phenomenex, Torrance, CA). Semi-preparative HPLC separation was performed on a Varian Prostar 210 HPLC system (Agilent) equipped with a PDA detector 330 using a Supelco Discovery[®]Bio wide pore C_{18} column (250 × 21.2 mm, 10 μm ; flow rate, 8 mL/min; Sigma-Aldrich, St. Louis, MO). All solvents used were of ACS grade and purchased from Pharmco-AAPER (Brookfield, CT). Sephadex LH-20 (25 ~ 100 μm) was purchased from GE Healthcare (Little Chalfont, United Kingdom). C_{18} -functionalized silica gel (40 ~ 63 μm) was purchased from Material Harvest Ltd. (Cambridge, United Kingdom). Amberlite[®] XAD16N resin (20-60 mesh) was purchased from Sigma-Aldrich (Saint Louis, MO, United States). Celite (TM) was purchased from Fisher Scientific (Pittsburgh, PA, United States). TLC silica gel plates (60 F_{254}) were purchased from EMD Chemicals Inc. (Darmstadt, Germany).

Isolation and Identification of *Streptomyces* sp. RM-5-8. The isolation of strain RM-5-8 followed the same protocol as that published.^{S1} The genomic DNA of this strain was isolated from a fully grown colony using GeneJET Genomic DNA Purification Kit (Thermo Scientific, Rockford, IL, USA). The partial 16S rRNA gene fragment was amplified using universal primers (27F, 5'-AGAGTTTGATCMTGGCTCAG-3'; 1492R, 5'-GGTTACCTTGTTACGACTT-3')^{S2} and Phusion High Fidelity DNA polymerase (New England Biolabs, Ipswich, MA, USA). QIAquick PCR purification kit (Qiagen, Valencia, CA, USA) was used to purify the amplified product. The amplified fragment (1,231 bp) displayed 99% identity (BLAST search) to the 16S rRNA gene sequence of *Streptomyces sporocinereus* strain NBRC 100766. The sequence of 16S rRNA has been deposited in the NCBI nucleotide database with the accession number KF732716.

Fermentation, Extraction, Isolation and Purification. *Streptomyces* sp. RM-5-8 was cultivated in three 250 mL Erlenmeyer flasks, each containing 50 mL of medium A (soluble starch, 20.0 g/L; glucose, 10.0 g/L; peptone, 5.0 g/L; yeast extract, 5.0 g/L; NaCl, 4.0 g/L; K_2HPO_4 , 0.5 g/L; $\text{MgSO}_4 \cdot 7\text{H}_2\text{O}$, 0.5 g/L; CaCO_3 , 2.0 g/L). After three days of incubation at 28°C with 200 rpm agitation, the cultures were used to inoculate 60 flasks (250 mL), each containing 100 mL of medium A. The fermentation was continued for seven days at 28°C with 200 rpm agitation. Cultures were subsequently combined, mixed with 300 g of celite followed by filtration under vacuum to separate the mycelium and water phase. The mycelial cake-celite portion was extracted with acetone (2 × 500 mL), filtered and the organic phase was evaporated to afford 0.5 g of a reddish-brown crude extract. The water phase was subjected to a XAD-16 resin column (800 g), washed with water until colorless, and then eluted with 5 L of methanol. The MeOH extract was concentrated under reduced pressure to obtain a crude reddish-brown crude extract (19.0 g). HPLC and TLC analysis indicated that both extracts (mycelium and water extracts) were identical. Therefore, the extracts were combined for further processing.

The crude extract (19.5 g) was subjected to a silica gel column chromatography using a gradient of CHCl_3 -MeOH (100:0 ~ 0:100) to yield six fractions (I-VI). Fraction I (3.5 g) was subjected to a Sephadex LH-20 column, using MeOH to elute compounds at the flow rate of 2 mL/min, affording six subfractions (I-1 to I-6). Subfraction I-2 (0.12 g) was further purified by a semi-preparative HPLC (250 × 21.2 mm, 10 μm ; 45% $\text{CH}_3\text{CN}/\text{H}_2\text{O}$; 8 mL/min; 254 nm) to yield geldanamycin (5 mg) and 17-O-demethyl-geldanamycin (9 mg) as yellow solids. Purification of subfraction I-4 (0.2 g) by semi-preparative HPLC

(250 × 21.2 mm, 10 μm; 16% CH₃CN/H₂O; 8 mL/min; 275 nm) afforded the new compounds **4** (15 mg) and **5** (5 mg) as white amorphous powders. Fraction II (2.4 g) was subjected to a C₁₈ column (10 × 1 cm) using a H₂O:CH₃CN (5-100%) gradient to afford eighteen subfractions (II-1 to II-18). Subfractions II-17 and II-18 were combined (0.22 g) followed by semi-preparative HPLC (250 × 21.2 mm, 10 μm; 35% CH₃CN/H₂O; 8 mL/min; 254 nm) to yield the new compounds **1** (9 mg), **2** (10 mg) and **3** (4 mg) as white amorphous powders. Finally, 500 mg from fraction IV (10 g) was dissolved in 10 mL MeOH followed by purification using a semi-preparative HPLC (250 × 21.2 mm, 10 μm; 9% CH₃CN/H₂O; 8 mL/min; 275 nm) to yield hygromycin A (32 mg), *epi*-hygromycin A (7 mg), methoxyhygromycin A (35 mg) and *epi*-methoxyhygromycin A (8 mg) as white solids.

Compounds **4** and **5** were obtained as white powders. The (–)-HR-ESI-MS of both compounds revealed a molecular formula of C₁₆H₁₈O₈ (*m/z* 337.0961 [M–H][–], calcd 337.0923 for C₁₆H₁₇O₈). The presence of a 3,4-dihydroxy- α -methylcinnamic acid and a 6-deoxy-5-keto-D-*arabino*-hexofuranose moiety in both compounds was established based upon a comparison of corresponding NMR spectra with hygromycin A and its epimer,^{S3-S5} the two main secondary metabolites isolated from this strain, and revealed both **4** and **5** to notably lack the requisite aminocyclitol moiety of hygromycin A. Compounds **4** and **5** were also determined as 4'-epimers on basis of the NMR data (Figure 4, Table 2). While compound **4** was previously reported as one of the intermediates during the total synthesis of hygromycin,^{S6} it is a new natural product. Thus, **4** was given the name prehygromycin and its full NMR assignments (Figure 4 and Table 2) are reported here for the first time. In addition, the 4'-epimer of **4**, compound **5** is a new compound which has been named as 4'-*epi*-prehygromycin (Figures S1).

Terfestatin B (1): White amorphous powder; [α]_D²⁵ –0.10 (*c* 0.3, MeOH); UV (MeOH) λ_{\max} (log ϵ) 260 (9.67) nm; ¹H and ¹³C NMR data, see Table 1; (–)-APCI-MS: *m/z* 449 [M – H][–], 899 [2M – H][–]; (+)-APCI-MS: *m/z* 468 [M + NH₄]⁺, 475 [M + Na]⁺; (+)-HR-ESI-MS: *m/z* 451.1379 [M + H]⁺ (calcd for C₂₅H₂₃O₈, 451.1393), *m/z* 473.1200 [M + Na]⁺ (calcd for C₂₅H₂₂O₈Na, 473.1212); (–)-HR-ESI-MS: *m/z* 449.1248 [M – H][–] (calcd for C₂₅H₂₁O₈, *m/z* 449.1236).

Terfestatin C (2): White amorphous powder; [α]_D²⁵ –0.07 (*c* 0.3, MeOH); UV (MeOH) λ_{\max} (log ϵ) 265 (15.0) nm; ¹H and ¹³C NMR data, see Table 1; (–)-APCI-MS: *m/z* 435 [M – H][–], 871 [2M – H][–]; (+)-APCI-MS: *m/z* 437 [M + H]⁺, 454 [M + NH₄]⁺, 459 [M + Na]⁺; (–)-HR-ESI-MS: *m/z* 435.1089 [M – H][–] (calcd for C₂₄H₁₉O₈, *m/z* 435.1080).

10-O-(4''-deoxy- α -L-threo-hex-4''-enopyranosid)-uronic acid-5-isoprenylindole-3-carboxylate (3): White amorphous powder; [α]_D²⁵ +0.07 (*c* 0.3, MeOH); UV (MeOH) λ_{\max} (log ϵ) 233 (9.88), 284 (4.43) nm; ¹H and ¹³C NMR data, see Table 2; (+)-HR-ESI-MS: *m/z* 388.1395 [M + H]⁺ (calcd for C₂₀H₂₂NO₇, 388.1396), *m/z* 405.1660 [M + NH₄]⁺ (calcd for C₂₀H₂₅NO₇, 405.1662), *m/z* 410.1210 [M + Na]⁺ (calcd for C₂₀H₂₁NO₇Na, 410.1216).

Prehygromycin (4): White amorphous powder; [α]_D²⁵ –0.23 (*c* 1.2, MeOH); UV (MeOH) λ_{\max} (log ϵ) 279 (10.08) nm; ¹H and ¹³C NMR data, see Table 2; (–)-APCI-MS: *m/z* 337.0 [M – H][–], 675.1 [2M – H][–]; (–)-HR-ESI-MS *m/z* 337.0961 [M – H][–] (calcd for C₁₆H₁₇O₈, *m/z* 337.0923).

4'-Epi-prehygromycin (5): White amorphous powder; [α]_D²⁵ –0.10 (*c* 0.5, MeOH); UV (MeOH) λ_{\max} (log ϵ) 282 (7.53) nm; ¹H and ¹³C NMR data, see Table 2; (–)-APCI-MS: *m/z* 337.0 [M – H][–], 675.2 [2M – H][–]; (–)-HR-ESI-MS *m/z* 337.0961 [M – H][–] (calcd for C₁₆H₁₇O₈, *m/z* 337.0923).

Organotypic Hippocampal Slice Culture Preparation. Whole brains were collected from eight-day-old Sprague-Dawley rats (Harlan Laboratories; Indianapolis, IN) and placed in cold dissecting medium composed of Minimum Essential Medium (MEM; Invitrogen, Carlsbad, CA), 25 mM HEPES (Sigma, St. Louis, MO), and 50 μM streptomycin/penicillin (Invitrogen). Hippocampi were removed from the whole

rain, cleaned of excess tissue using a dissecting microscope, and sectioned at 200 μM using a McIlwain Tissue Chopper (Mickle Laboratory Engineering Co. Ltd., Gomshall, UK). Hippocampi slices were plated onto Millicell-CM 0.4 μM biopore membrane inserts containing 1 mL of pre-incubated culture medium [dissecting medium, distilled water, 36 mM glucose (Fisher, Pittsburg, PA), 25% Hanks' Balanced Salt Solution (HBSS; Invitrogen), 25% v/v heat-inactivated horse serum (HIHS; Sigma), and 0.05% streptomycin/penicillin (Invitrogen)]. Hippocampi were maintained in an incubator at 37 °C with a gas composition of 5% CO_2 /95% air for 5 days before any experiments were conducted. Care of all animals was carried out in accordance with the National Institutes of Health Guide for the Care and Use of Laboratory Animals (NIH Publications No. 80-23, revised 1996) and the University of Kentucky's Institutional Animal Care and Use Committee.

Organotypic Hippocampal Slice Treatment. At 5 DIV, slices were transferred to new plates containing either 1 mL of standard culture medium (control) or culture medium with a calculated EtOH concentration of 100 mM. No single animal was represented in a given treatment group more than once. In an attempt to minimize EtOH evaporation, all plates containing EtOH in the medium were surrounded by 50 mL of ddH₂O containing EtOH (at a concentration of 100 mM) in topless polypropylene containers, and plates devoid of EtOH in the medium were surrounded by 50 mL of ddH₂O. Containers were placed into plastic bags, filled to capacity with 5% CO_2 /95% air, sealed and placed in a water-jacketed CO_2 incubator for 48 h. Prior work has demonstrated that rapid evaporation of EtOH occurs during the preparation such that the actual starting concentration of EtOH in medium is approximately 90 mM.^{S7}

In cultures exposed to compounds **1-3** and echoside B, with or without the addition of EtOH, the compounds were diluted in DMSO to a final working concentration of 0.01% DMSO in cell culture medium. EtOH-exposed and EtOH-naïve cultures were also exposed to 0.1% DMSO in cell culture medium. Each 1 mL of cell culture medium, for all groups, also contained the nucleic acid intercalating agent, propidium iodide (3.74 μM). Propidium iodide is a polar compound that is only able to enter cells with compromised membranes, after which it binds to DNA and is able to fluoresce when excited at 515-560 nm. Propidium iodide uptake is highly correlated with multiple other measures of cytotoxicity in cell culture.^{S8} After 48 h incubation, all cultures were removed from incubators and imaged to assess the intensity of propidium iodide uptake.

Fluorescent Microscopy and Statistical Analyses. Fluorescent intensity of propidium iodide was measured using densitometric measurement of the entire hippocampal slice. Images were taken using SPOT Advanced version 4.0.2 software for Windows (W. Nuhsbaum Inc., McHenry, IL, USA) with a 5x objective on an inverted Leica DMIRB microscope (W. Nuhsbaum Inc.) fitted for fluorescence detection (mercury-arc lamp) and connected to a personal computer via a SPOT 7.2 color mosaic camera (W. Nuhsbaum Inc.). Propidium iodide has a maximum excitation wavelength of 536 nm and was excited using a band-pass filter that excites the wavelengths between 515 and 560 nm. The emission of PI in the visual range is 620 nm. Fluorescent intensity was analyzed ImageJ software (National Institutes of Health, Bethesda, MD, USA) for the entirety of each hippocampal slice culture. Raw fluorescent values were analyzed using a one-way analysis of variance ANOVA to assess effects of ethanol and treatment of compounds on propidium iodide uptake. When appropriate, Tukey's post-hoc analyses were conducted. The significance level was set at $P < 0.05$. For purposes of graphical illustration, all data were converted to percentage of EtOH-naïve control values.

Antimicrobial, Antifungal and Cancer Cell Line Cytotoxicity Assays. Assays for antibacterial (*Staphylococcus aureus* ATCC 6538, *Salmonella enterica* ATCC 10708), antifungal (*Saccharomyces cerevisiae* ATCC 204508) and cancer cell line cytotoxicity (non-small cell lung A549, prostate PC3) followed our previously reported protocols.^{S9,S10}

Supplemental References

- S1. Wang, X.; Shaaban, K. A.; Elshahawi, S. I.; Ponomareva, L. V.; Sunkara, M.; Zhang, Y.; Copley, G. C.; Hower, J. C.; Kharel, M. K.; Thorson, J. T. *J. Nat. Prod.* **2013**, *76*, 1441–1447.
- S2. Lane, D. J.; Stackebrandt, E.; Goodfellow, M., Nucleic acid techniques in bacterial systematics. *John Wiley and Sons Ltd.: New York* **1991**, 115-147.
- S3. Kakinuma, K.; Sakagami, Y. *Agr. Biol. Chem.* **1978**, *42*, 279-286.
- S4. Wakisaka, Y.; Koizumi, K.; Nishimoto, Y.; Kobayashi, M.; Tsuji, N. *J. Antibiot.* **1980**, *33*, 695-704.
- S5. Yoshida, M.; Takahashi, E.; Uozumi, T.; Beppu, T. *Agr. Biol. Chem.* **1986**, *50*, 143-149.
- S6. Buchanan, J. G.; Hill, D. G.; Wightman, R. H.; Boddy, I. K.; Hewitt, B. D. *Tetrahedron* **1995**, *51*, 6033-6050.
- S7. Prendergast, M. A.; Harris, B. R.; Mullholland, P. J.; Blanchard, J. A., 2nd; Gibson, D. A.; Holley, R. C.; Littleton, J. M. *Neuroscience* **2004**, *124*, 869-877.
- S8. Zimmer, J.; Kristensen, B. W.; Jakobsen, B.; Noraberg, J. *Amino acids* **2000**, *19*, 7-21.
- S9. Wang, X.; Elshahawi, S. I.; Shaaban, K. A.; Fang, L.; Ponomareva, L. V.; Zhang, Y.; Copley, G. C.; Hower, J. C.; Zhan, C. G.; Kharel, M. K.; Thorson, J. S. *Org. Lett.* **2014**, *16*, 456-459.
- S10. Shaaban, K. A.; Singh, S.; Elshahawi, S. I.; Wang, X.; Ponomareva, L. V.; Sunkara, M.; Copley, G. C.; Hower, J. C.; Morris, A. J.; Kharel, M. K.; Thorson, J. S. *J. Antibiot.* **2014**, *67*, 223-230.

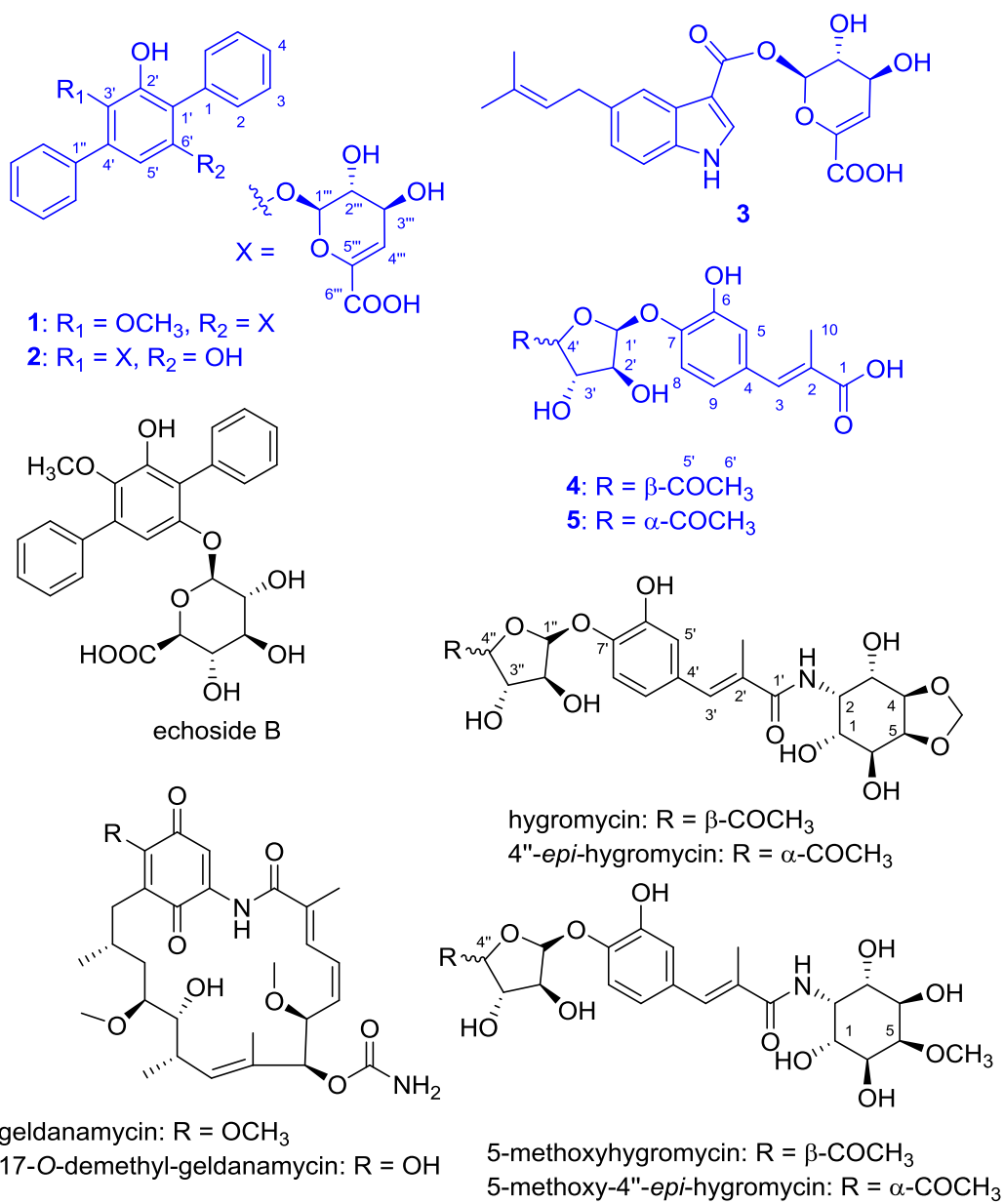


Figure S1. Structures of the compounds isolated from *Streptomyces* sp. RM-5-8. Compound highlighted in blue, new natural products; compounds highlighted in black, known natural products.

Table S1. ^1H and ^{13}C NMR data for terfestatins B (1) and C (2) in $\text{DMSO}-d_6$ (J in Hz).

Position	terfestatin B (1)			terfestatin C (2)		
	$\delta_{\text{H}}^{\text{a}}$	$\delta_{\text{C}}^{\text{b}}$, type	HMBC	$\delta_{\text{H}}^{\text{a}}$	$\delta_{\text{C}}^{\text{b}}$, type	HMBC
1		133.4, C			134.4, C	
2, 6	7.41, m	130.9, CH	C-4, C-1'	7.33, m	130.8, CH	C-1', C-3, C-4, C-5
3, 5	7.35, m	127.5, CH	C-1	7.38, m	127.3, CH	C-1, C-2, C-6
4	7.29, m	126.7, CH	C-2, C-6	7.24, m	126.2, CH	C-2, C-6
1'		119.9, C			116.0, C	
2'		148.3, C			148.5, C	
3'		141.0, C			133.0, C	
4'		133.1, C			132.8, C	
5'	6.76, s	108.8, CH	C-1', C-3', C-4', C-6', C-1''	6.39, s	107.4, CH	C-1'', C-1', C-3', C-6'
6'		150.0, C			151.5, C	
1''		137.6, C			137.7, C	
2'', 6''	7.62, dd, (7.5)	128.6, CH	C-4', C-3'', C-4'', C-5''	7.54, dd (7.2, 1.2)	128.6, CH	C-3'', C-4'', C-5'', C-4'
3'', 5''	7.46, t (7.5)	128.4, CH	C-1'', C-2'', C-6''	7.45, t (7.3)	128.4, CH	C-1'', C-2'', C-6''
4''	7.35, m	127.5, CH	C-2'', C-6''	7.35, m	127.4, CH	C-2'', C-6''
1'''	5.54, d (4.6)	99.1, CH	C-6', C-2''', C-3''', C-5'''	4.83, d (2.2)	99.5, CH	C-5'''
2'''	3.46, m	69.9, CH		3.70, br s	68.1, CH	
3'''	3.91, br s	66.2, CH		3.81, br s	63.9, CH	C-1''', C-4'''
4'''	5.87, br s	112.6, CH	C-2''', C-5''', C-6'''	5.97, d (4.4)	110.7, CH	C-2''', C-5''', C-6'''
5'''		140.6, C			140.3, C	
6'''		163.2, C			162.9, C	
3'-OCH ₃	3.30, s	60.3, CH ₃	C-3'			
2'-OH	8.91, s		C-1', C-2', C-3'	8.28, s		
6'-OH				9.21, s		C-1', C-5', C-6'
2''-OH	5.37, br s			5.53, d (4.3)		C-1''', C-3'''
3''-OH	4.35, br s			5.68, d (6.6)		C-3''', C-4'''

^a400 MHz; ^b100 MHz

Table S2. ¹H and ¹³C NMR data for 10-*O*-(4''-deoxy- α -L-*threo*-hex-4''-enopyranosid)-uronic acid-5-isoprenylindole-3-carboxylate (**3**), prehygromycin (**4**) and 4'-*epi*-prehygromycin (**5**), (*J* in Hz)

Position	Compound 3		prehygromycin (4)		4'- <i>epi</i> -prehygromycin (5)	
	δ_{H}^a	δ_{C}^b , type	δ_{H}^a	δ_{C}^b , type	δ_{H}^c	δ_{C}^d , type
1				169.5, C		172.3, C
2	8.10, s	133.5, CH		126.8, C		128.3, C
3		105.3, C	7.47, s	137.5, CH	7.58, s	140.0, CH
4	7.25, s	111.3, CH		130.9, C		132.4, C
5		135.9, C	6.95, br s	116.9, CH	6.97, d (2.0)	118.5, CH
6	7.00, d (7.8)	122.5, CH		146.5, C		148.1, C
7	7.97, d (7.8)	120.5, CH		144.6, C		146.4, C
8		123.7, C	7.15, d (8.4)	115.5, CH	7.24, d (8.5)	117.3, CH
9		136.8, C	6.92, d (8.4)	121.6, CH	6.91, dd (8.5, 2.0)	123.2, CH
10		162.6, C	2.01, s	13.9, CH ₃	2.08, s	14.4, CH ₃
1'	3.40, d (7.2)	33.8, CH ₂	5.66, d (3.8)	101.1, CH	5.84, d (4.0)	103.1, CH
2'	5.34, m	123.8, CH	4.02, br s	77.0, CH	4.25, t (4.5)	78.8, CH
3'		131.3, C	4.19, br s	75.9, CH	4.56, dd (6.0, 4.5)	77.4, CH
4'	1.71, s	17.6, CH ₃	4.19, br s	87.1, CH	4.82, d (6.0)	86.1, CH
5'	1.71, s	25.5, CH ₃		207.4, C		208.9, C
6'			2.01, s	25.8, CH ₃	2.12, s	28.3, CH ₃
1''	6.21, d (4.5)	91.3, CH				
2''	3.72, br.s	69.7, CH				
3''	4.11, br.s	66.2, CH				
4''	5.88, br.s	110.9, CH				
5''		142.4, C				
6''		163.7, C				
1-OH			12.38, s			
6-OH			8.82, s			
2'-OH/3'-OH			5.33, 5.85			

^aDMSO-*d*₆, 400 MHz; ^bDMSO-*d*₆, 100 MHz; ^cCD₃OD, 400 MHz; ^dCD₃OD, 100 MHz.

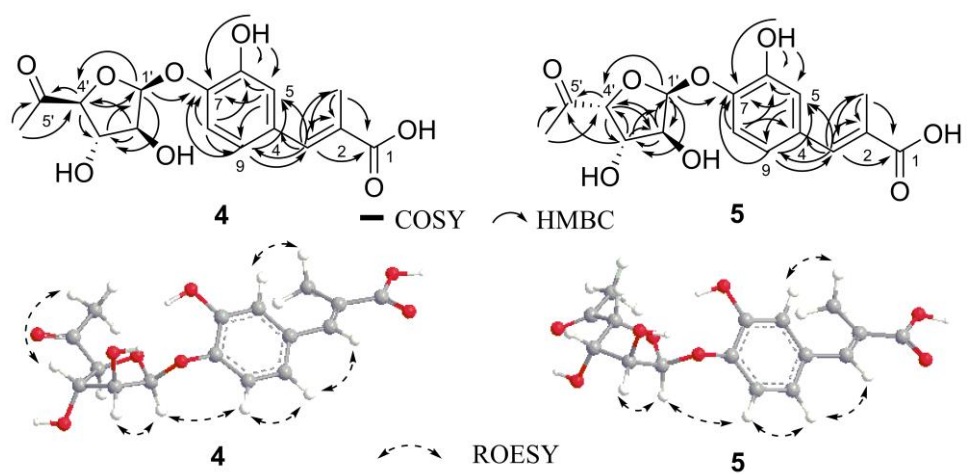


Figure S2. ^1H , ^1H -COSY (—), selected HMBC (→) and key ROESY correlations of prehygromycin (**4**) and 4'-*epi*-prehygromycin (**5**).

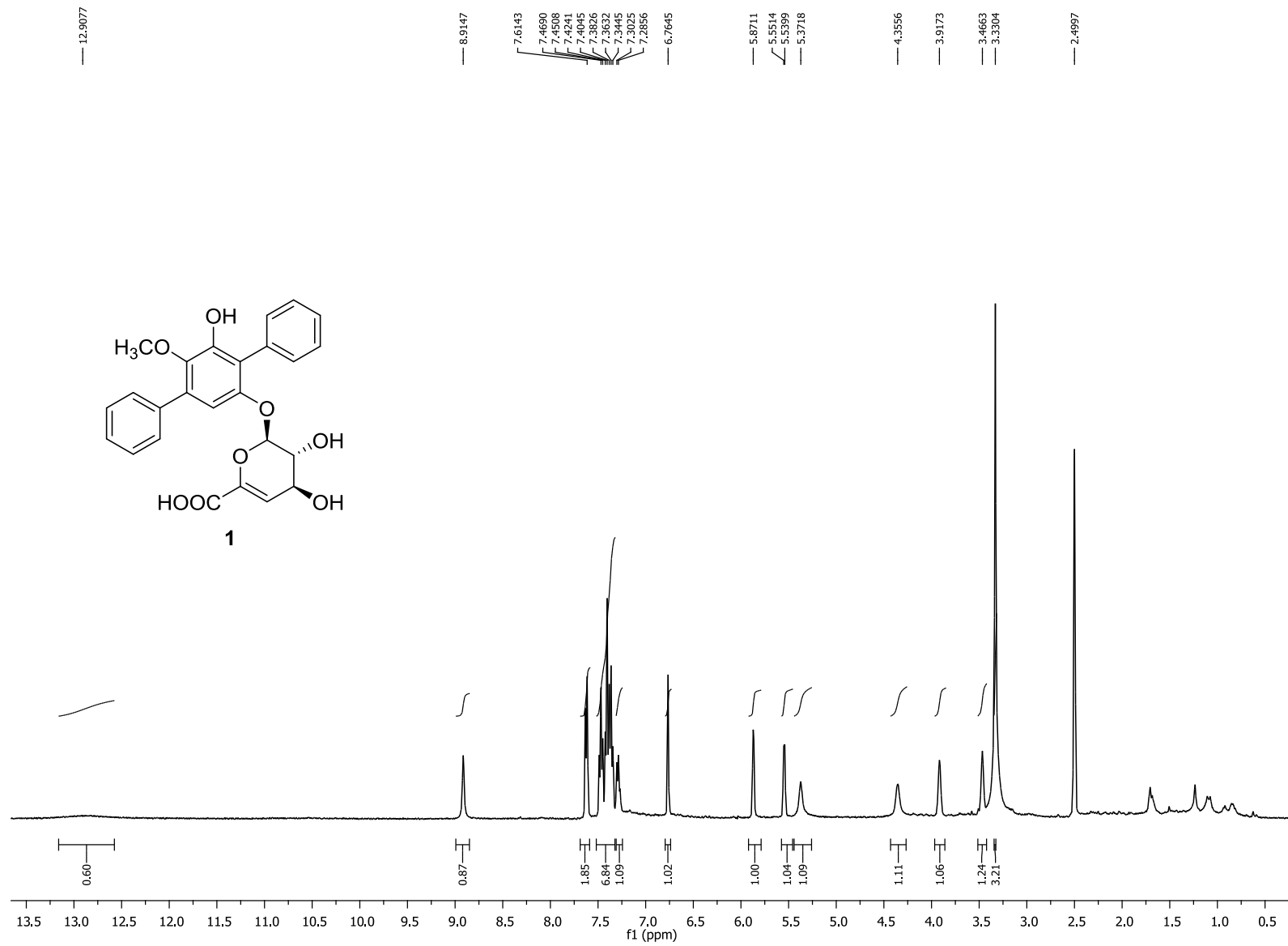


Figure S3. ¹H NMR spectrum (DMSO-*d*₆, 400 MHz) of terfestatin B (1).

RM5-8-15 CNMR, DMSO-d₆, 100MHz

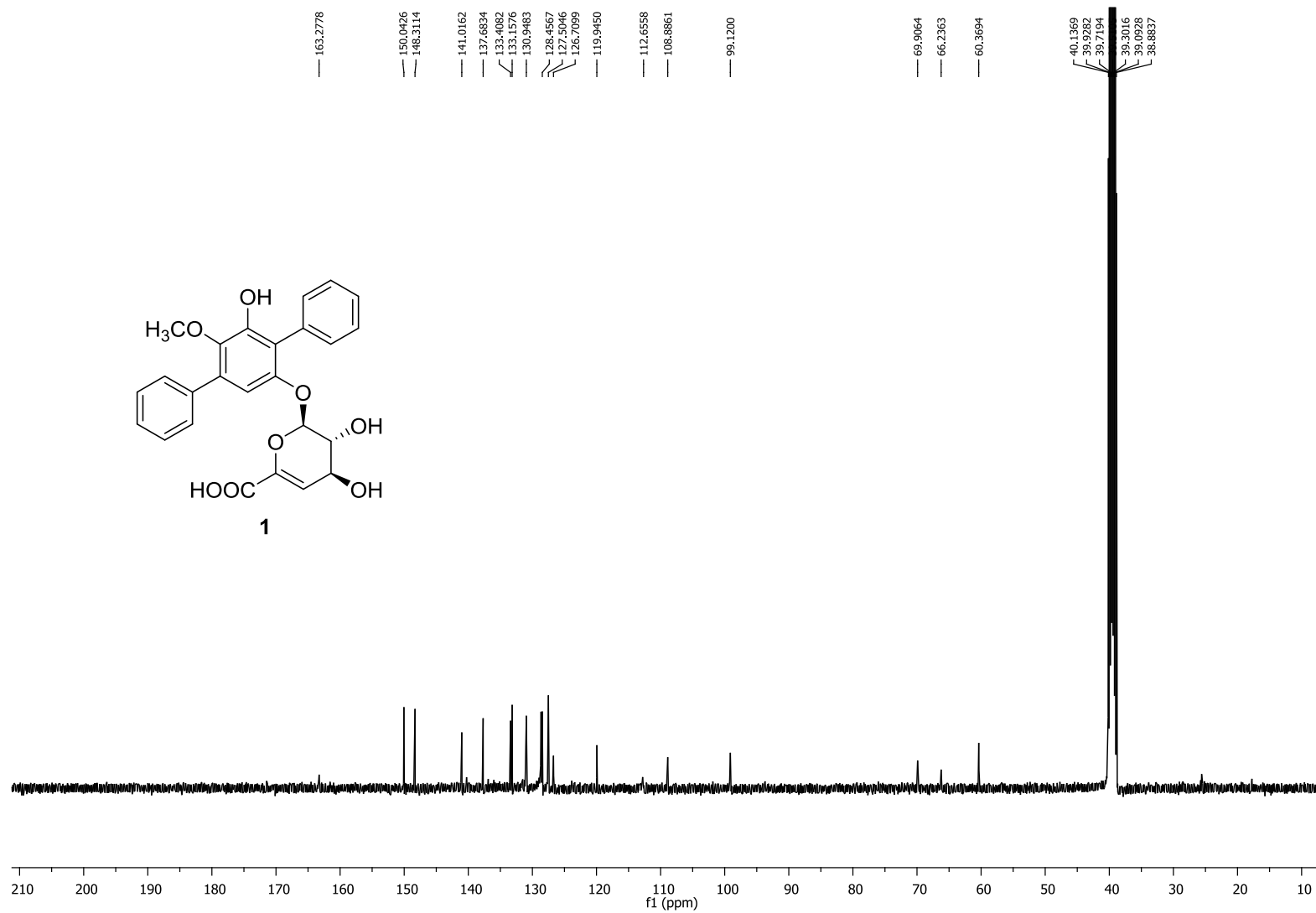


Figure S4. ¹³C NMR spectrum (DMSO-d₆, 100 MHz) of terfestatin B (1).

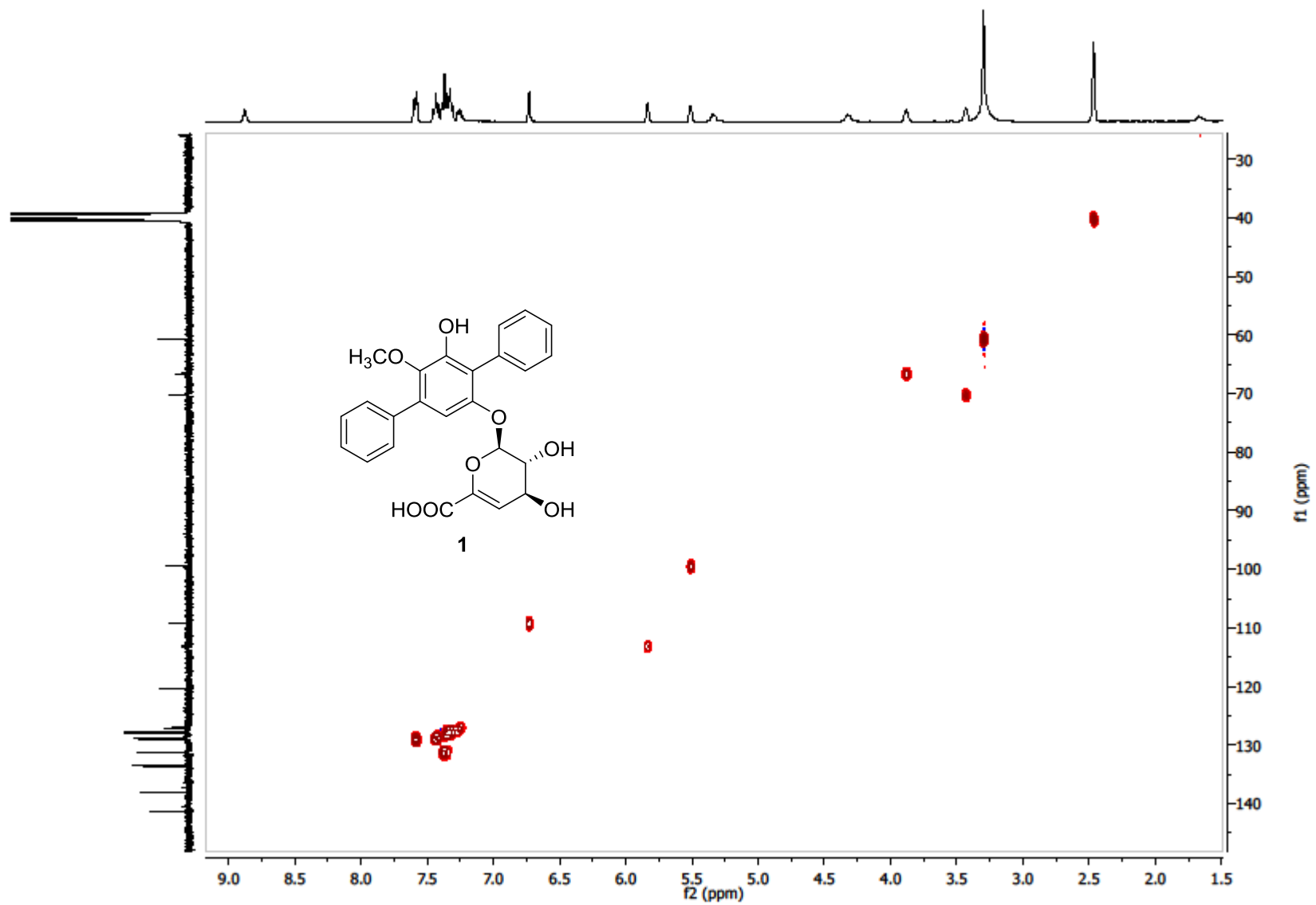


Figure S5. HSQC spectrum (DMSO- d_6 , 400 MHz) of terfestatin B (1).

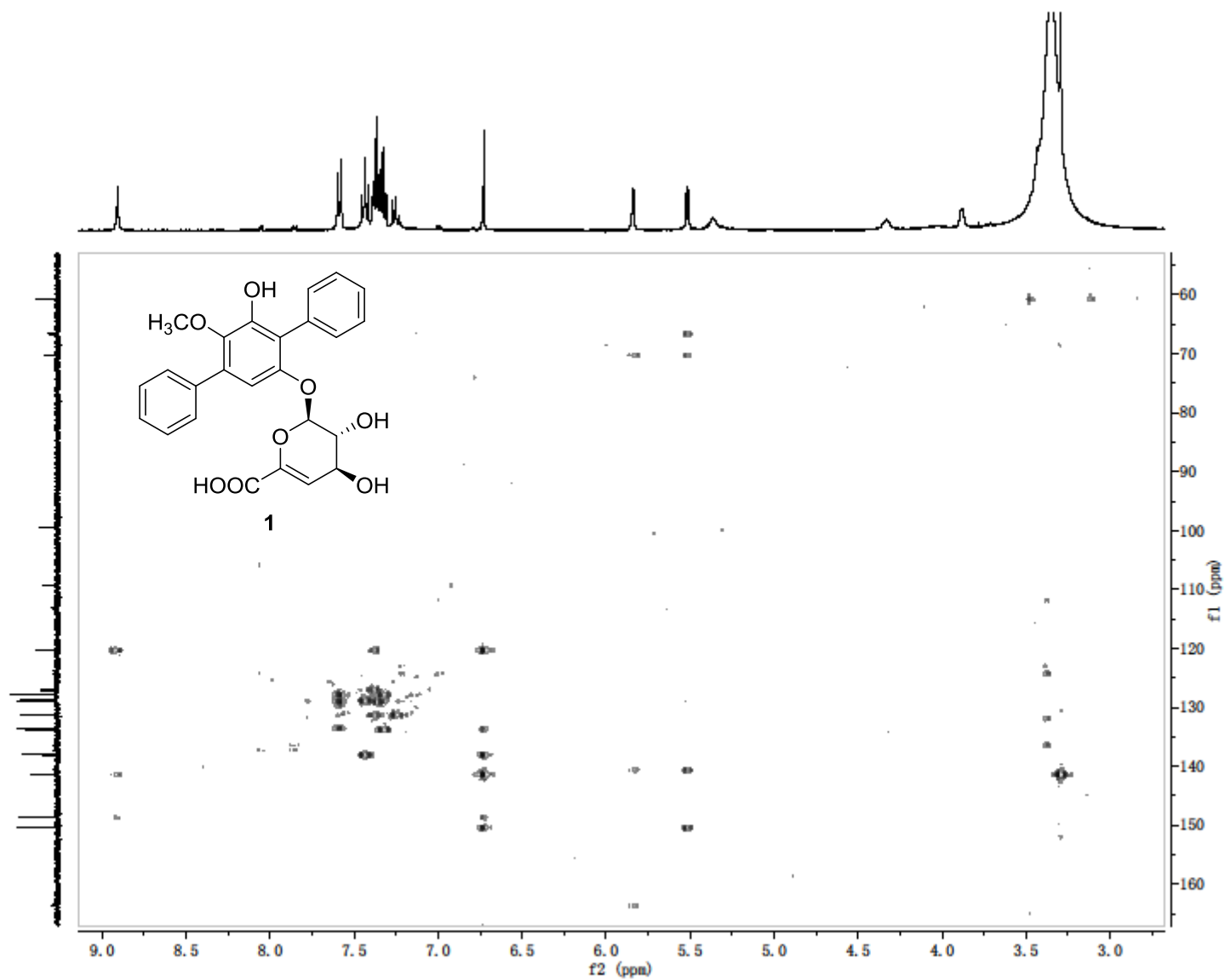


Figure S6. HMBC spectrum (DMSO- d_6 , 400 MHz) of terfestatin B (1).

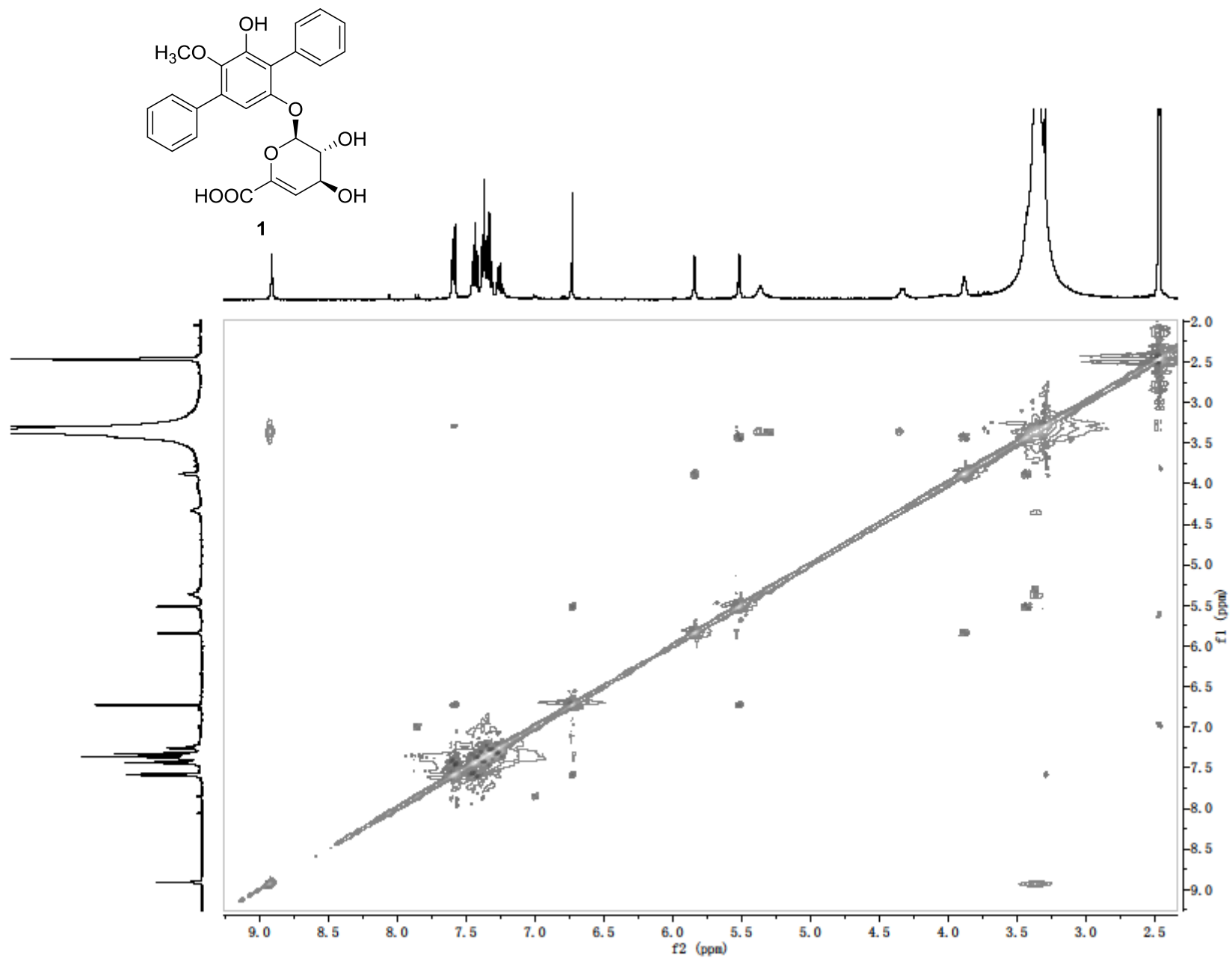


Figure S7. ROESY spectrum ($\text{DMSO-}d_6$, 400 MHz) of terfestatin B (1).

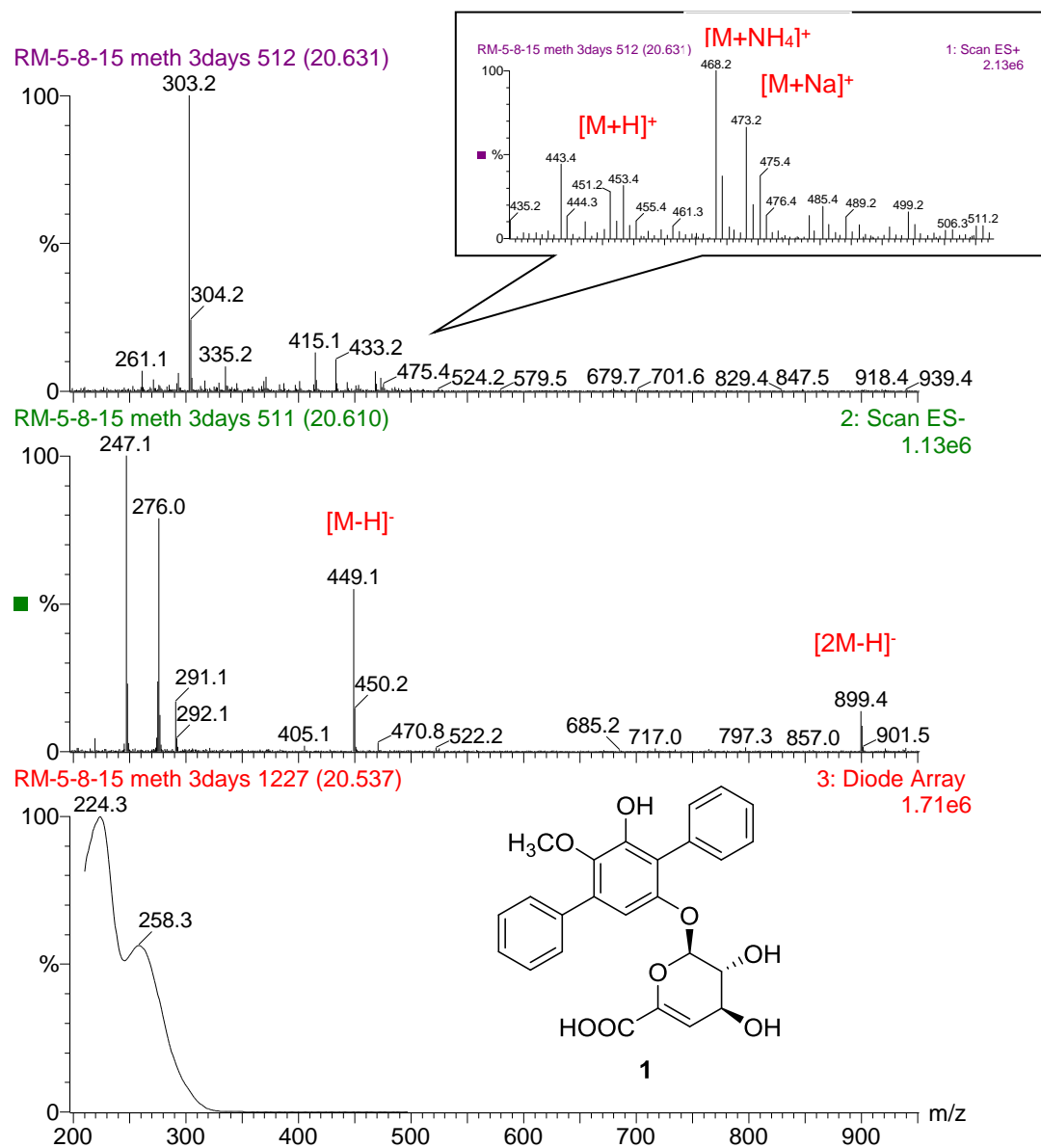


Figure S8. APCI-MS/UV of terfestatin B (1).

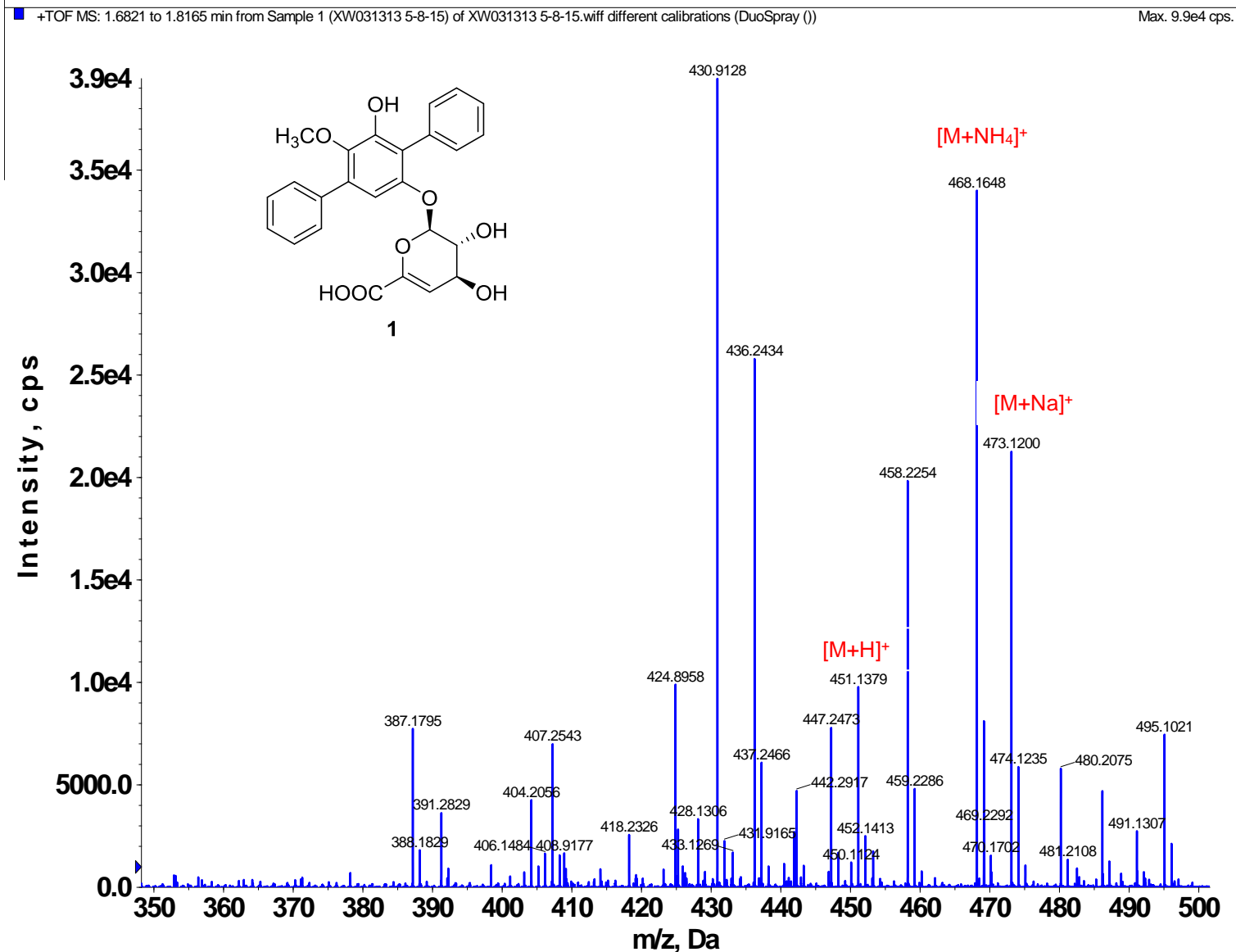


Figure S9. (+)-HRESI-MS (positive mode) of terfestatin B (1).

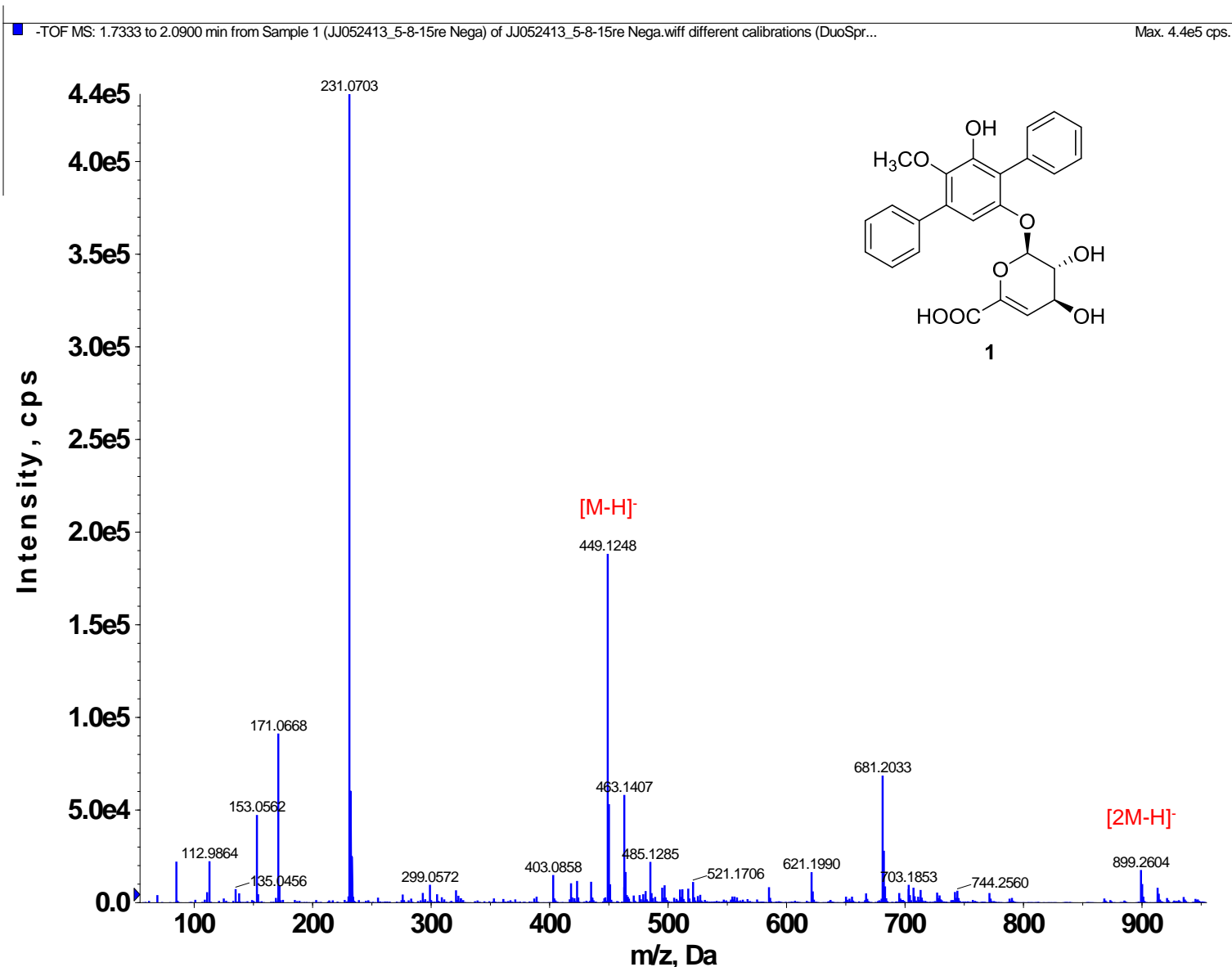


Figure S10. (-)-HRESI-MS of terfestatin B (1).

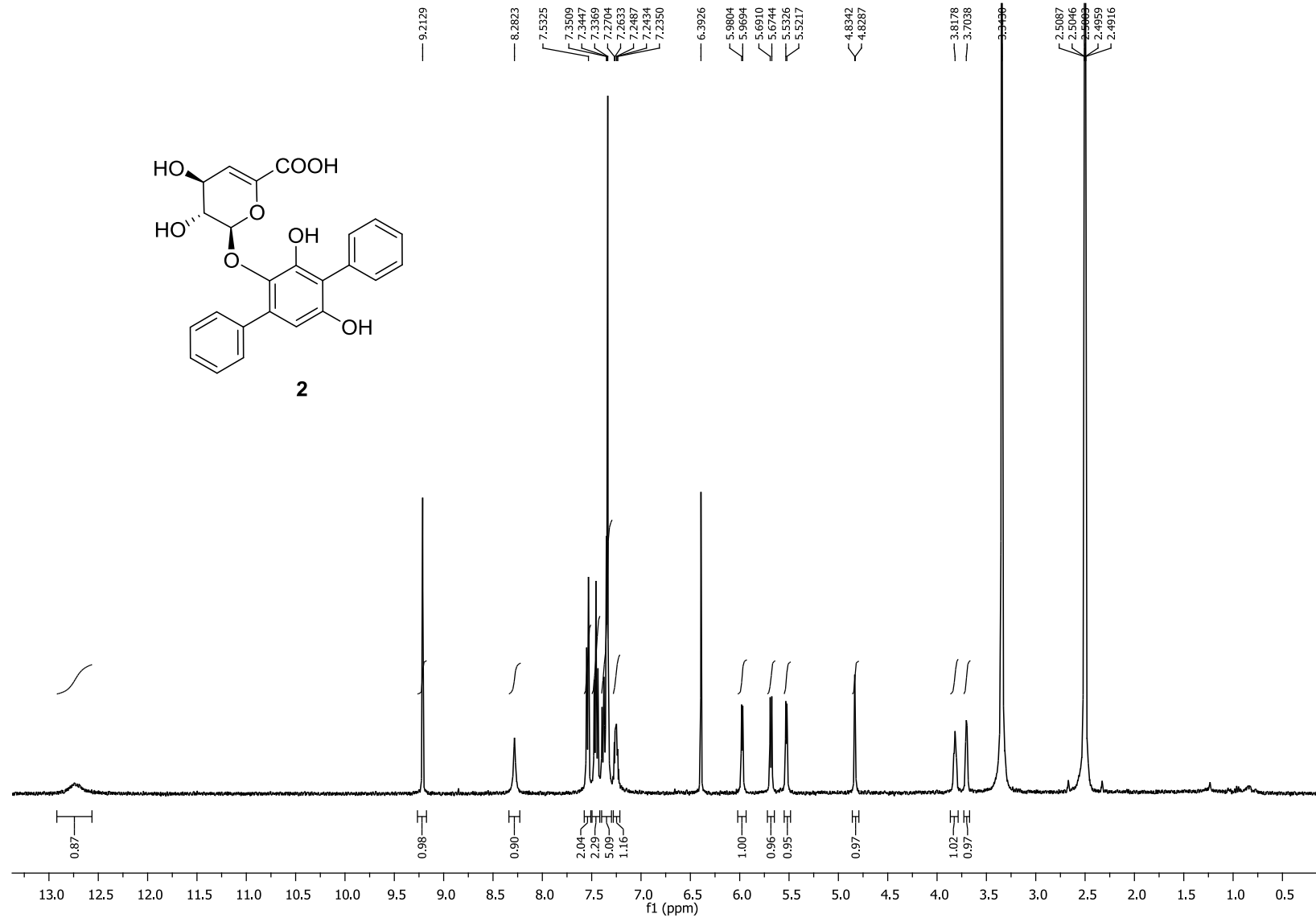


Figure S11. ^1H NMR spectrum ($\text{DMSO}-d_6$, 400 MHz) of terfestatin C (**2**).

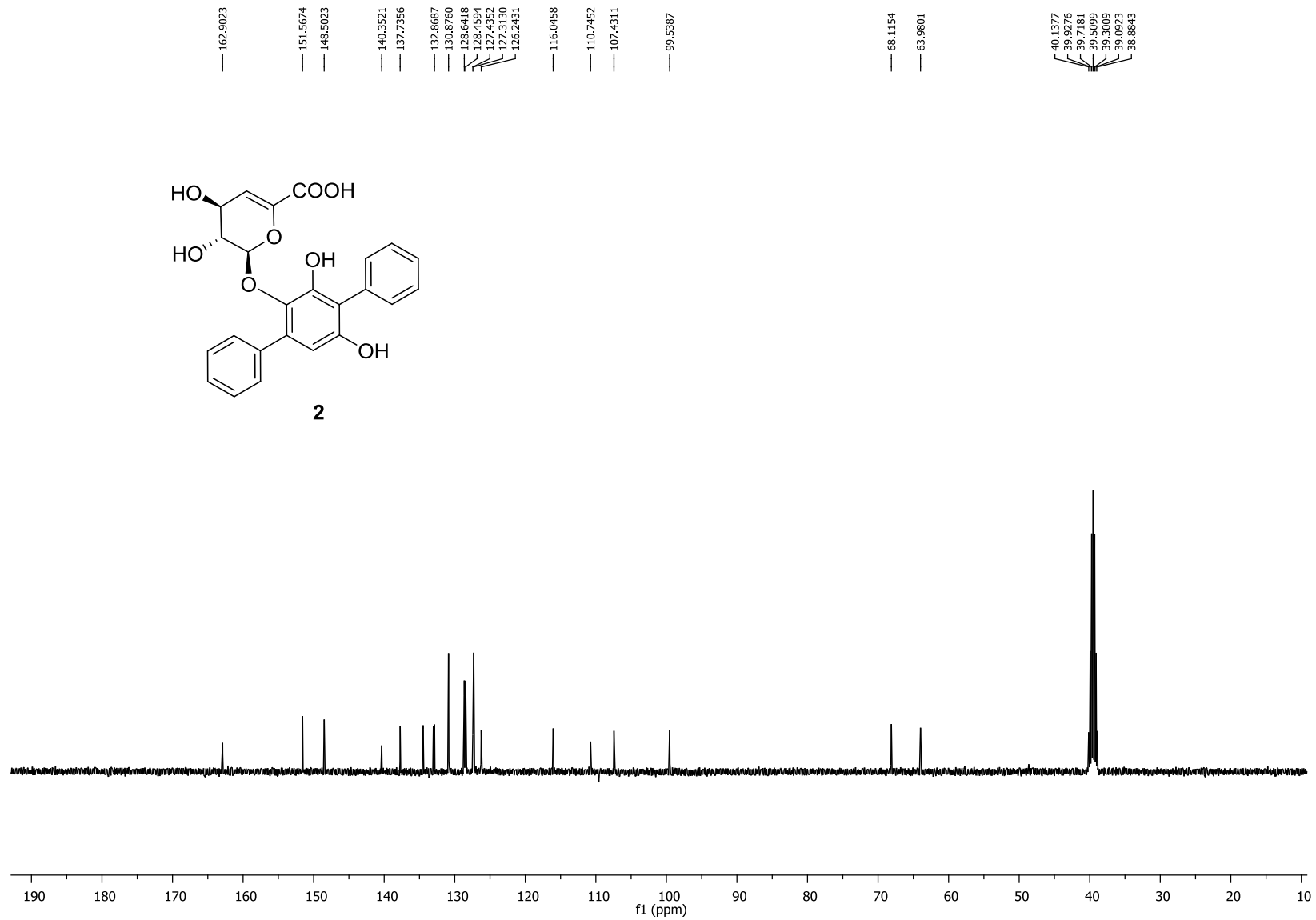


Figure S12. ¹³C NMR spectrum (DMSO-*d*₆, 100 MHz) of terfestatin C (2).

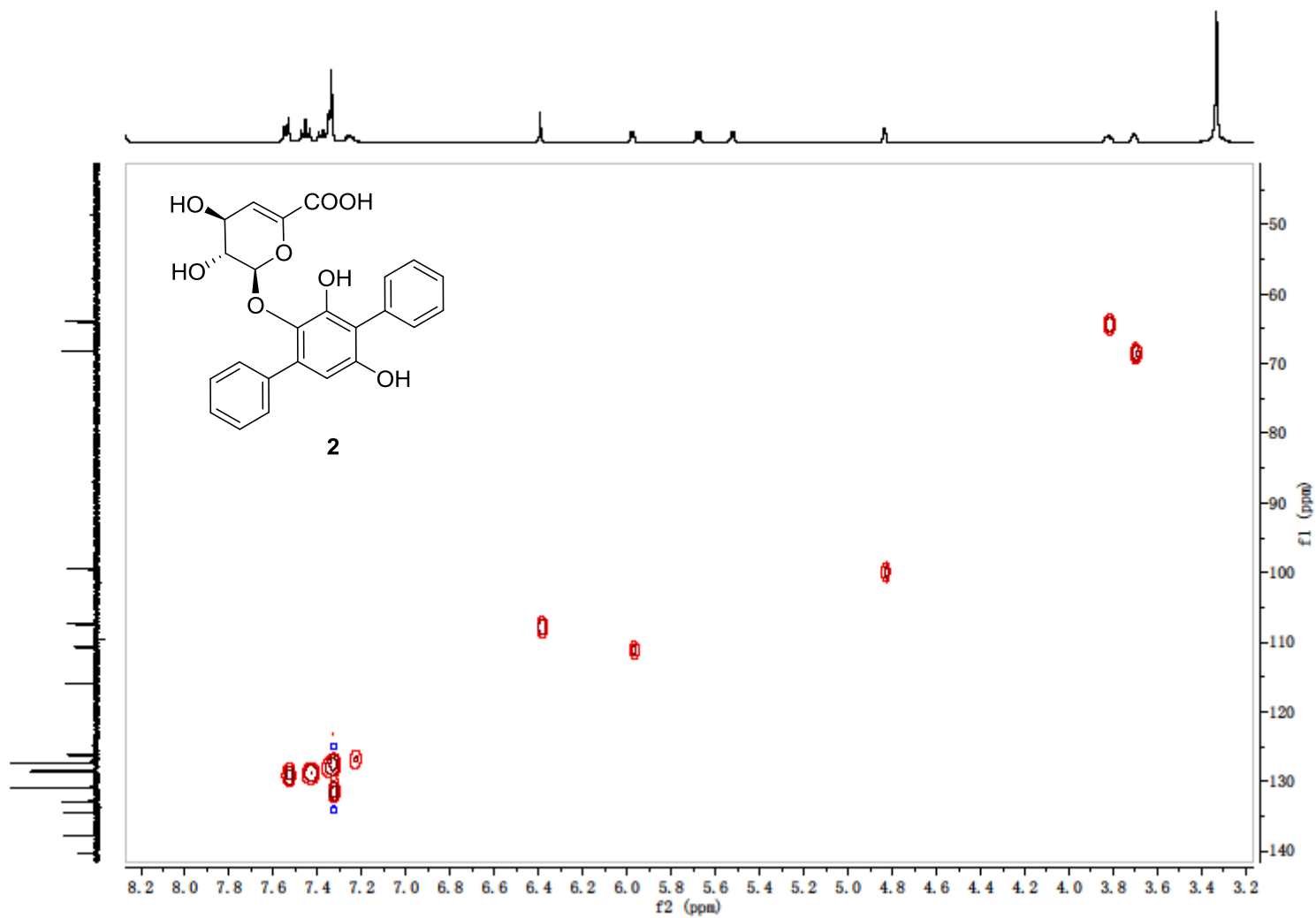


Figure S13. HSQC spectrum (DMSO- d_6 , 400 MHz) of terfestatin C (2).

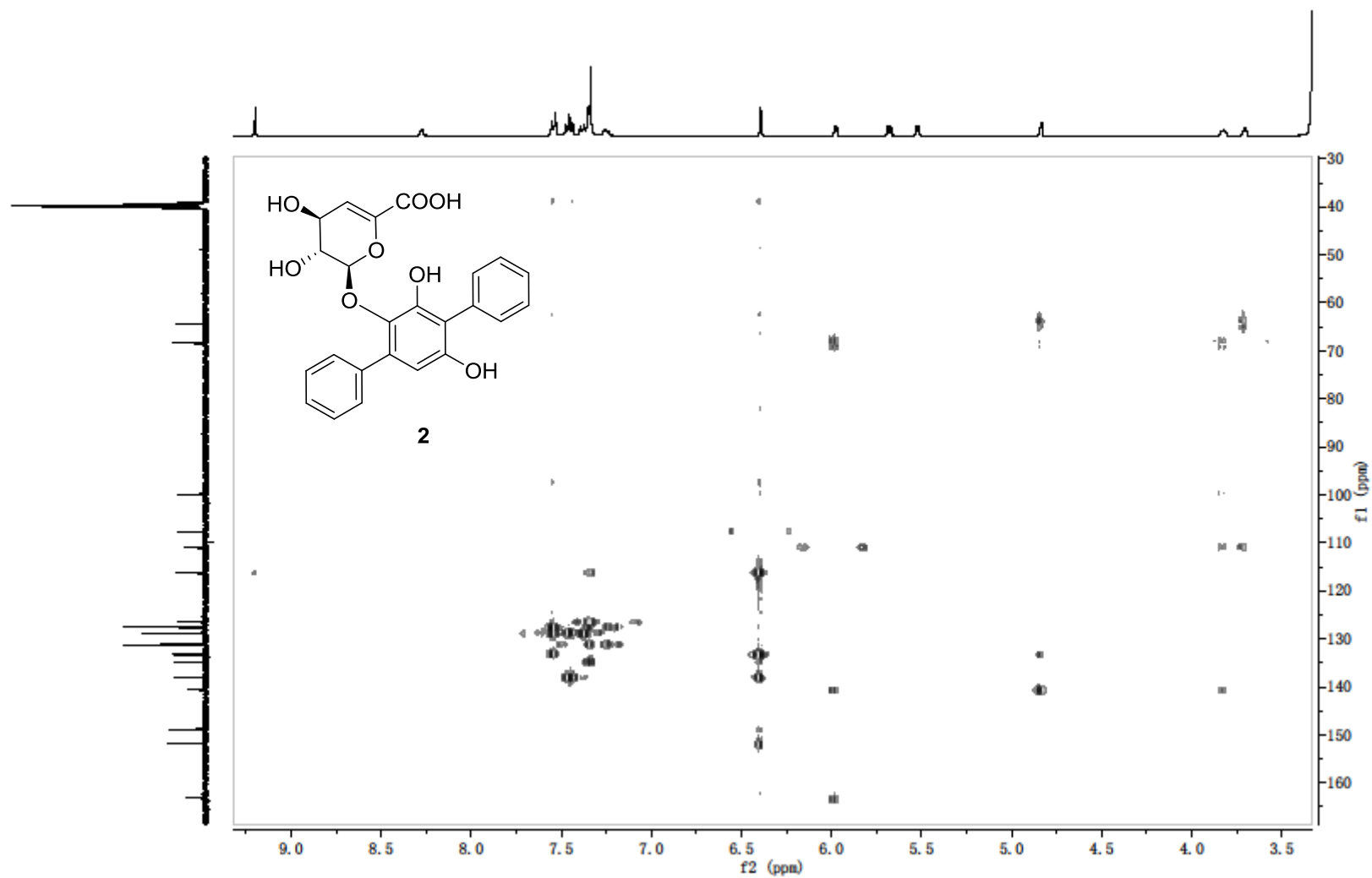


Figure S14. HMBC spectrum (DMSO-*d*₆, 400 MHz) of terfestatin C (2).

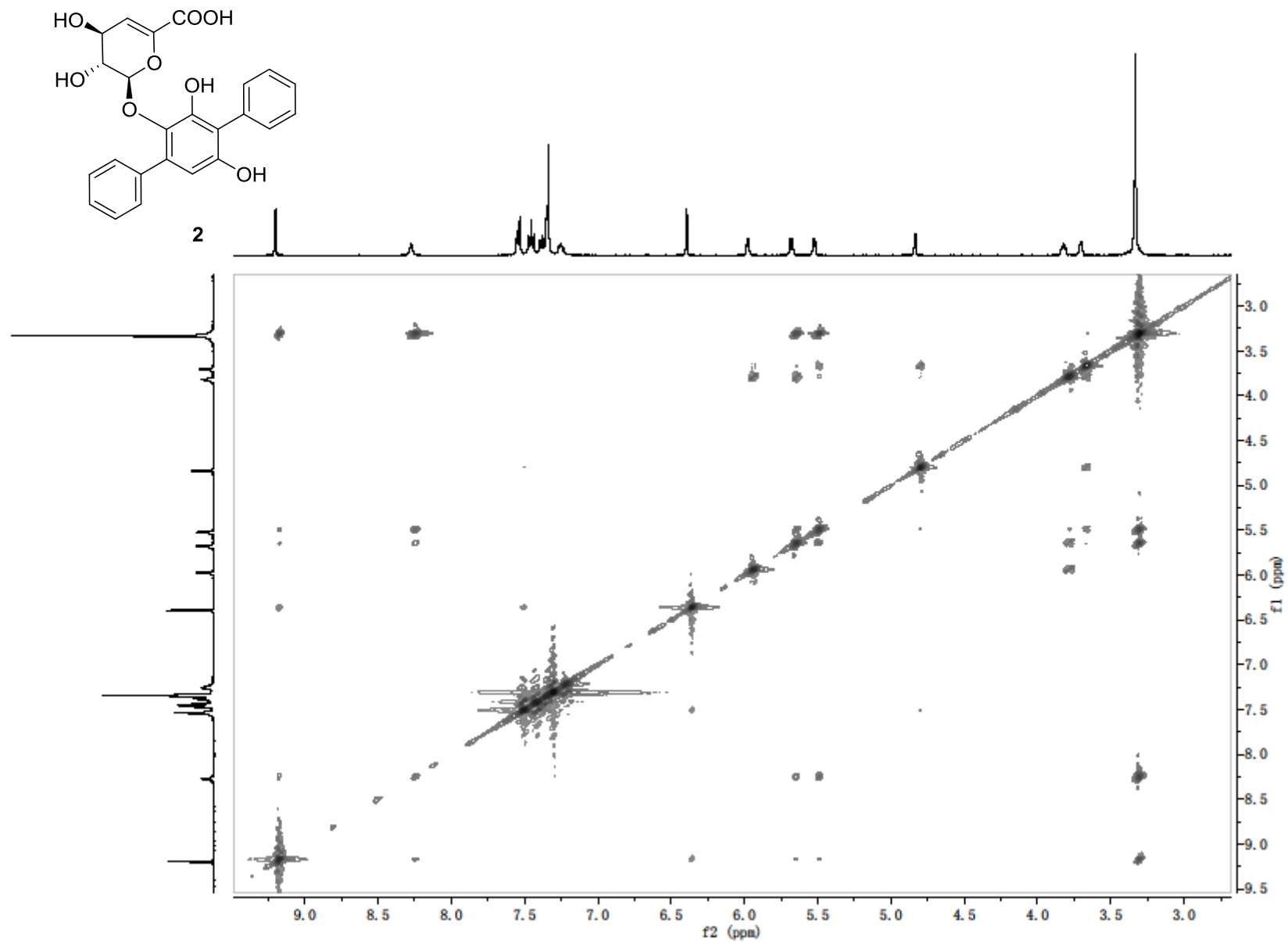


Figure S15. ROESY spectrum (DMSO-*d*₆, 400 MHz) of terfestatin C (2).

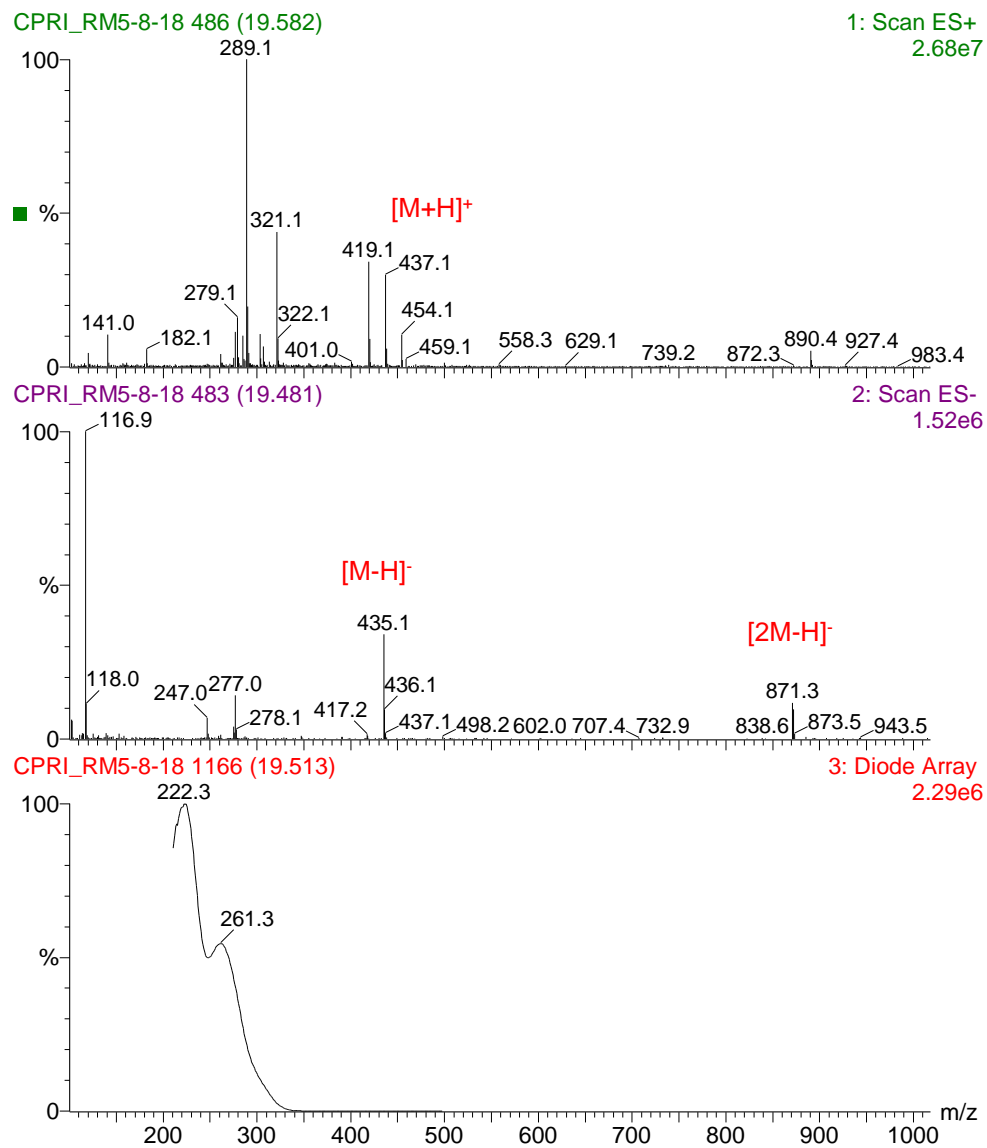


Figure S16. APCI-MS/UV of terfestatin C (**2**).

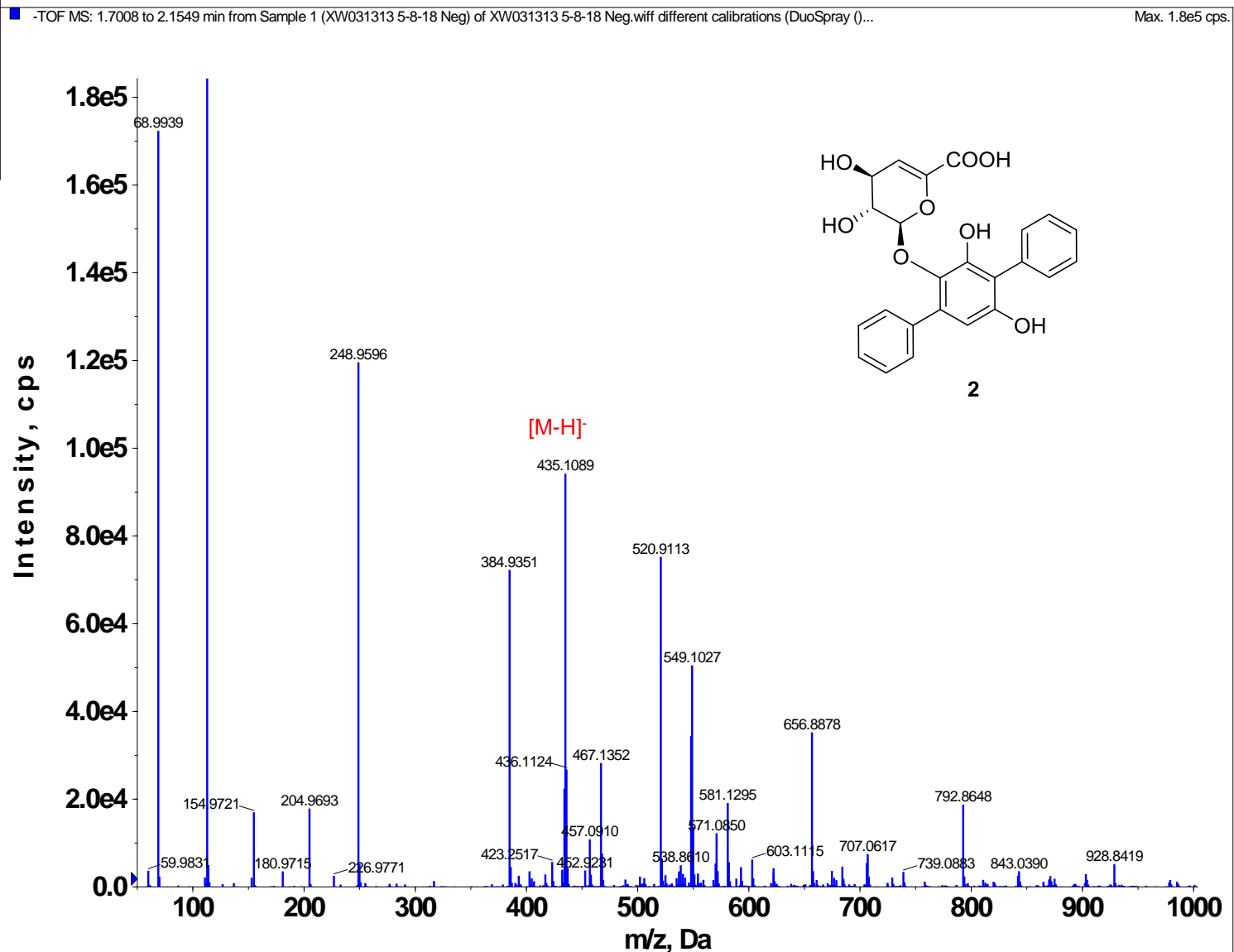


Figure S17. (-)-HRESI-MS of terfestatin C (2).

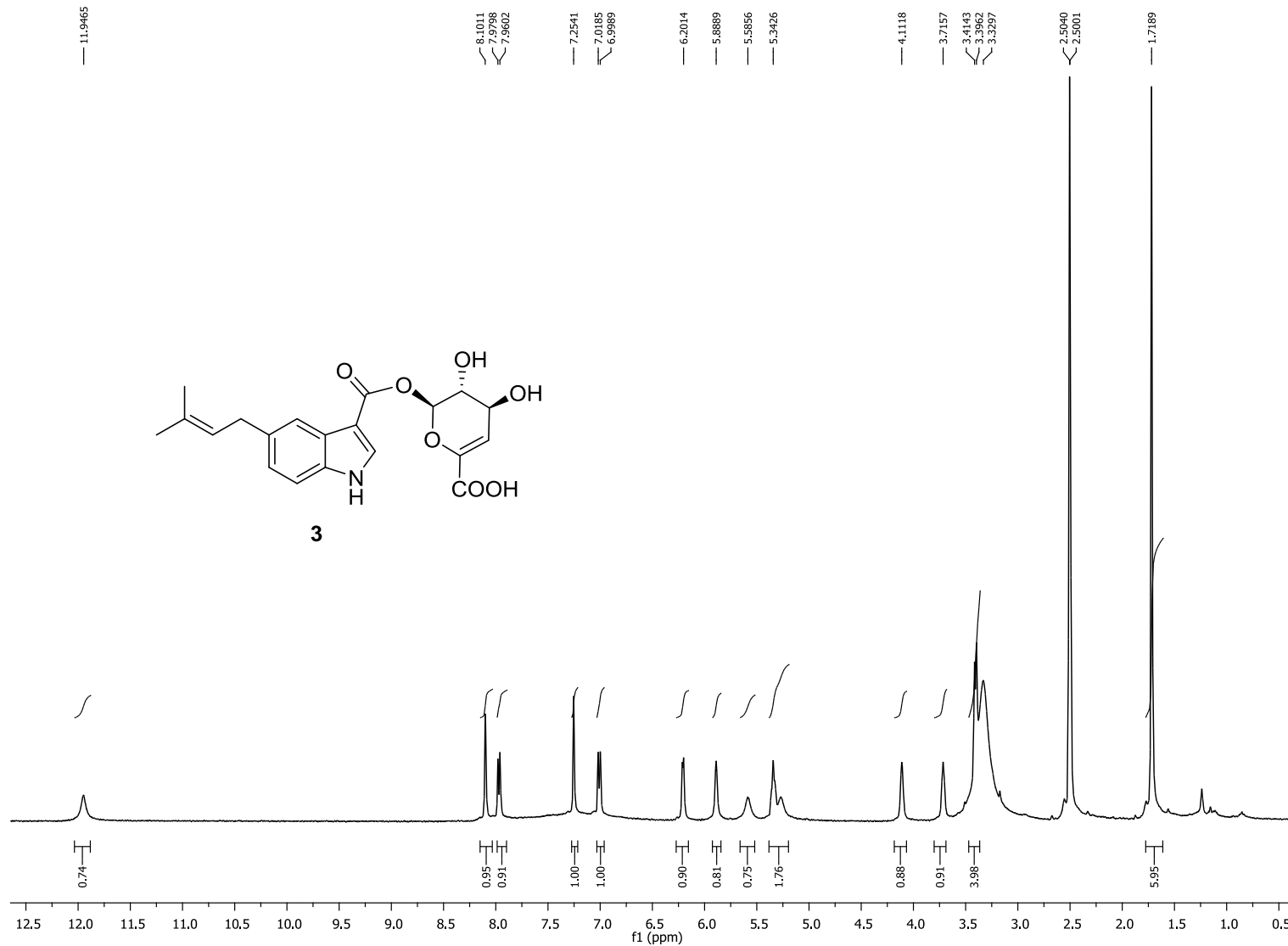


Figure S18. ^1H NMR spectrum (DMSO- d_6 , 400 MHz) of 10-O-(4''-deoxy- α -L-threo-hex-4''-enopyranosid)-uronic acid-5-isoprenylindole-3-carboxylate (**3**).

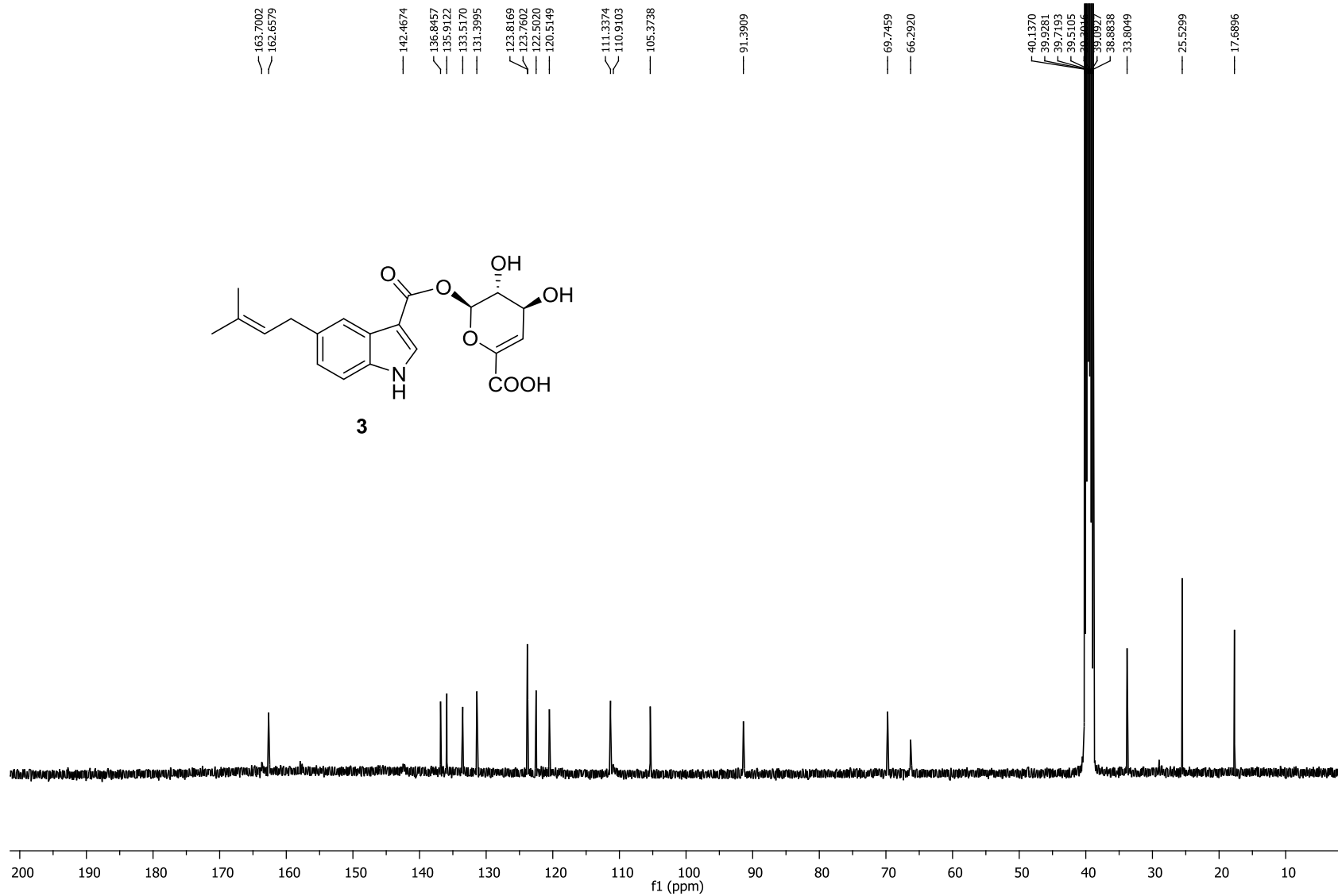


Figure S19. ^{13}C NMR spectrum (DMSO- d_6 , 100 MHz) of 10-O-(4''-deoxy- α -L-threo-hex-4''-enopyranosid)-uronic acid-5-isoprenylindole-3-carboxylate (**3**).

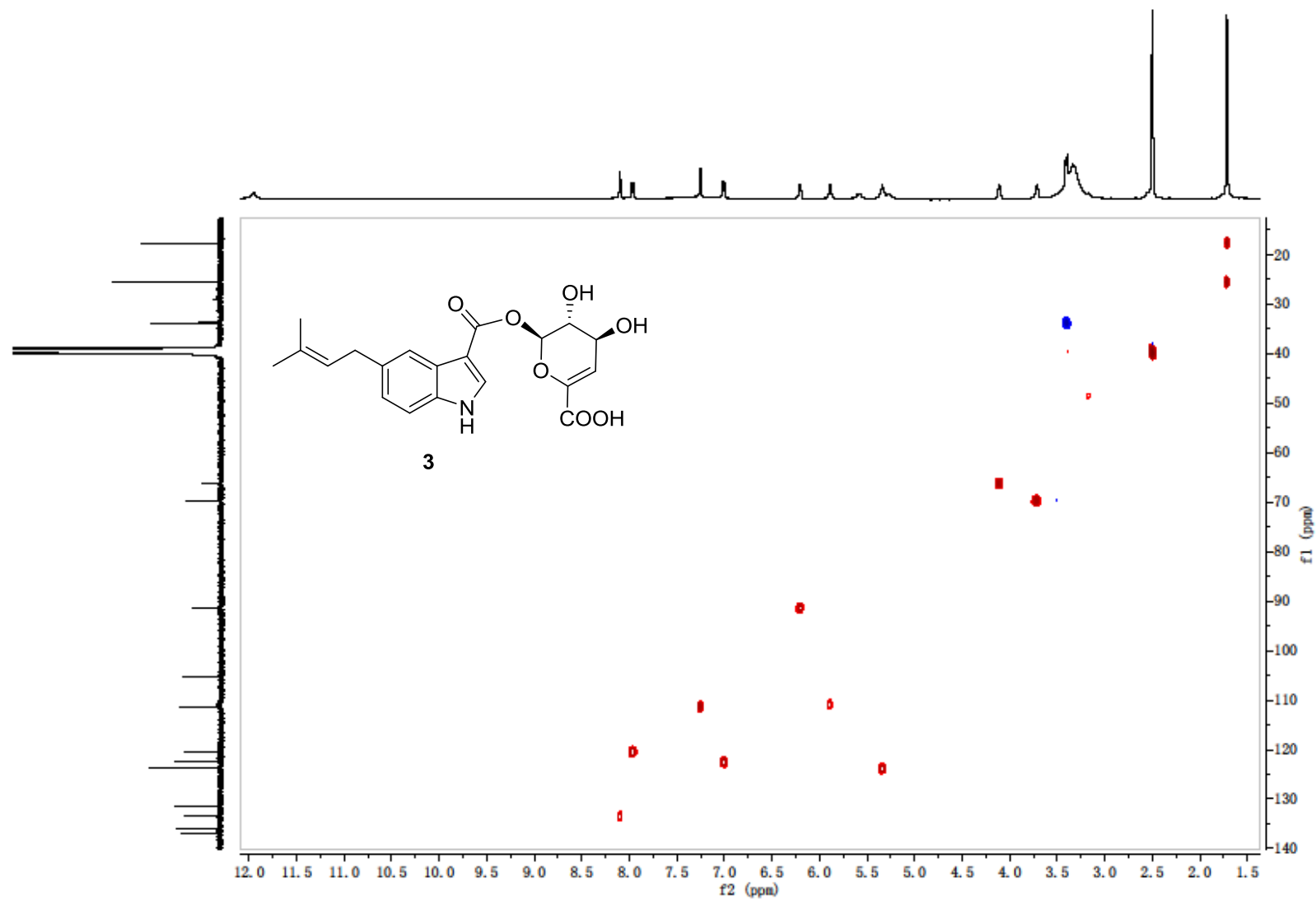


Figure S20. HSQC spectrum (DMSO-*d*₆, 400 MHz) of 10-*O*-(4''-deoxy- α -L-*threo*-hex-4''-enopyranosid)-uronic acid-5-isoprenylindole-3-carboxylate (**3**).

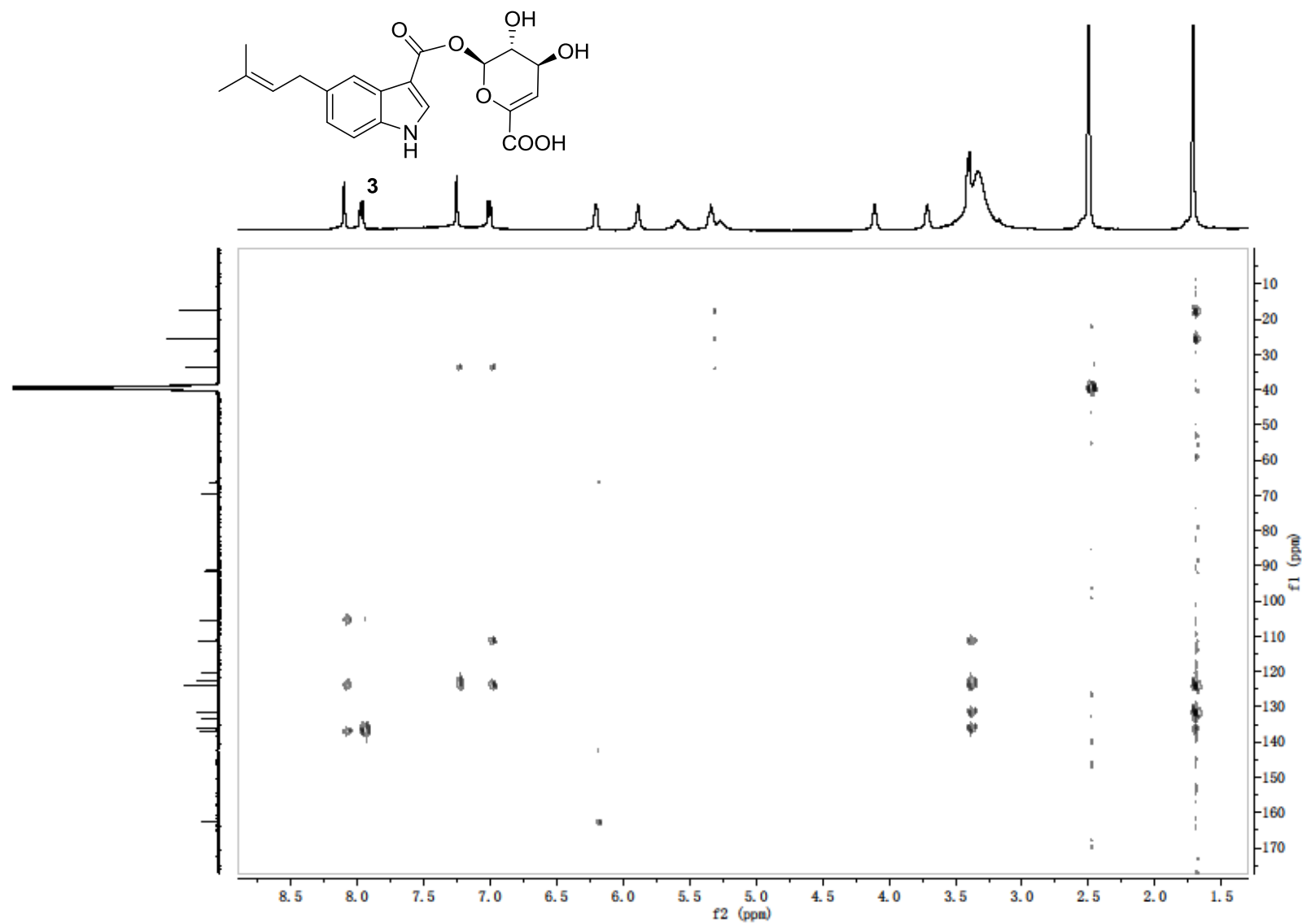


Figure S21. HMBC spectrum (DMSO- d_6 , 400 MHz) of 10-O-(4''-deoxy- α -L-threo-hex-4''-enopyranosid)-uronic acid-5-isoprenylindole-3-carboxylate (**3**).

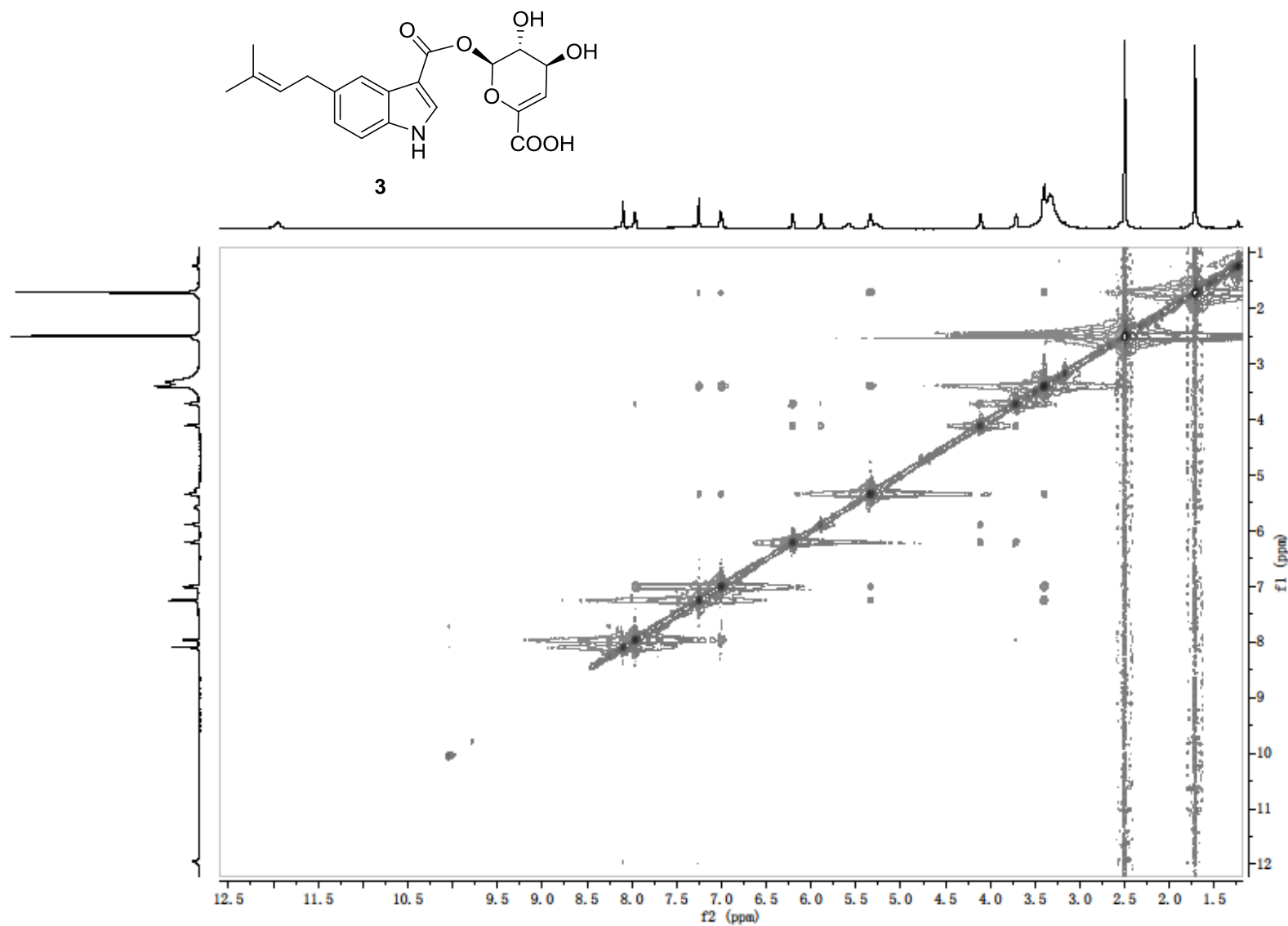


Figure S22. ROESY spectrum (DMSO- d_6 , 400 MHz) of 10-*O*-(4''-deoxy- α -L-*threo*-hex-4''-enopyranosid)-uronic acid-5-isoprenylindole-3-carboxylate (**3**).

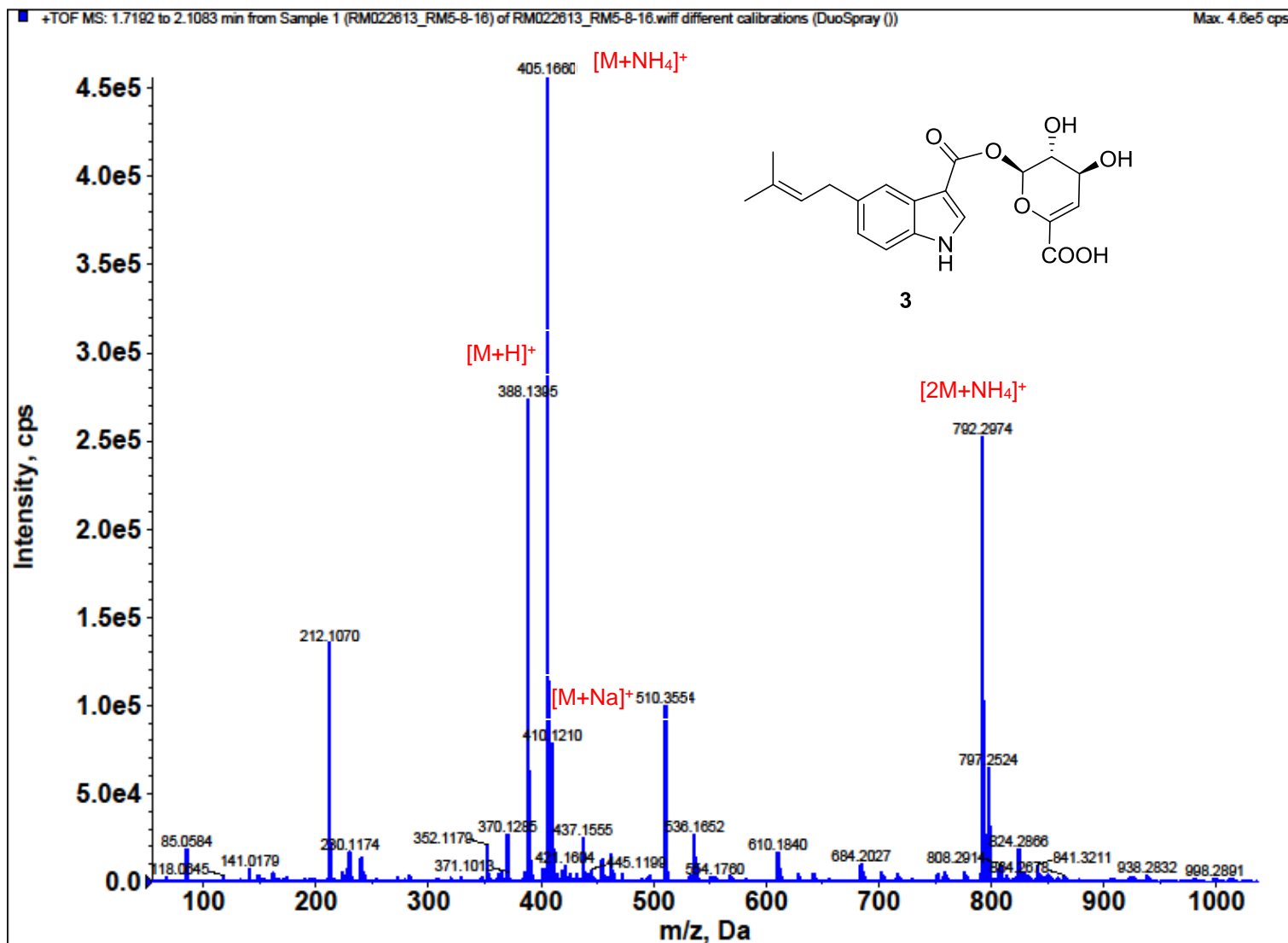


Figure S23. (+)-HRESI-MS of 10-O-(4''-deoxy- α -L-threo-hex-4''-enopyranosid)-uronic acid-5-isoprenylindole-3-carboxylate (**3**).

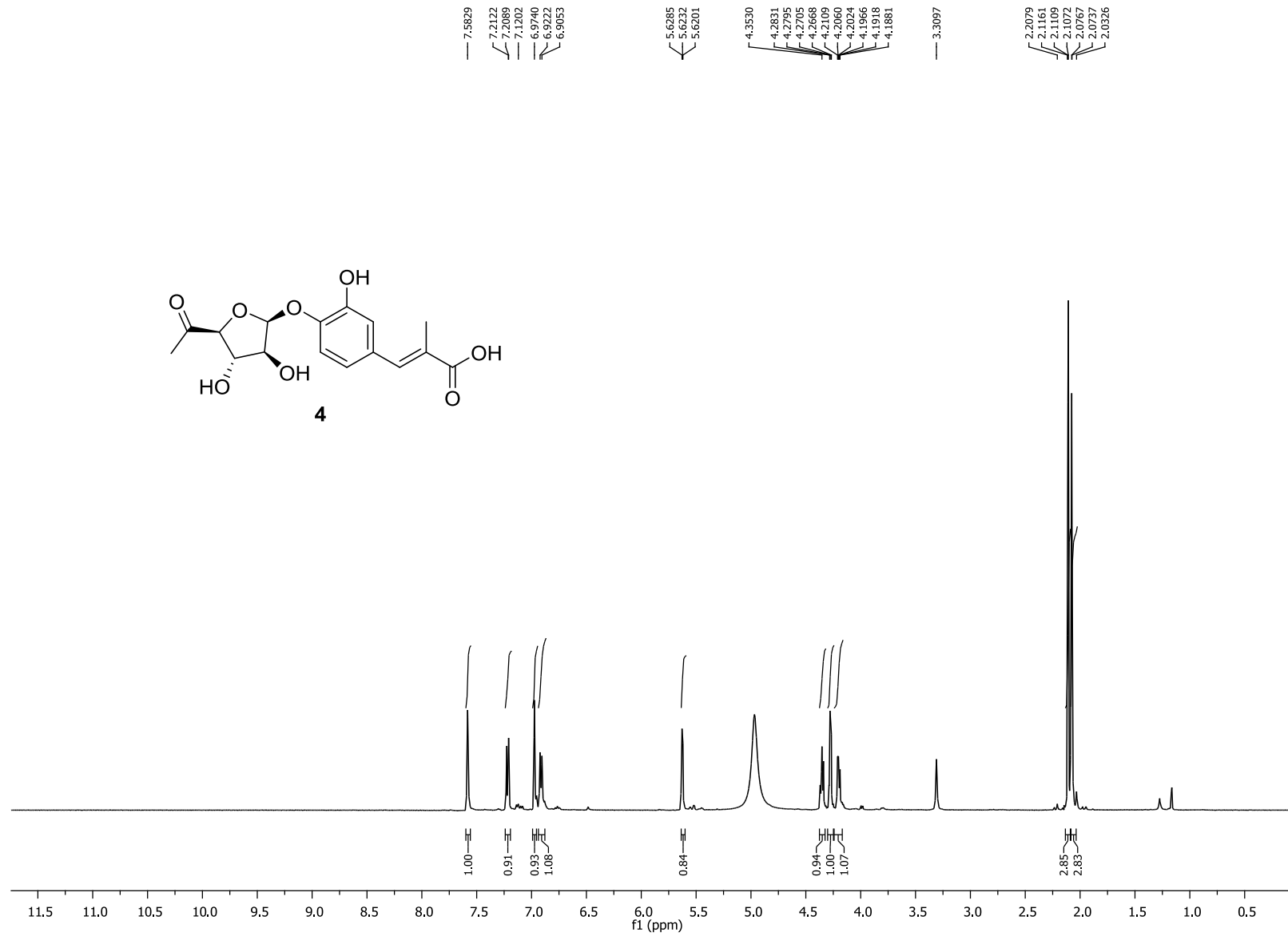
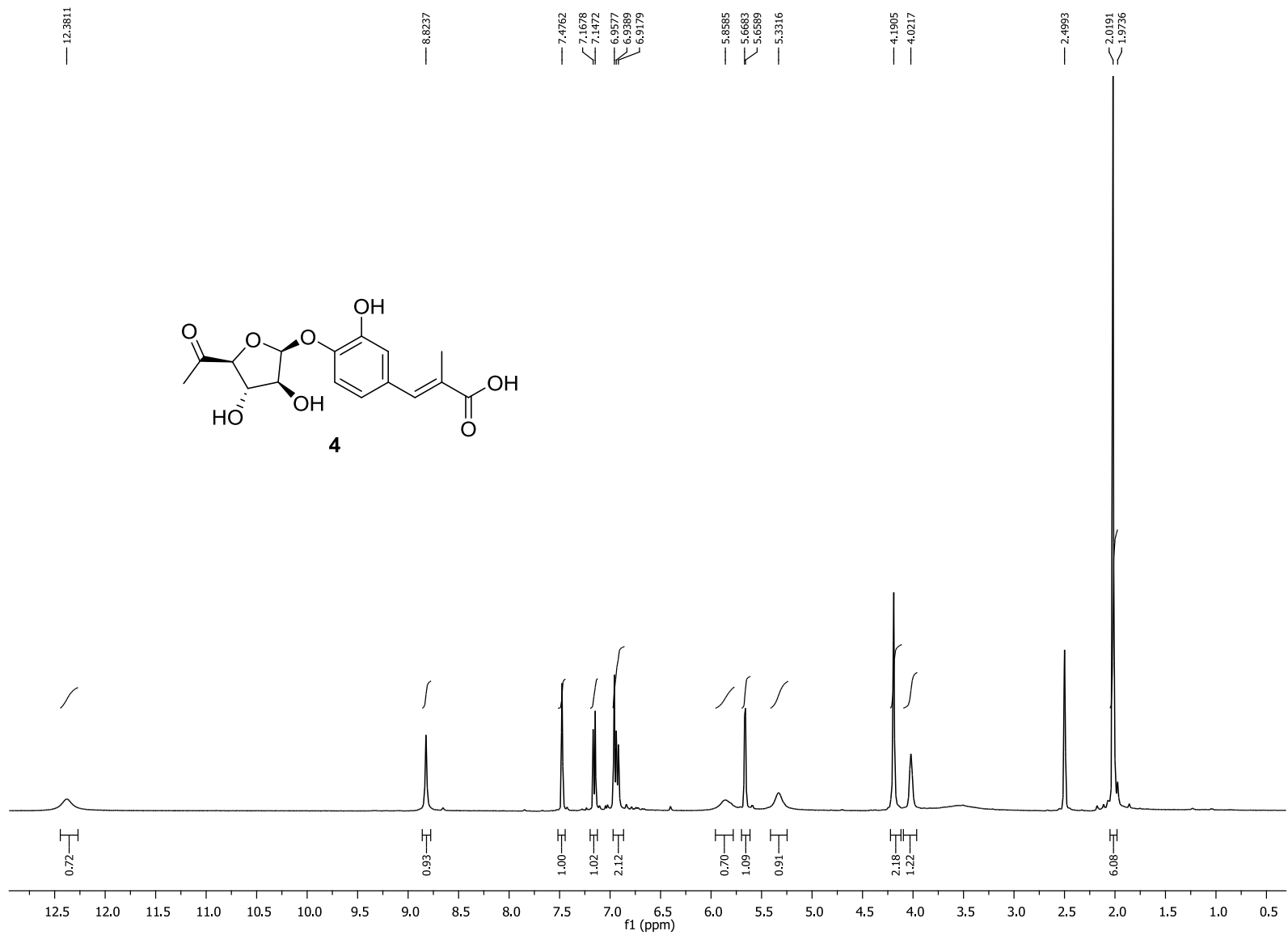


Figure S24. ¹H NMR spectrum (CD₃OD, 500 MHz) of prehygromycin (4).



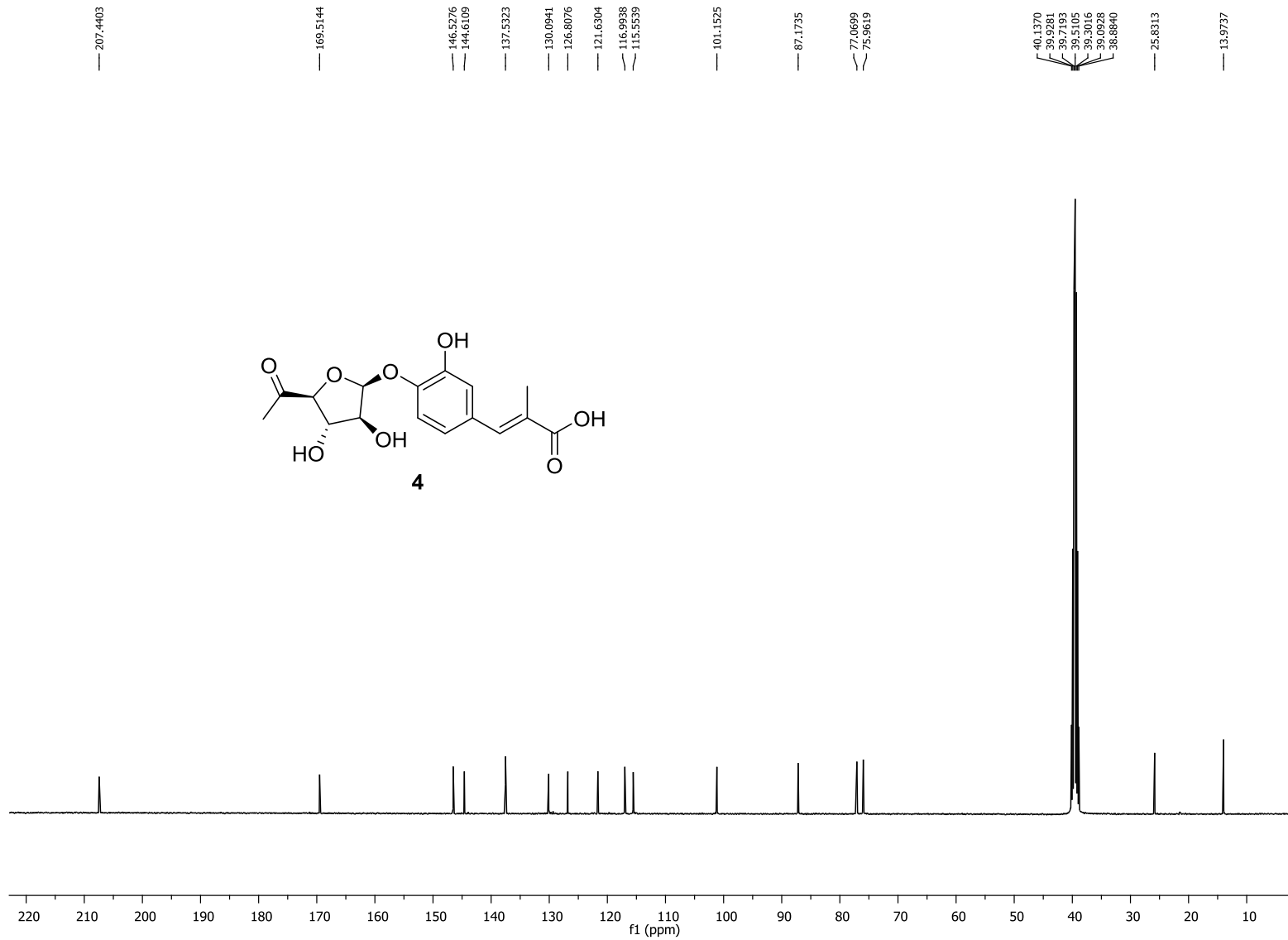


Figure S26. ¹³C NMR spectrum (DMSO-*d*₆, 100 MHz) of prehygromycin (**4**).

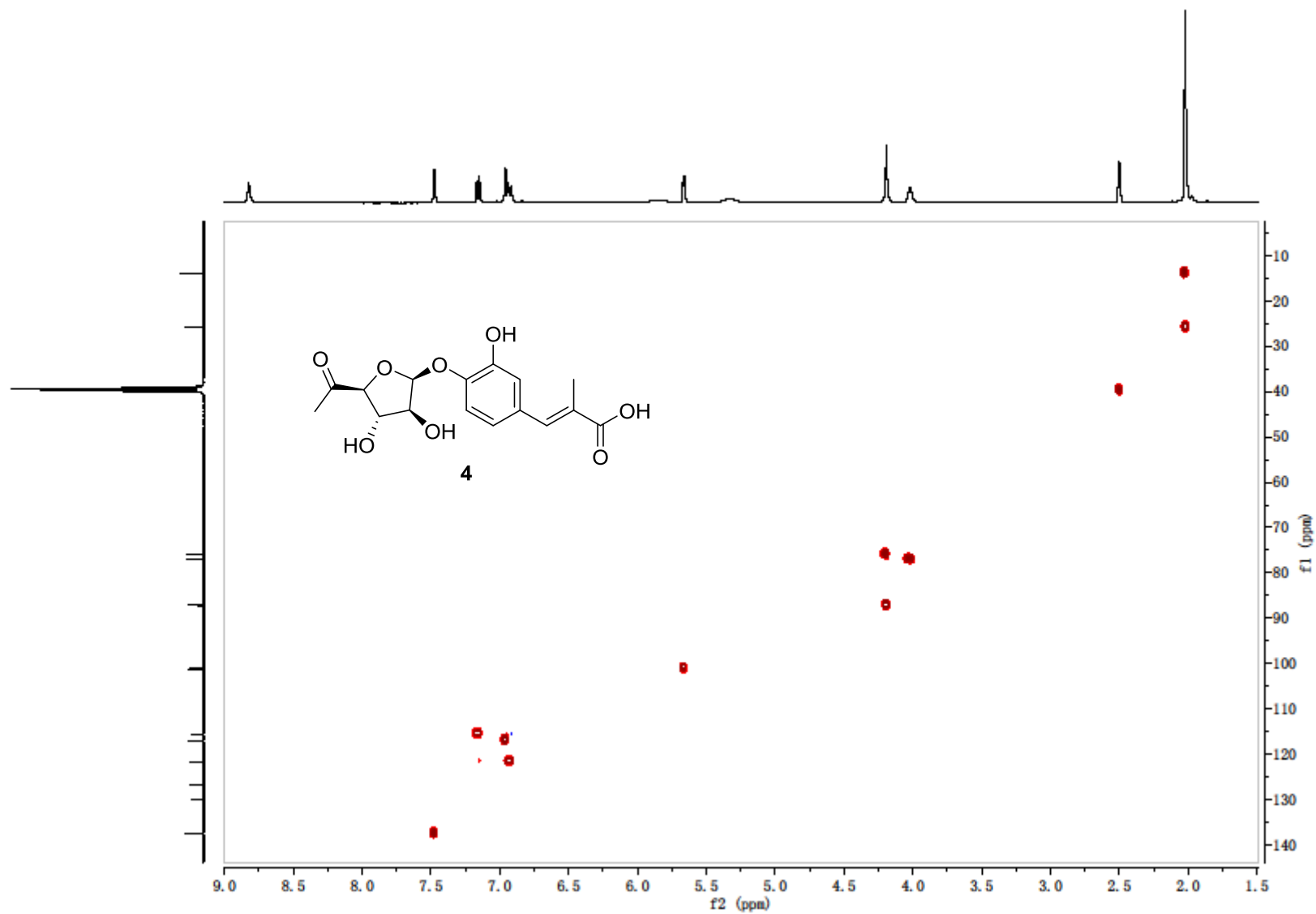


Figure S27. HSQC spectrum (DMSO-*d*₆, 400 MHz) of prehygromycin (**4**).

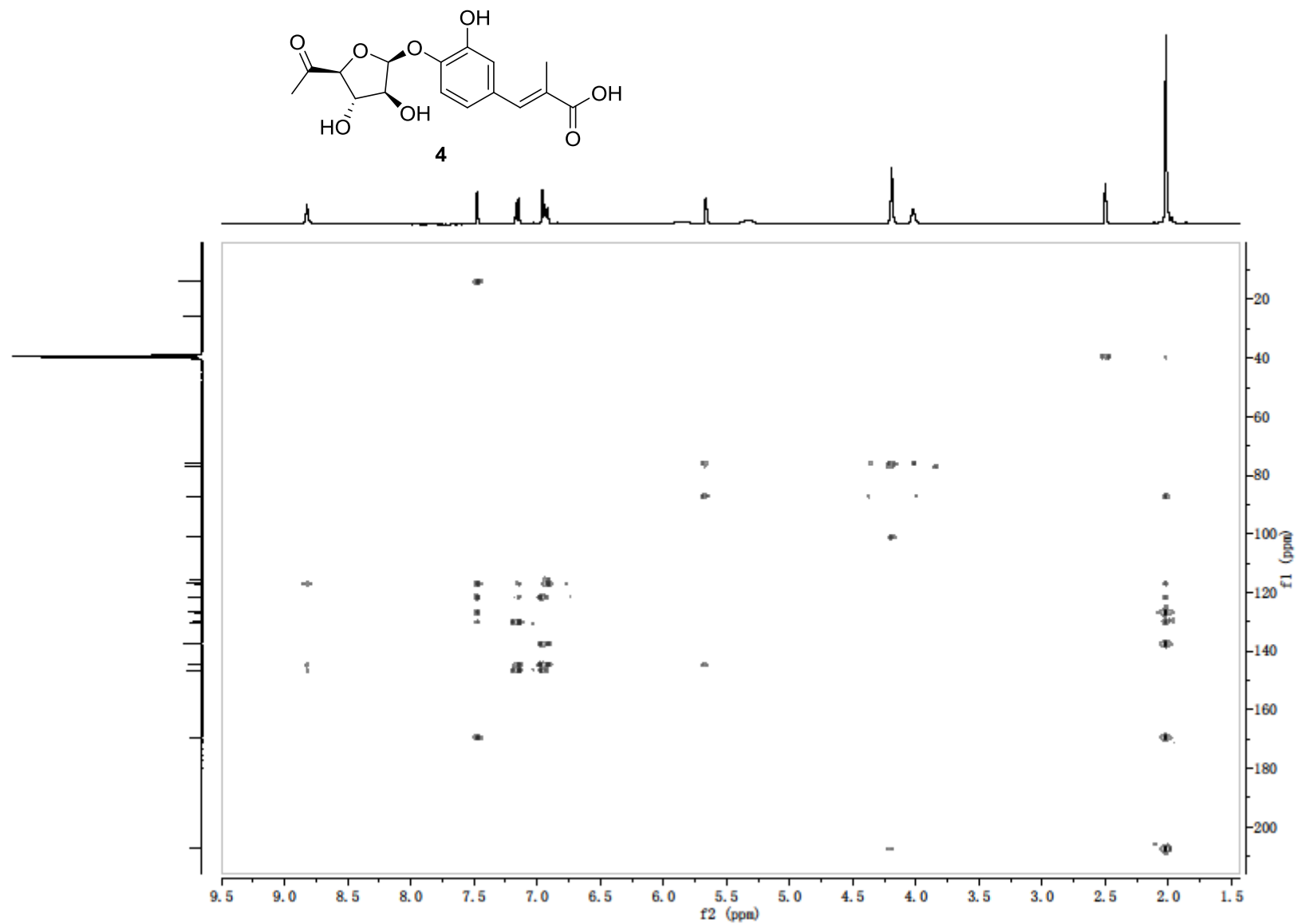
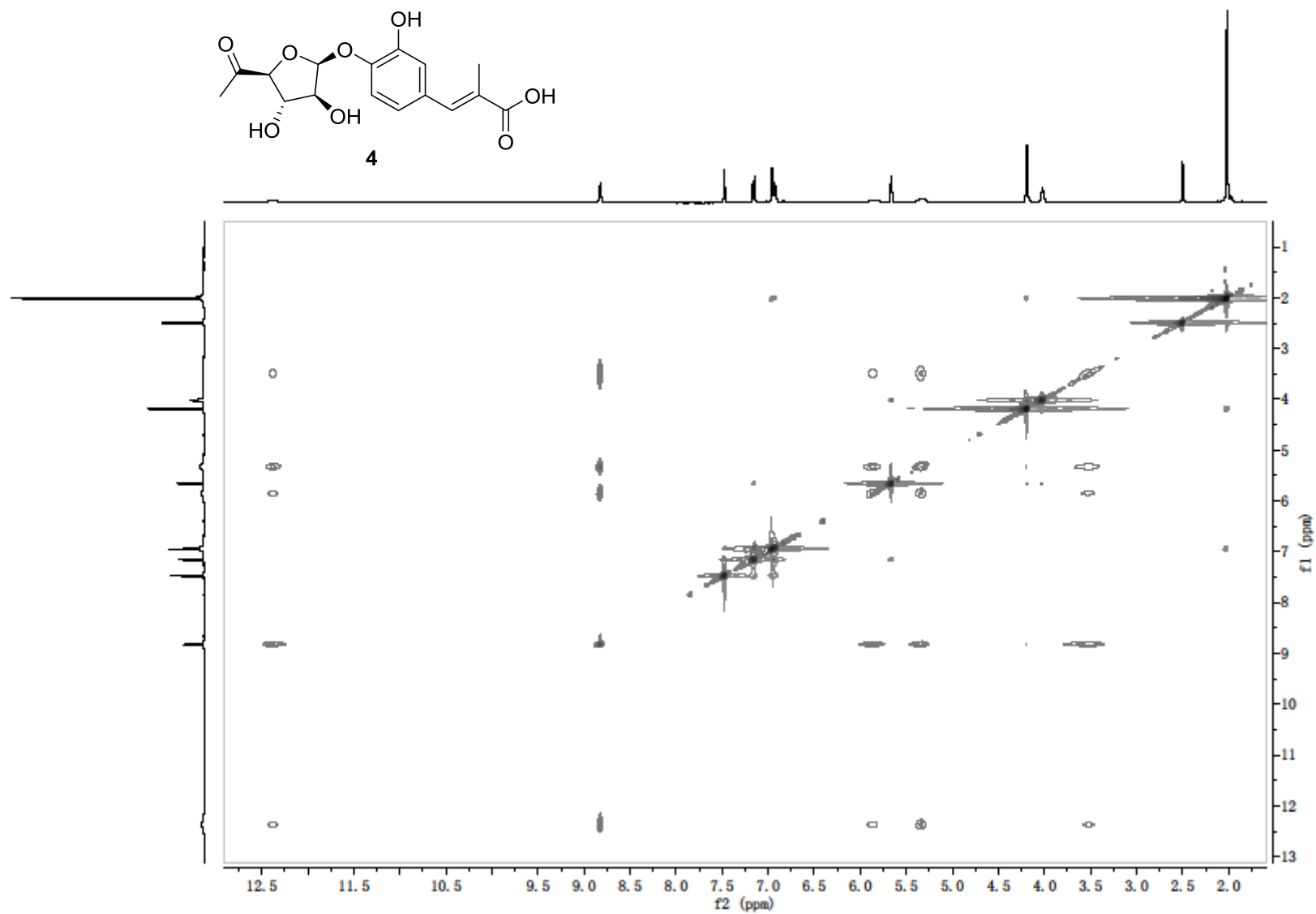


Figure S28. HMBC spectrum (DMSO- d_6 , 400 MHz) of prehygromycin (4).



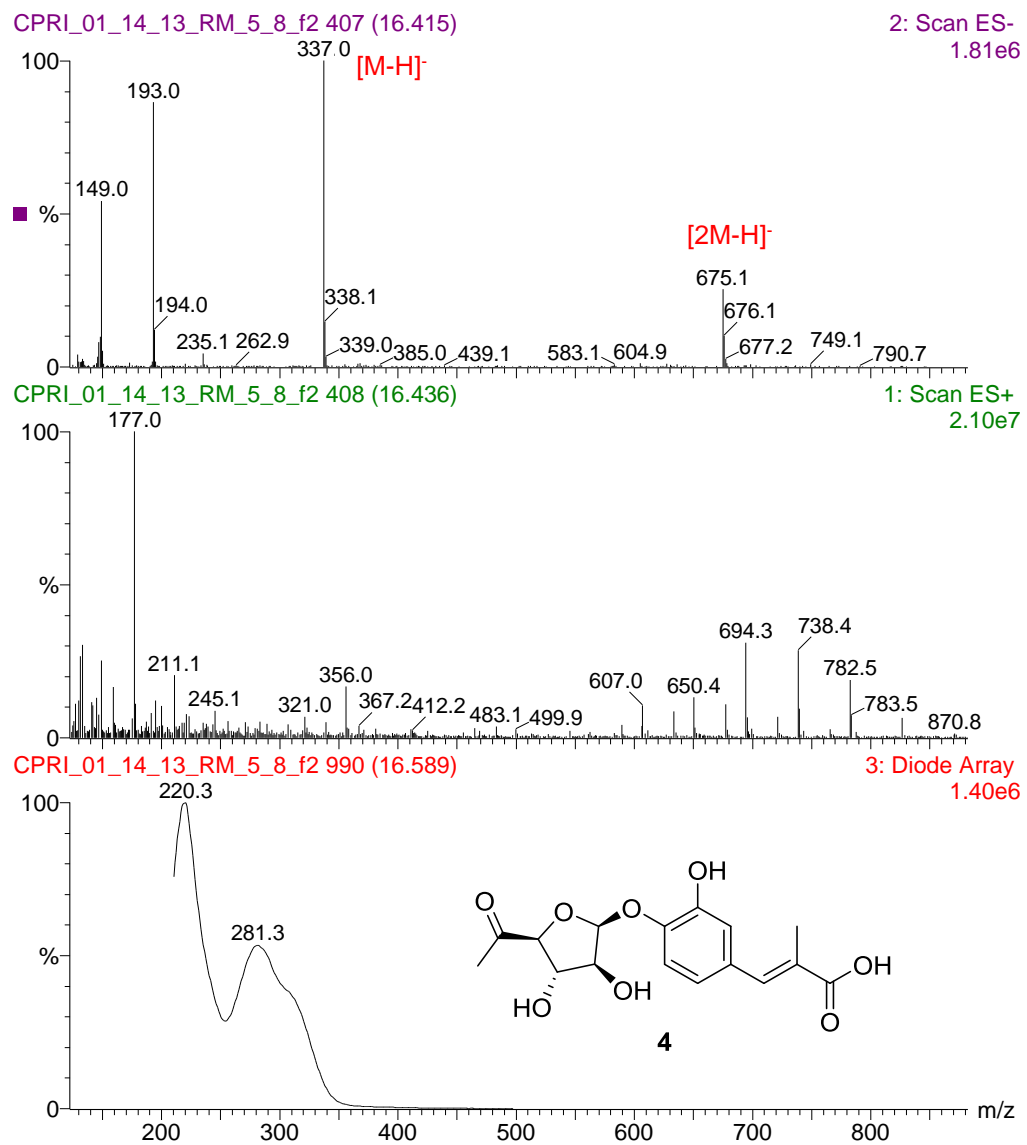


Figure S30. APCI-MS/UV of prehygromycin (**4**).

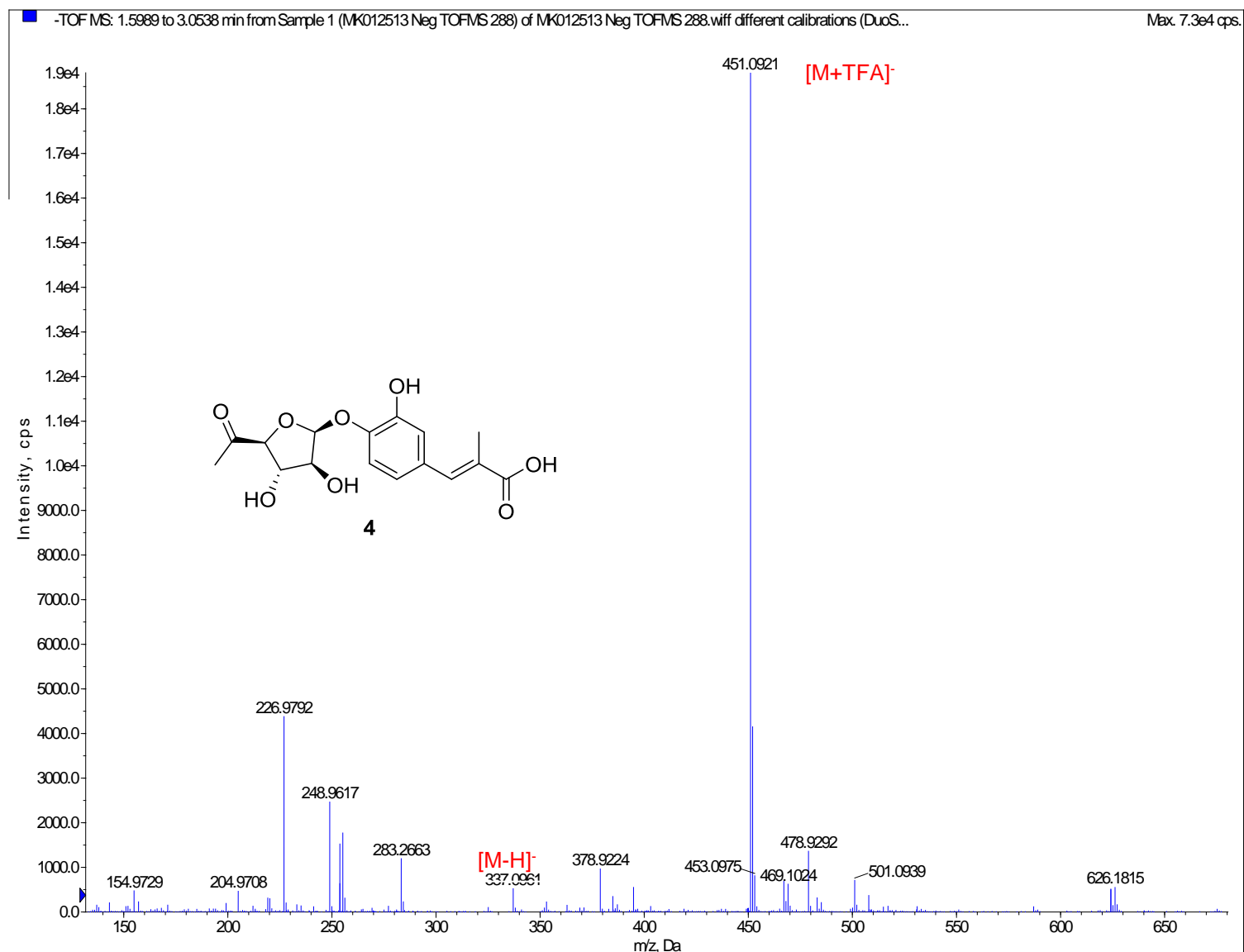


Figure S31. (-)-HRESI-MS (negative mode) of prehygromycin (**4**).

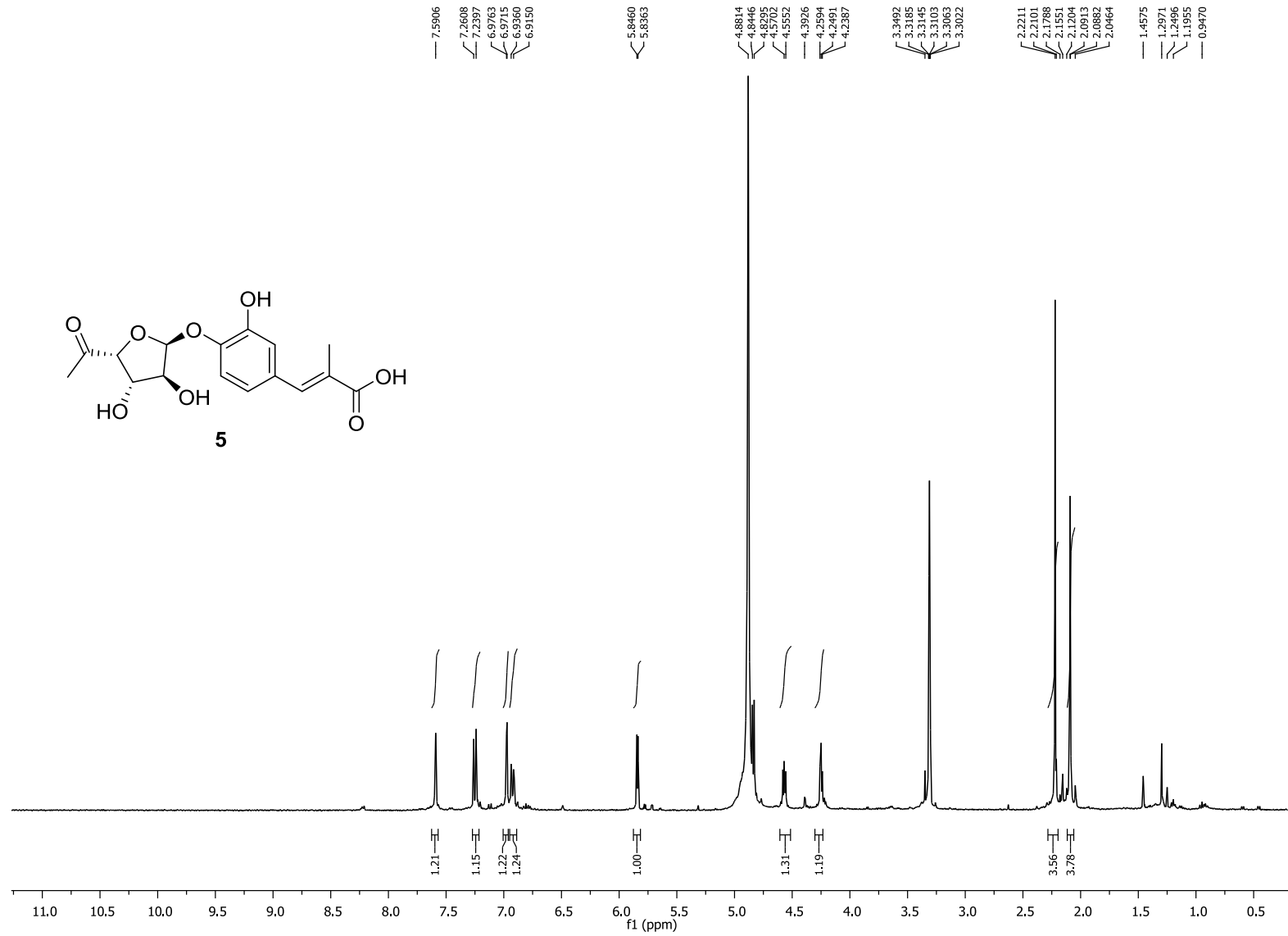


Figure S32. ¹H NMR spectrum (CD₃OD, 400 MHz) of 4'-epi-prehygromycin (5).



Figure S33. ¹³C NMR spectrum (CD₃OD, 100 MHz) of 4'-epi-prehygromycin (5).

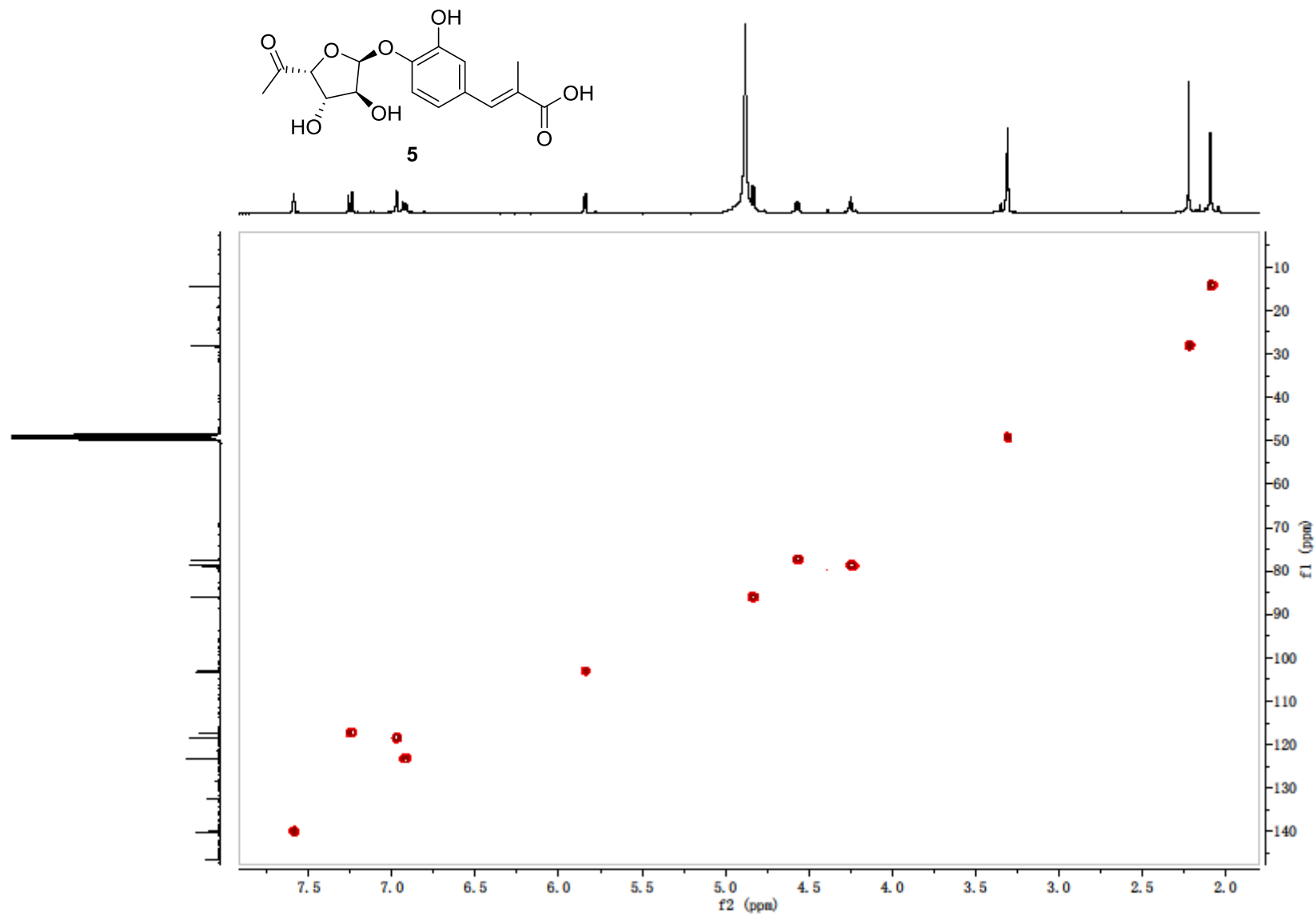


Figure S34. HSQC spectrum (CD₃OD, 400 MHz) of 4'-*epi*-prehygromycin (5).

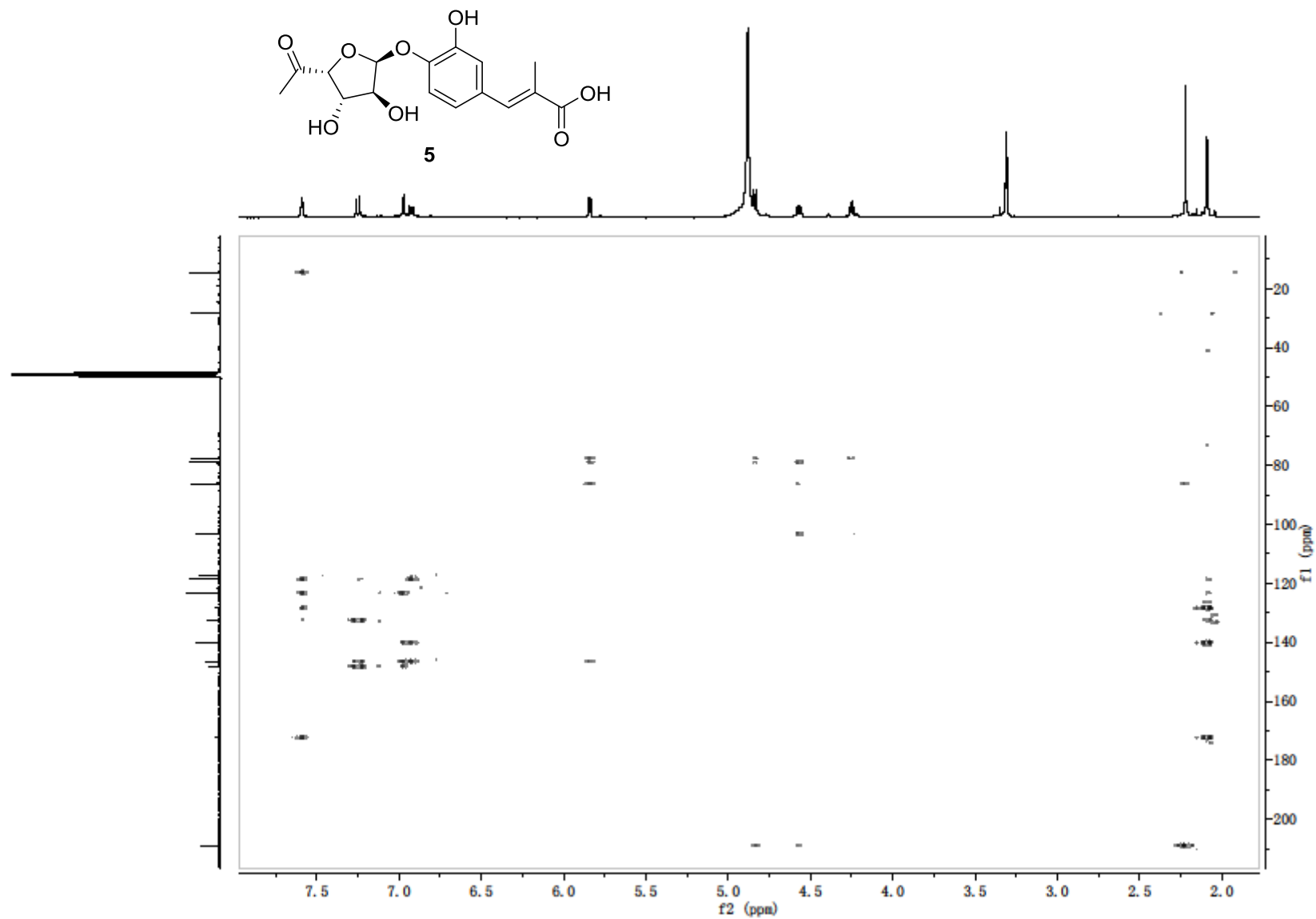


Figure S35. HMBC spectrum (CD₃OD, 400 MHz) of 4'-epi-prehygromycin (5).

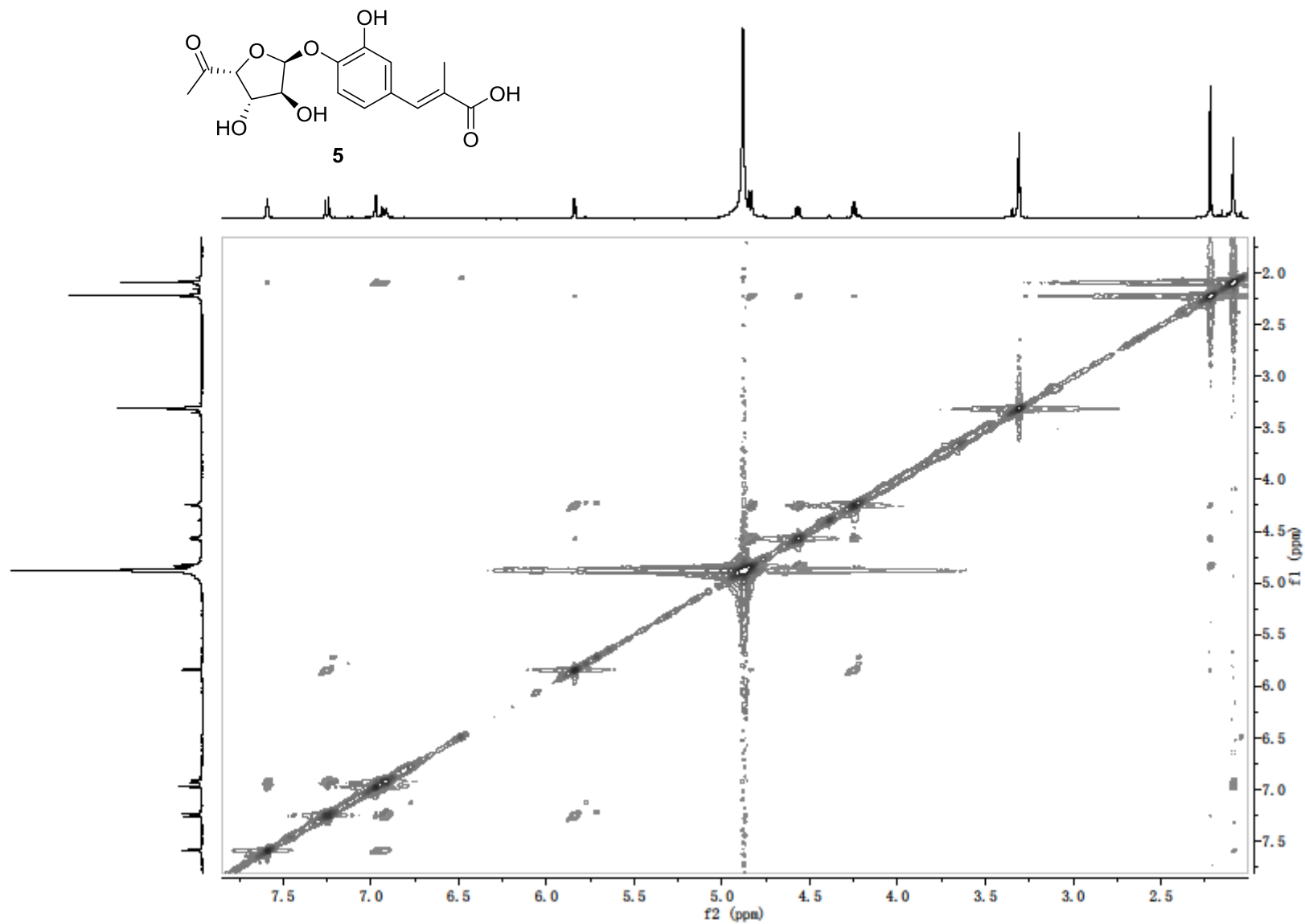


Figure S36. ROESY spectrum (CD₃OD, 400 MHz) of 4'-*epi*-prehygromycin (5).

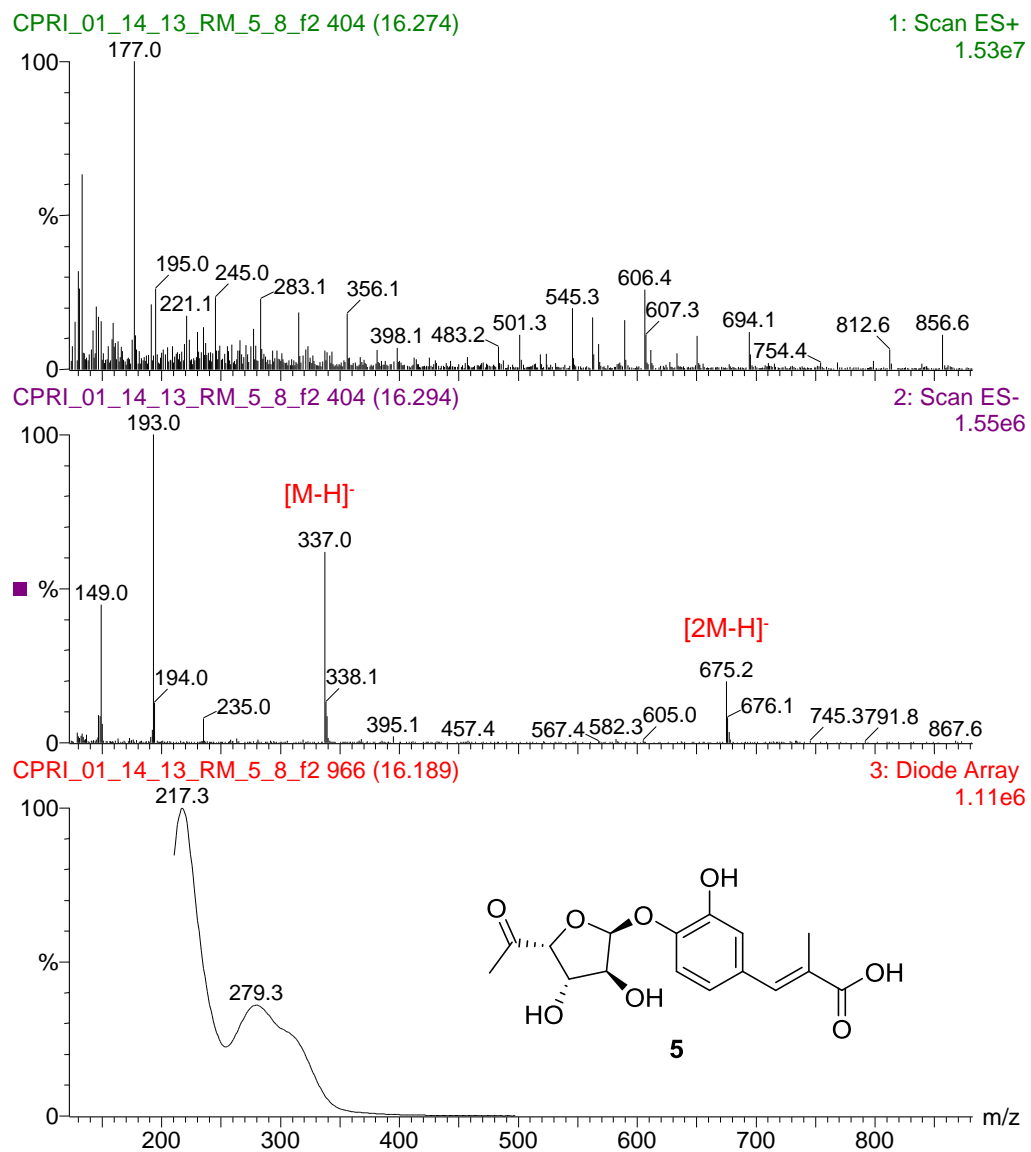


Figure S37. APCI-MS/UV of 4'-*epi*-prehygromycin (5).

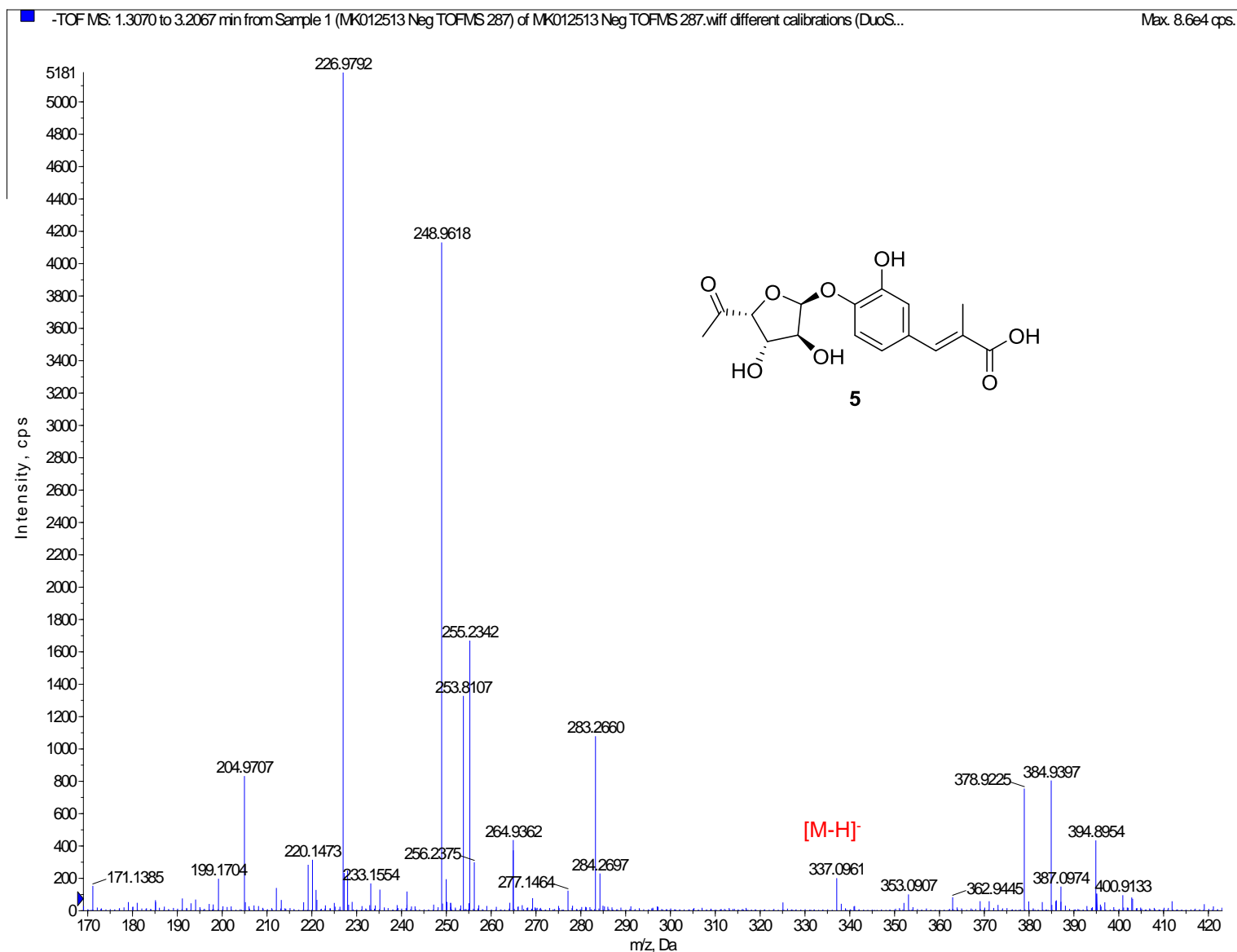


Figure S38. (-)-HRESI-MS of 4'-epi-prehygromycin (5).

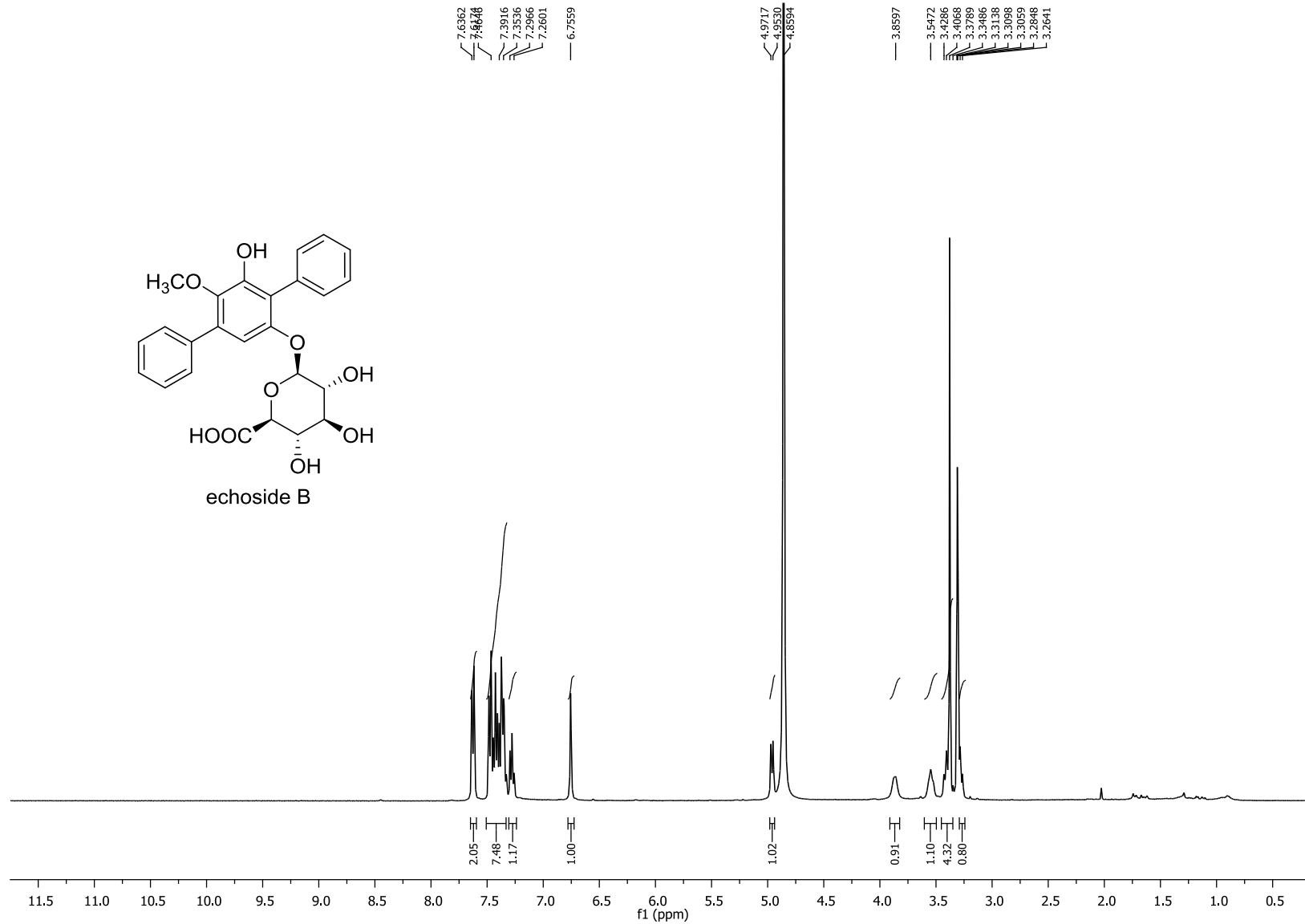


Figure S39. ¹H NMR spectrum (CD₃OD, 400 MHz) of echoside B.

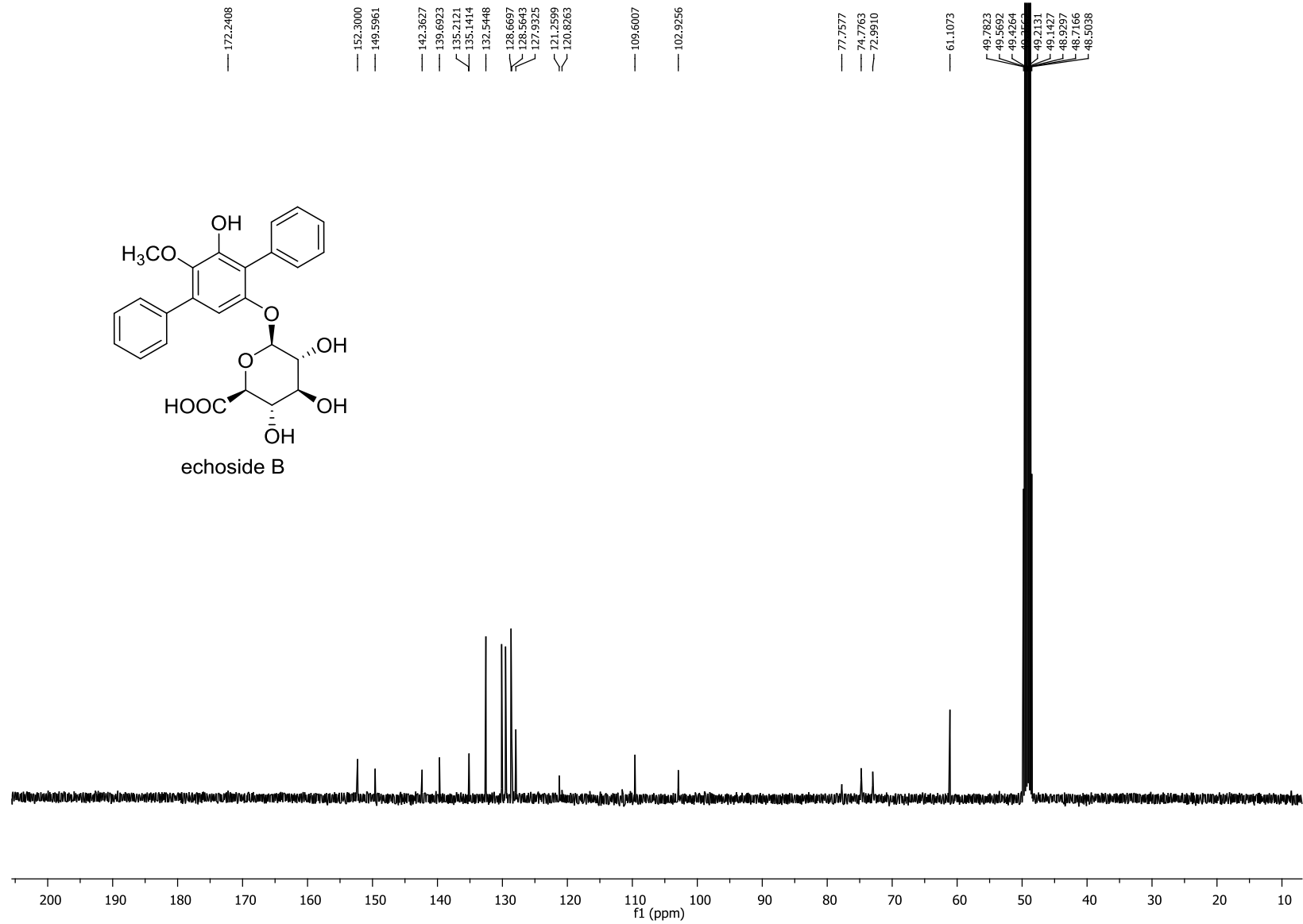


Figure S40. ¹³C NMR spectrum (CD₃OD, 100 MHz) of echoside B.

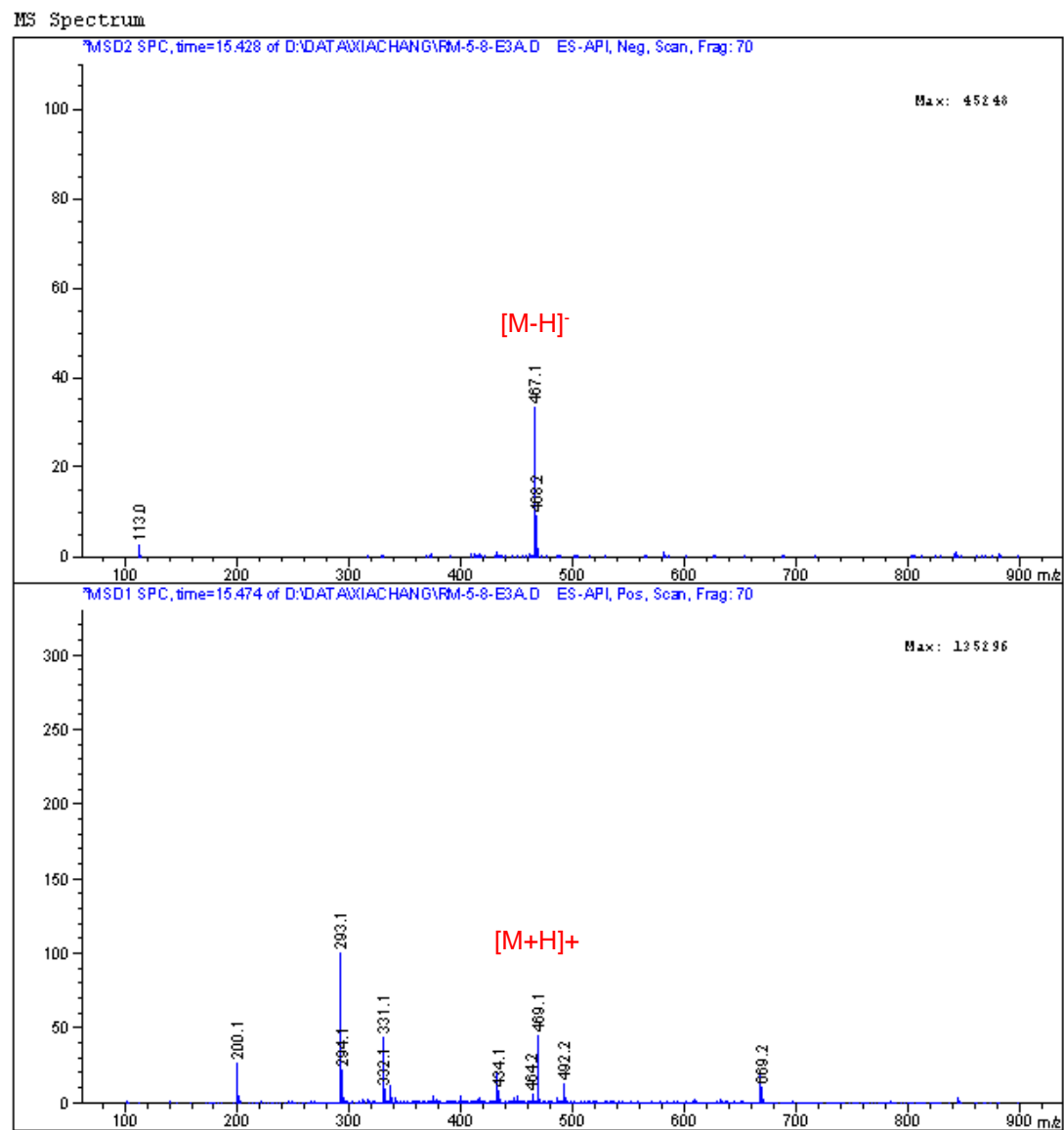


Figure S41. ESI-MS of echoside B

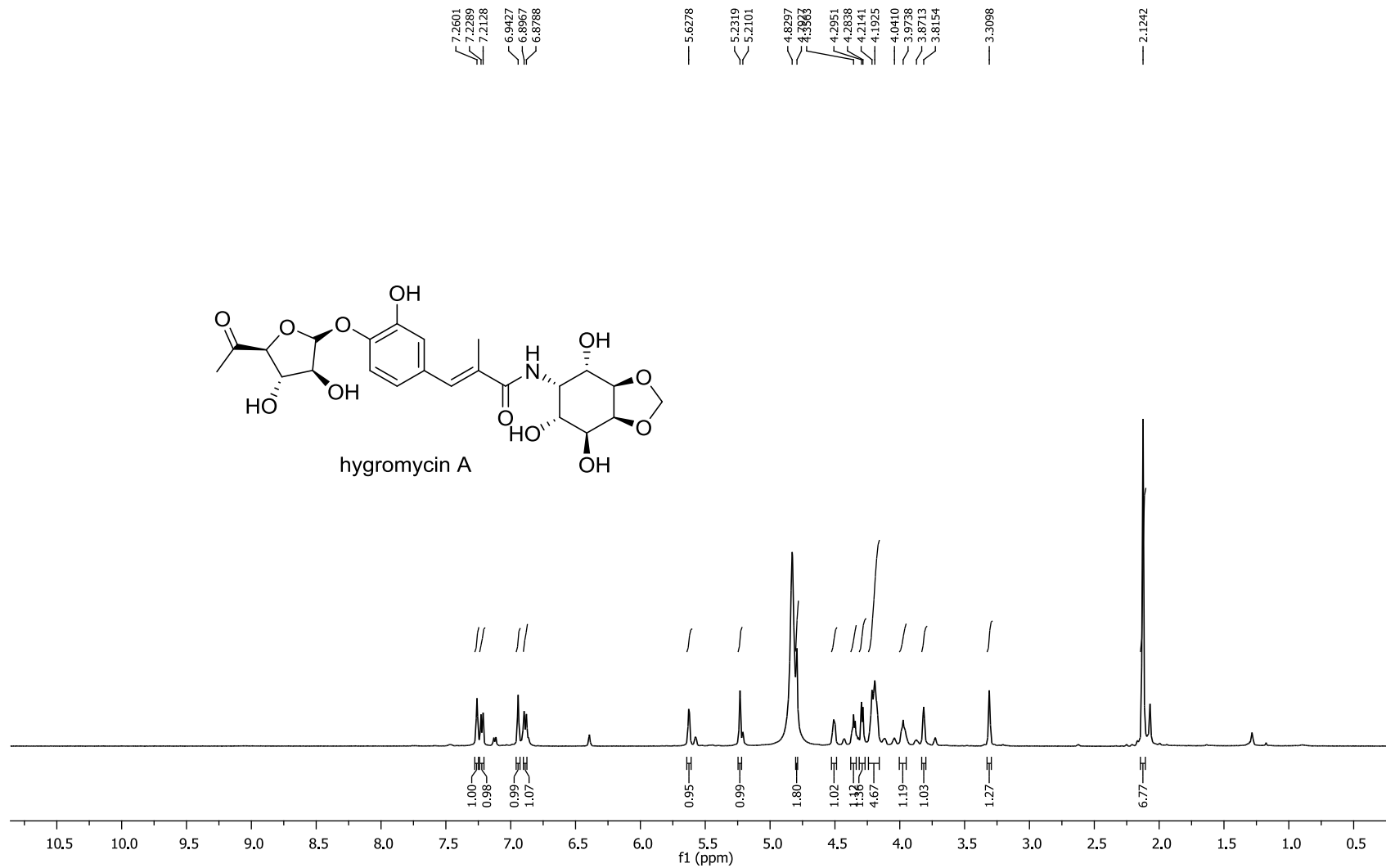


Figure S42. ¹H NMR spectrum (CD₃OD, 400 MHz) of hygromycin A.

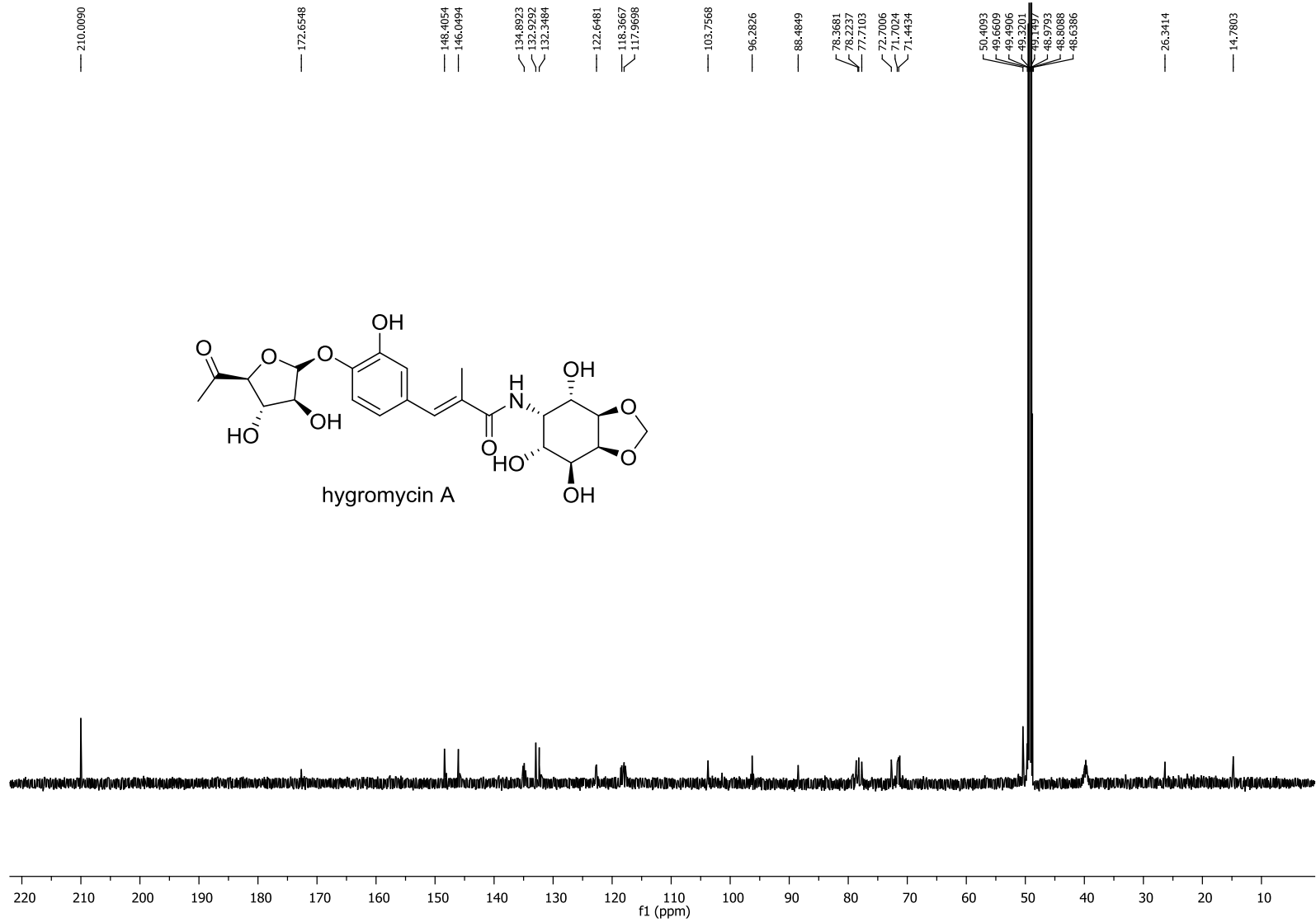


Figure S43. ¹³C NMR spectrum (CD₃OD, 100 MHz) of hygromycin A.

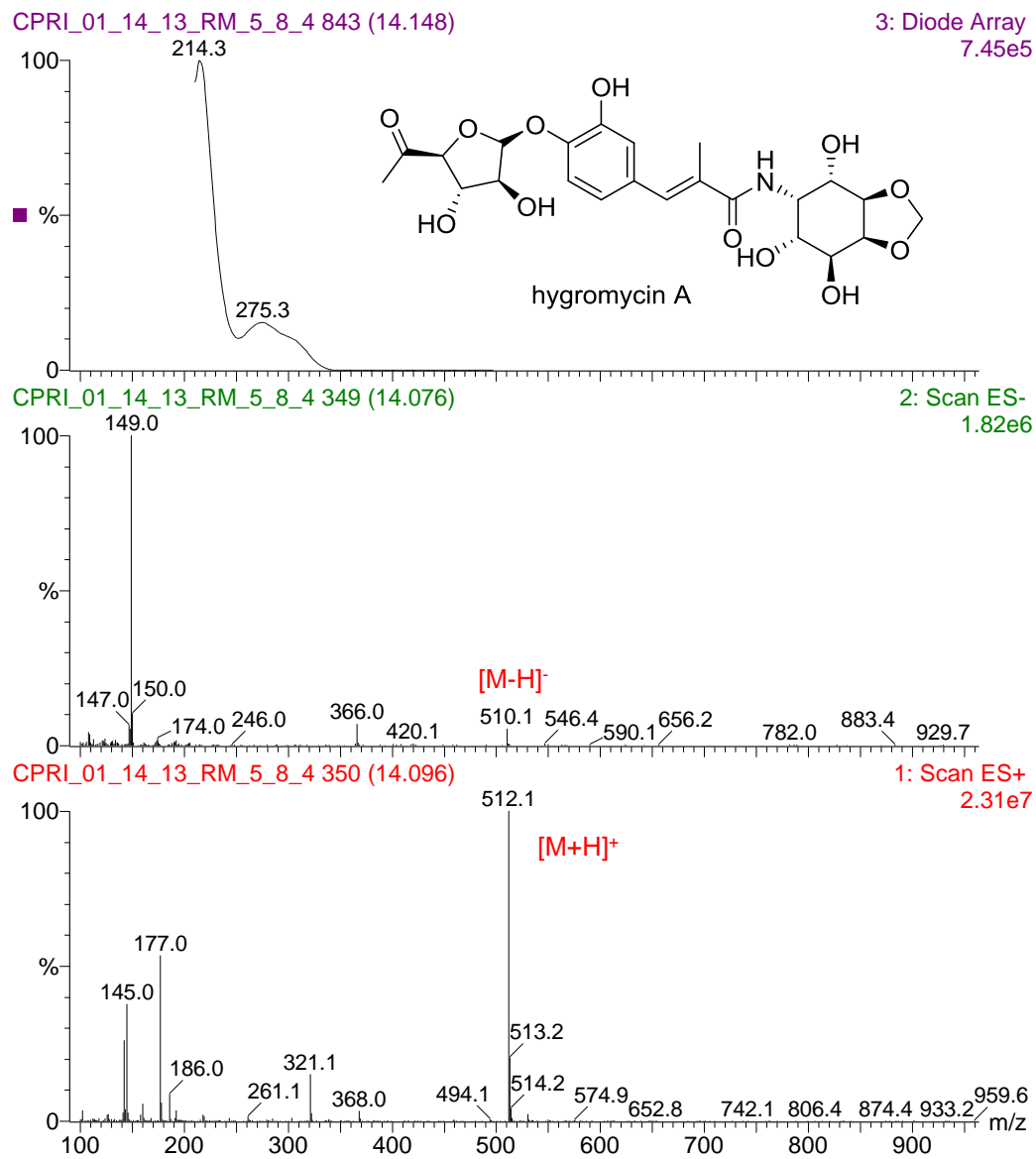


Figure S44. APCI-MS/UV of hygromycin A.

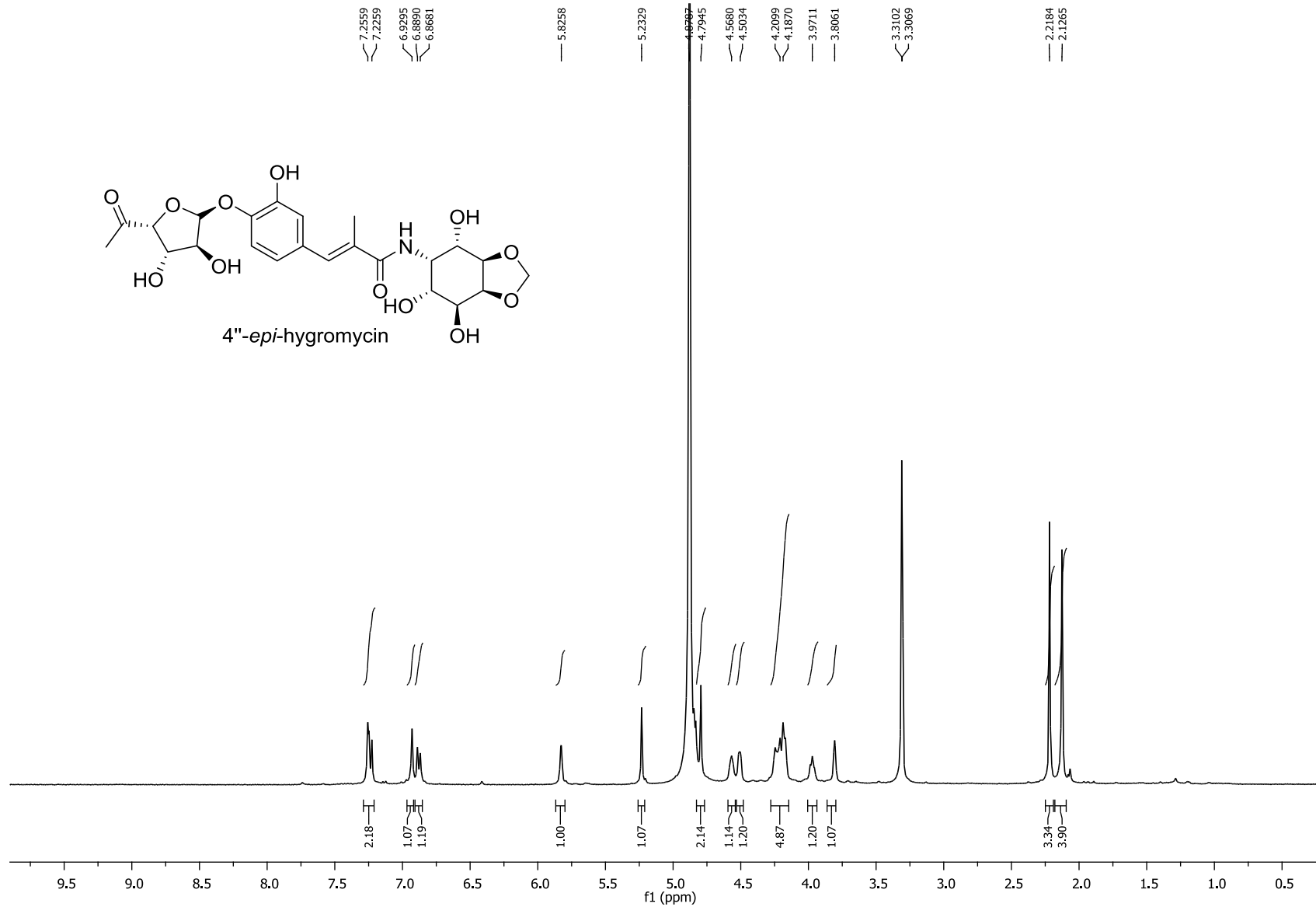


Figure S45. ¹H NMR spectrum (CD₃OD, 400 MHz) of 4''-epi-hygroscopicin.

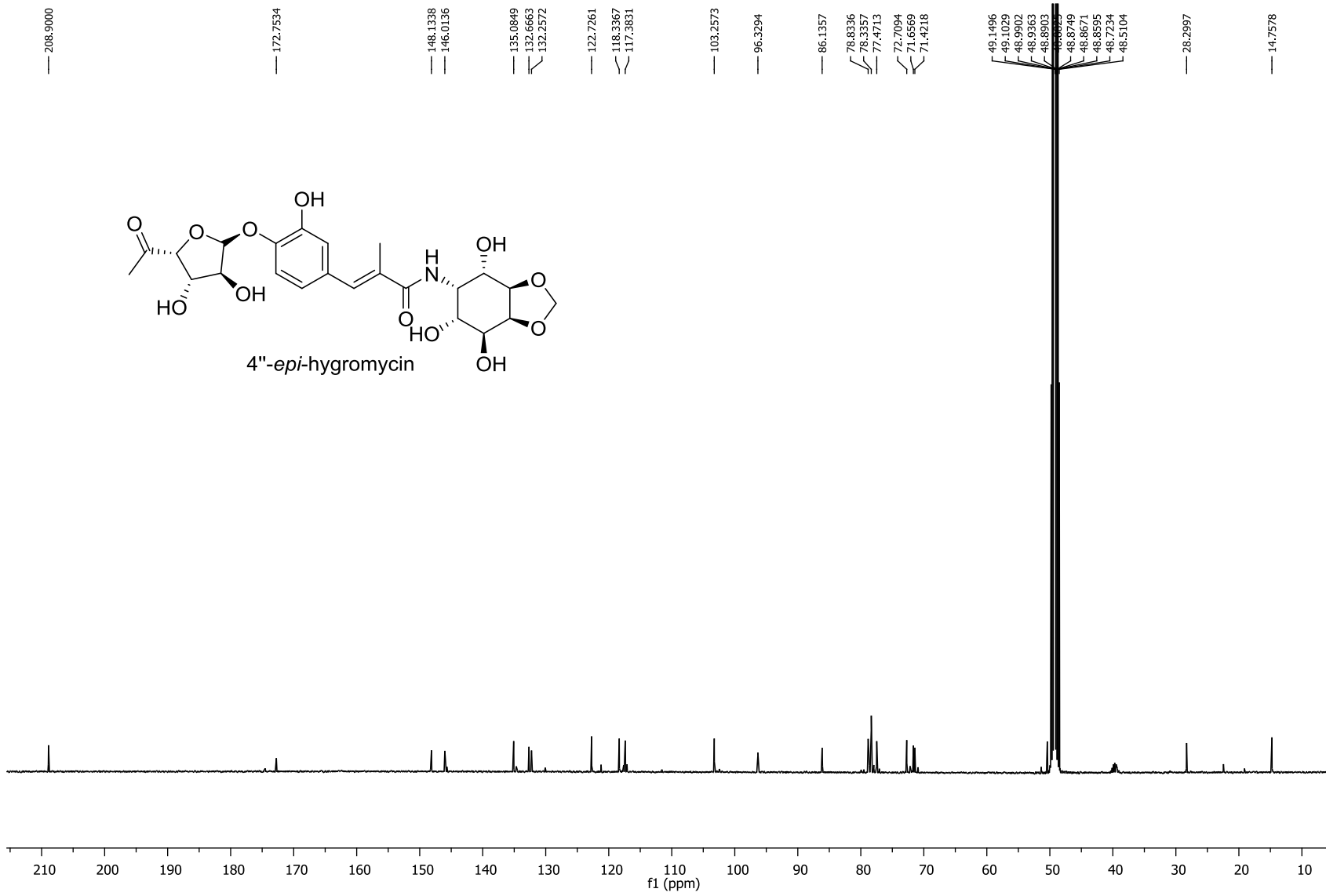


Figure S46. ¹³C NMR spectrum (CD₃OD, 100 MHz) of 4''-epi-hygroscopicin.

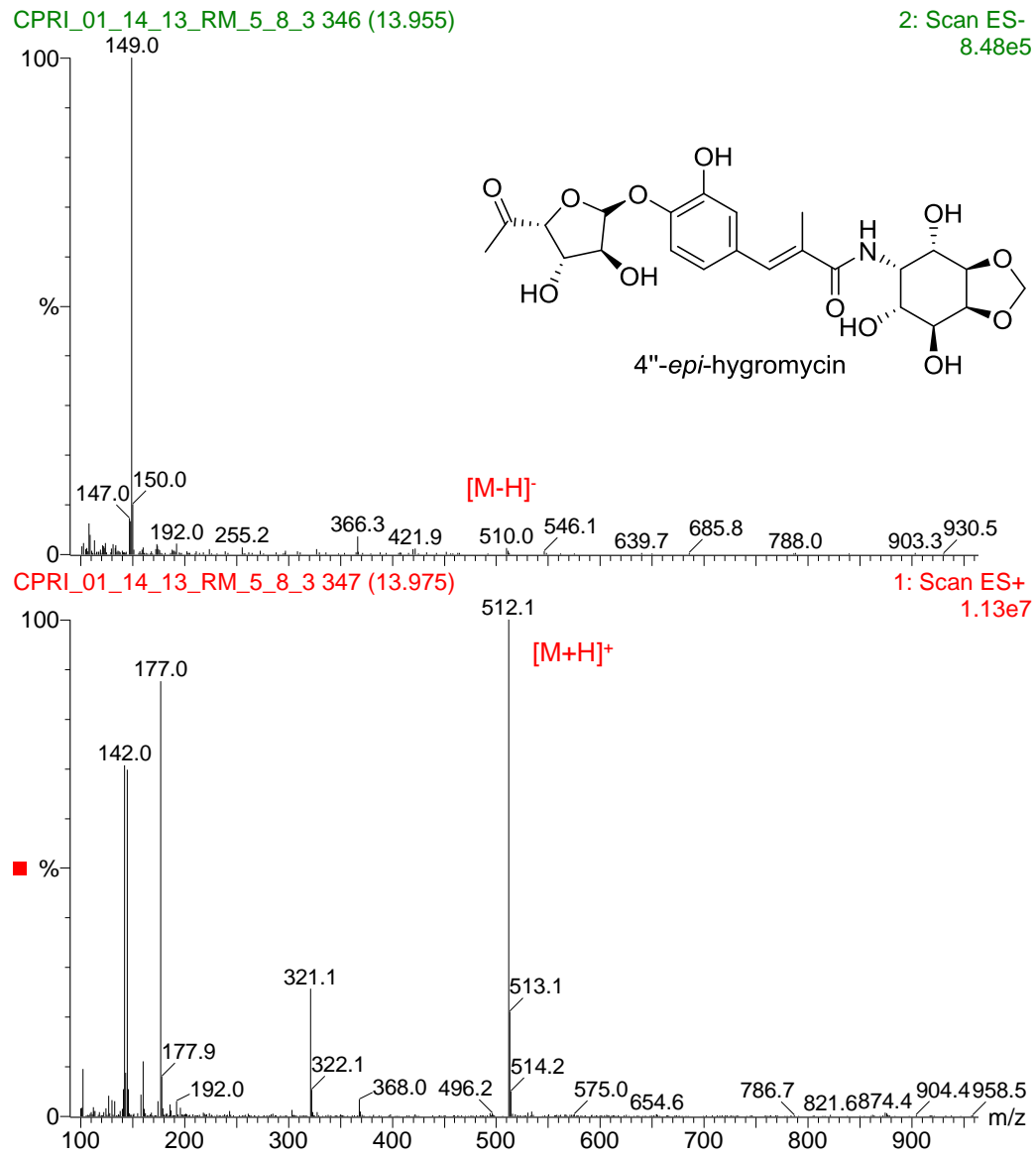


Figure S47. APCI-MS of 4''-*epi*-hygromycin.

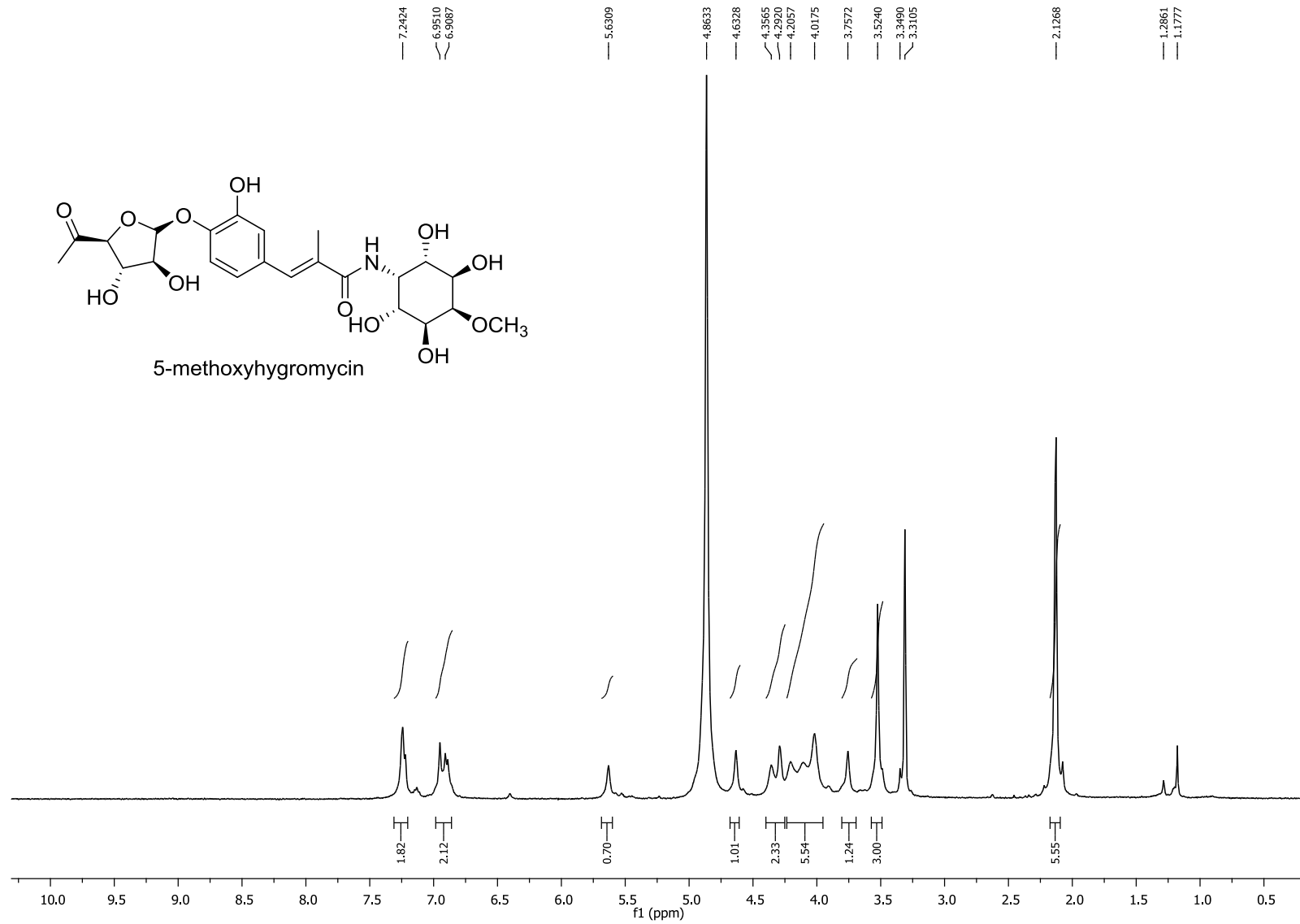


Figure S48. ^1H NMR spectrum (CD_3OD , 400 MHz) of 5-methoxyhygromycin.

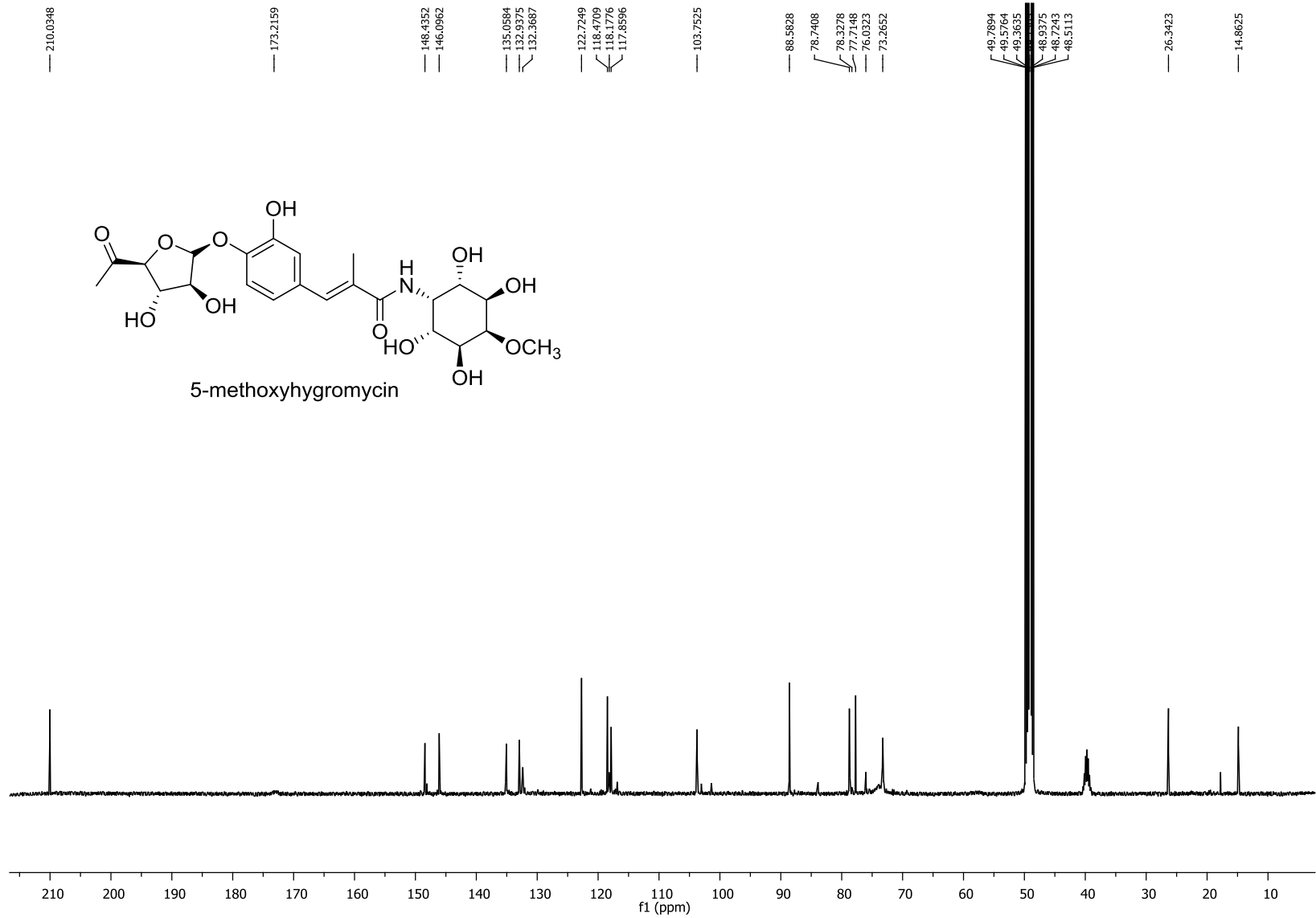


Figure S49. ¹³C NMR spectrum (CD₃OD, 100 MHz) of 5-methoxyhygromycin.

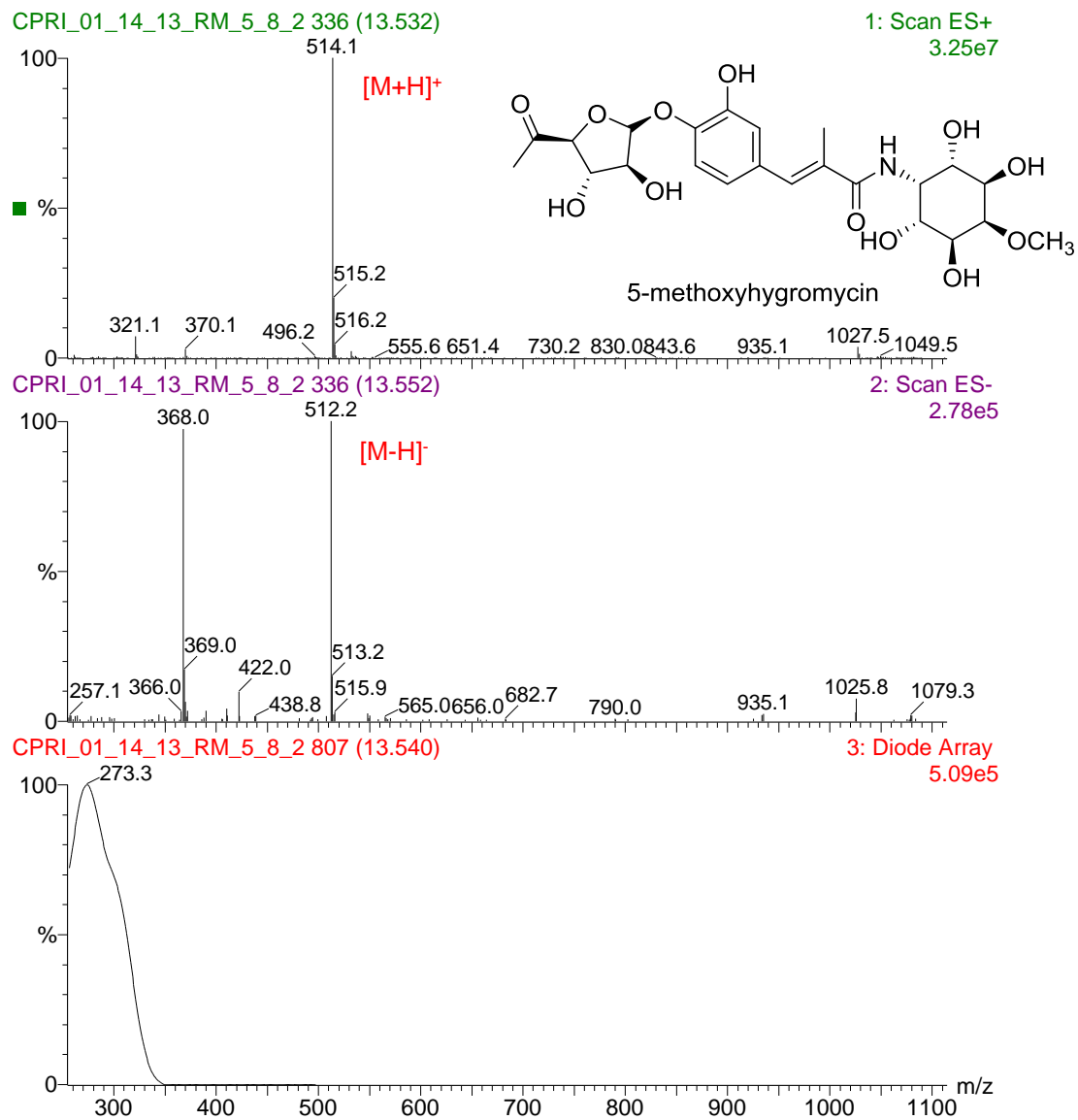


Figure S50. APCI-MS/UV of 5-methoxyhygromycin.

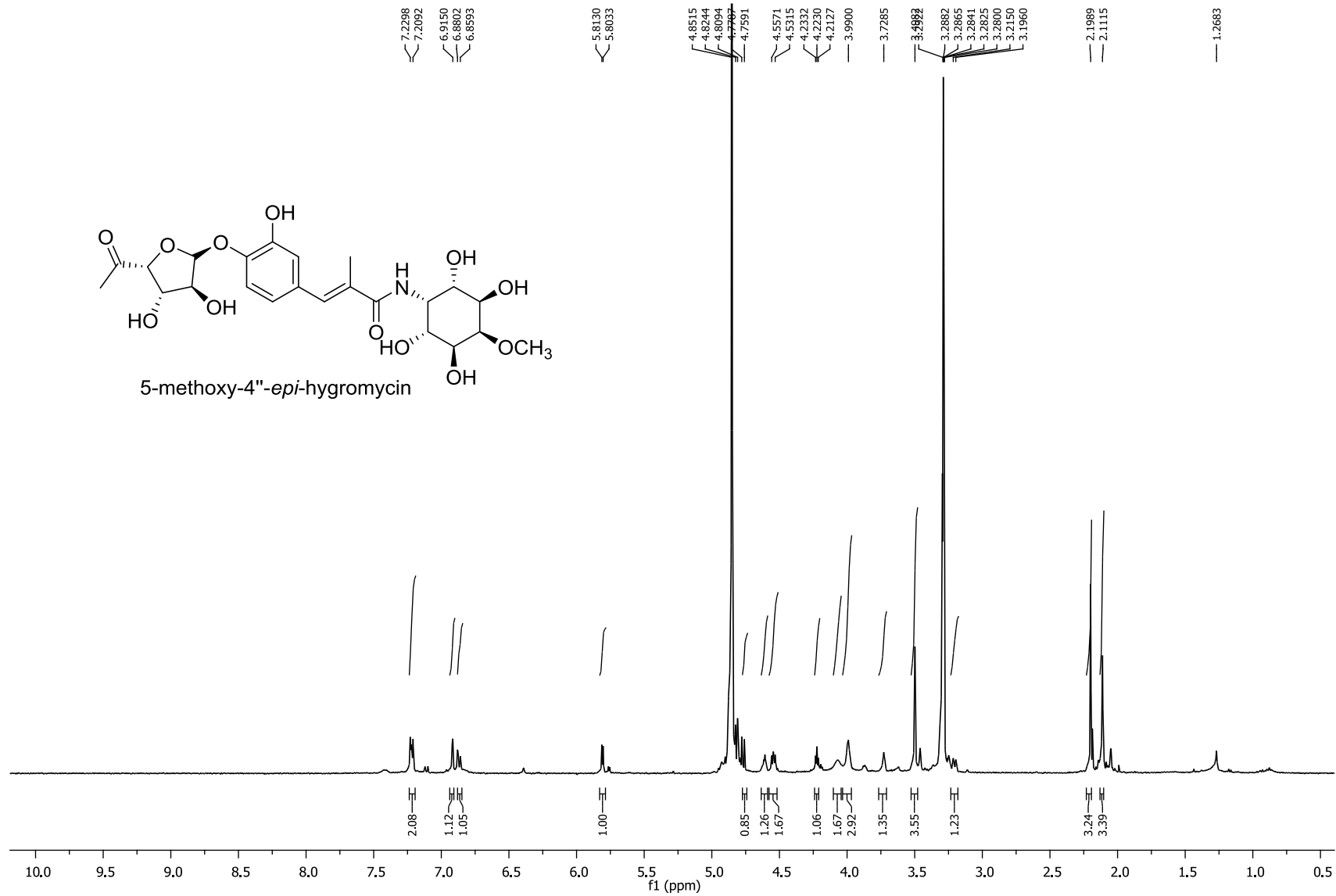


Figure S51. ¹H NMR spectrum (CD₃OD, 400 MHz) of 5-methoxy-4''-epi-hygrocin.

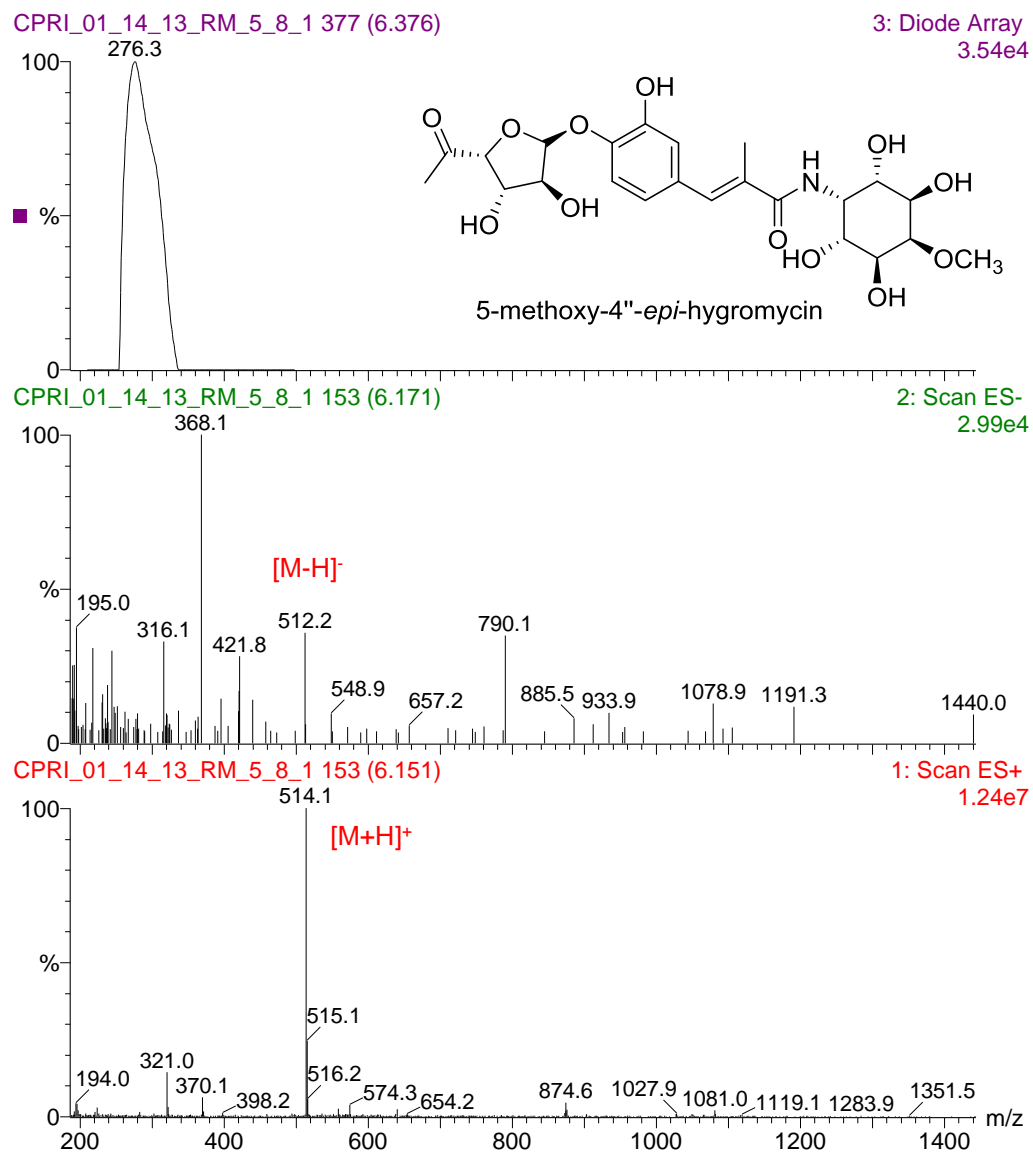


Figure S52. APCI-MS/UV of 5-methoxy-4''-*epi*-hygromycin.

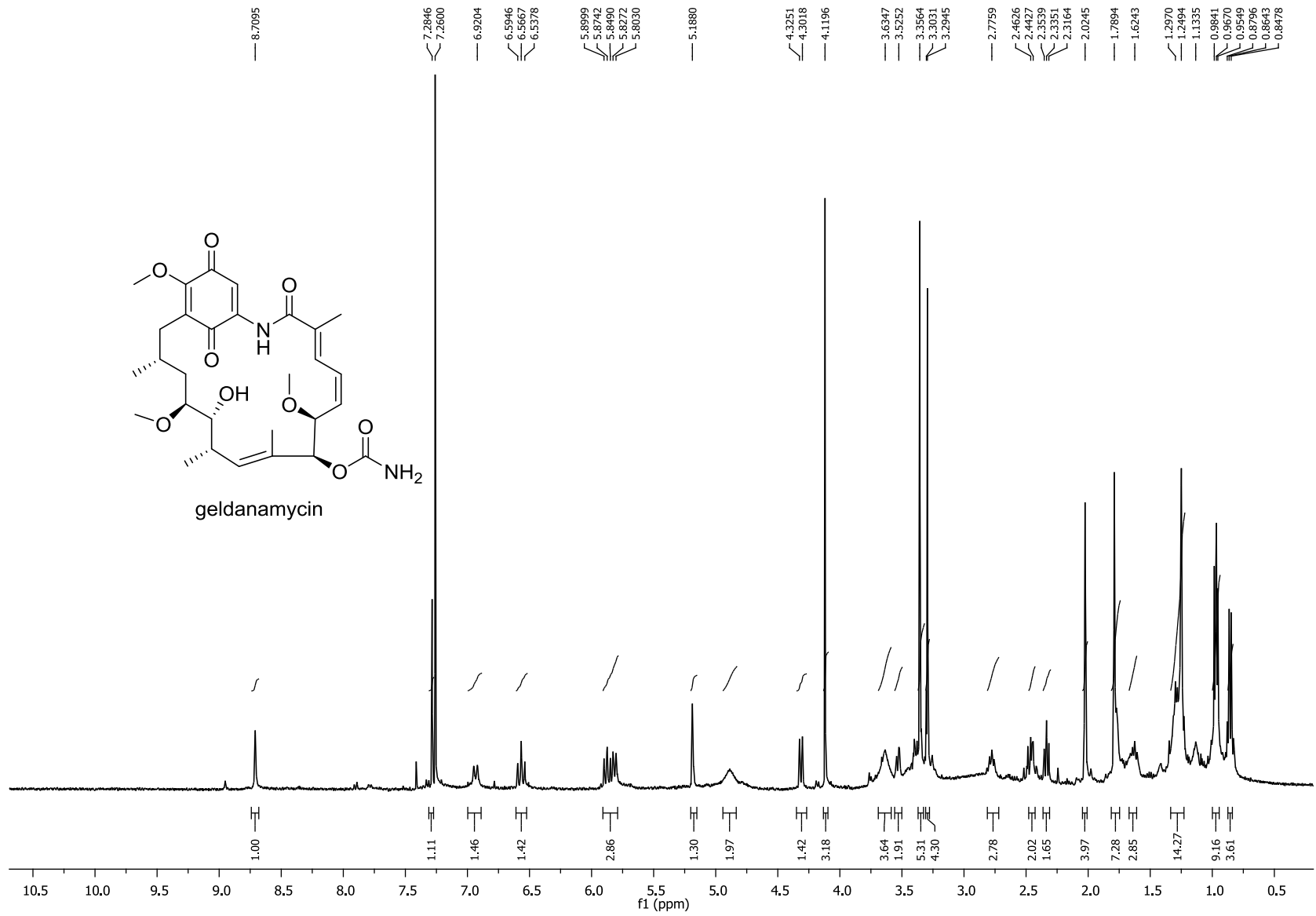


Figure S53. ¹H NMR spectrum (CDCl₃, 400 MHz) of geldanamycin.

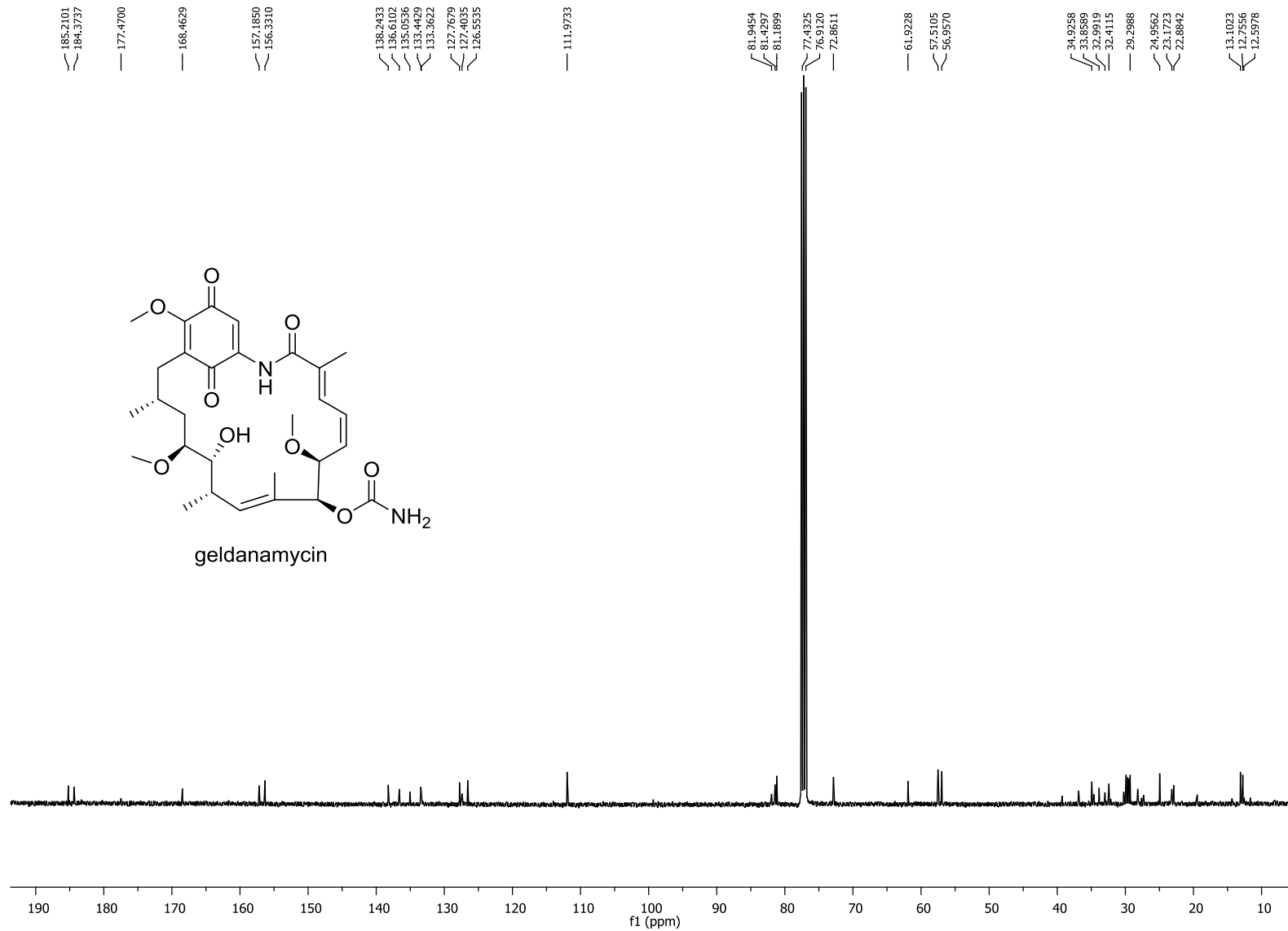


Figure S54. ¹³C NMR spectrum (CDCl₃, 100 MHz) of geldanamycin.

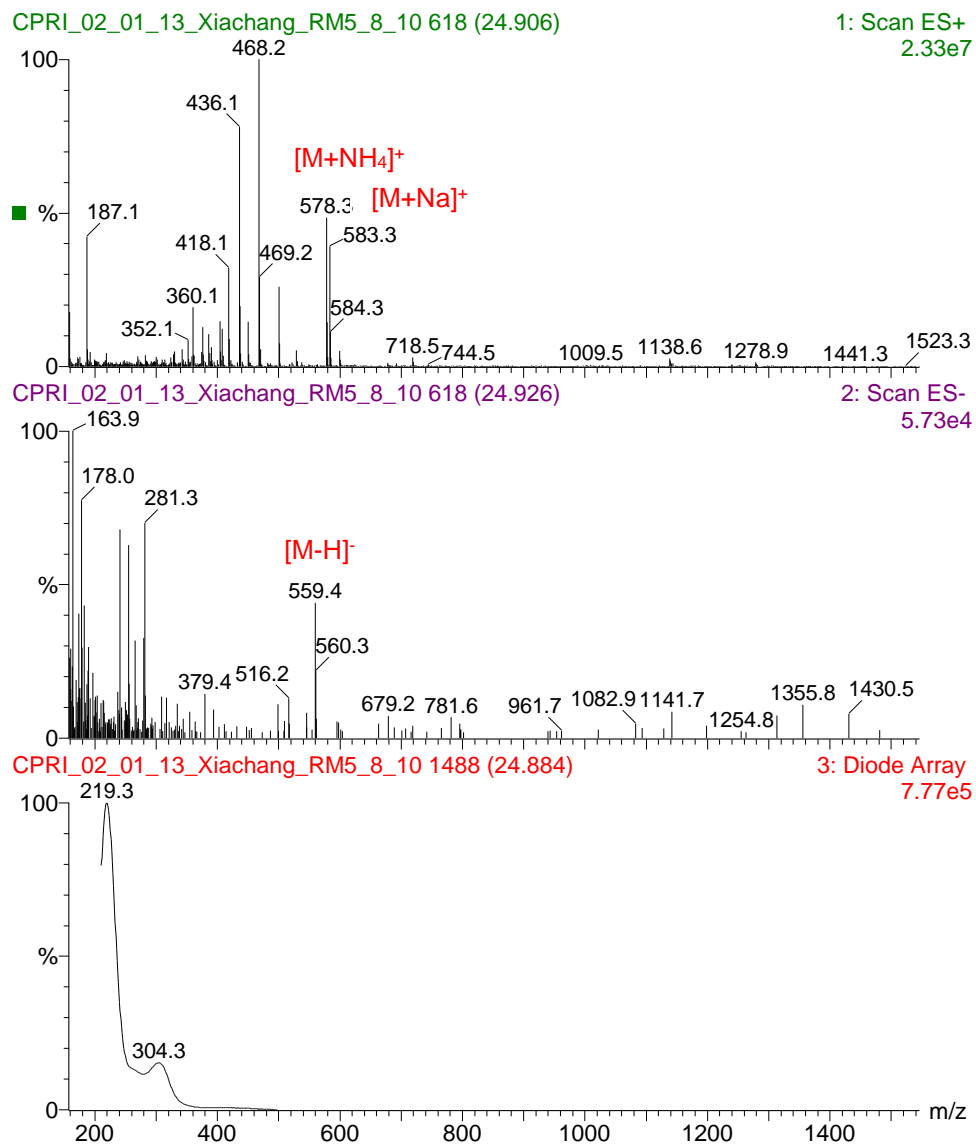


Figure S55. APCI-MS/UV of geldanamycin.

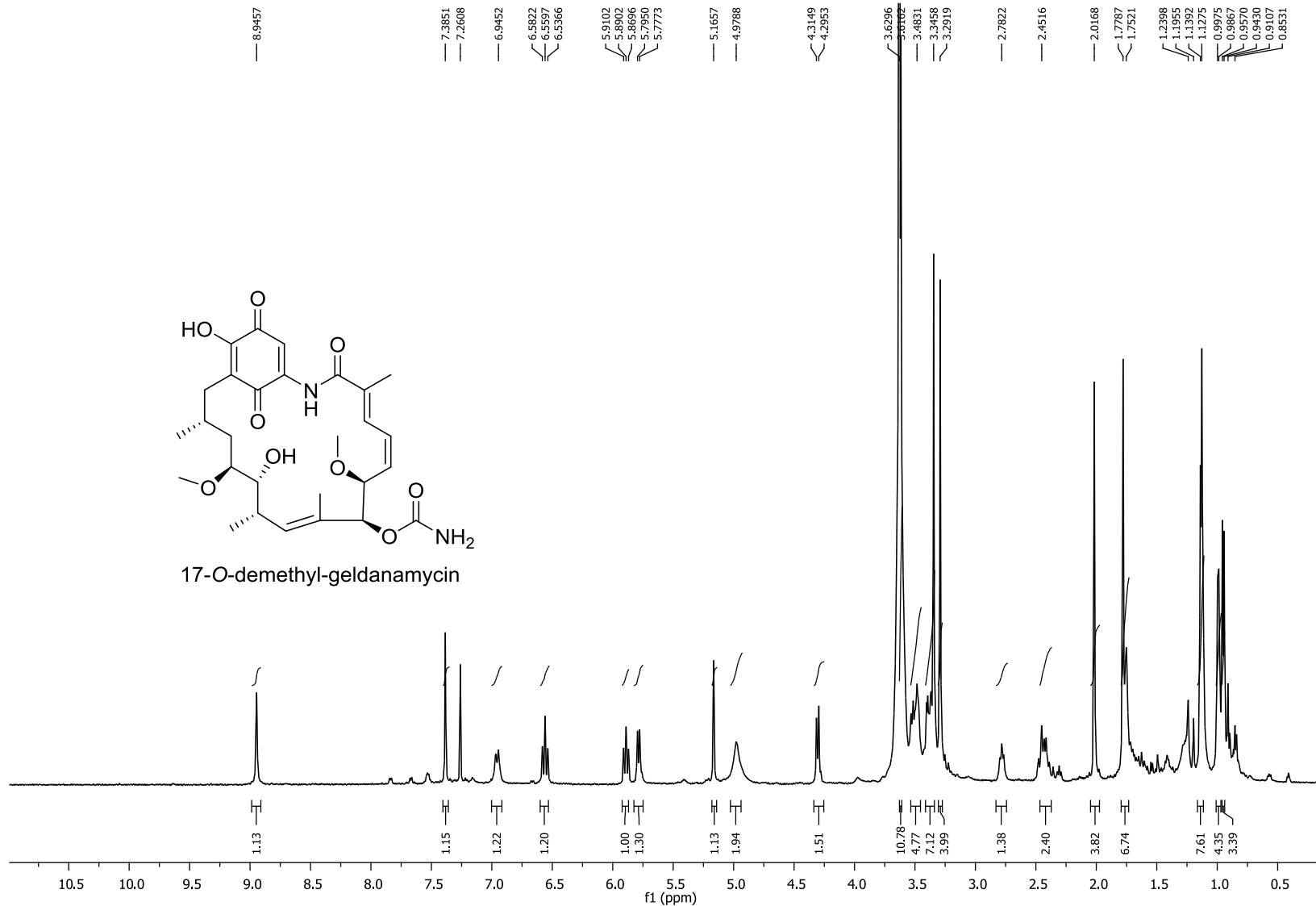


Figure S56. ^1H NMR spectrum (CDCl_3 , 500 MHz) of 17-O-demethyl-geldanamycin.

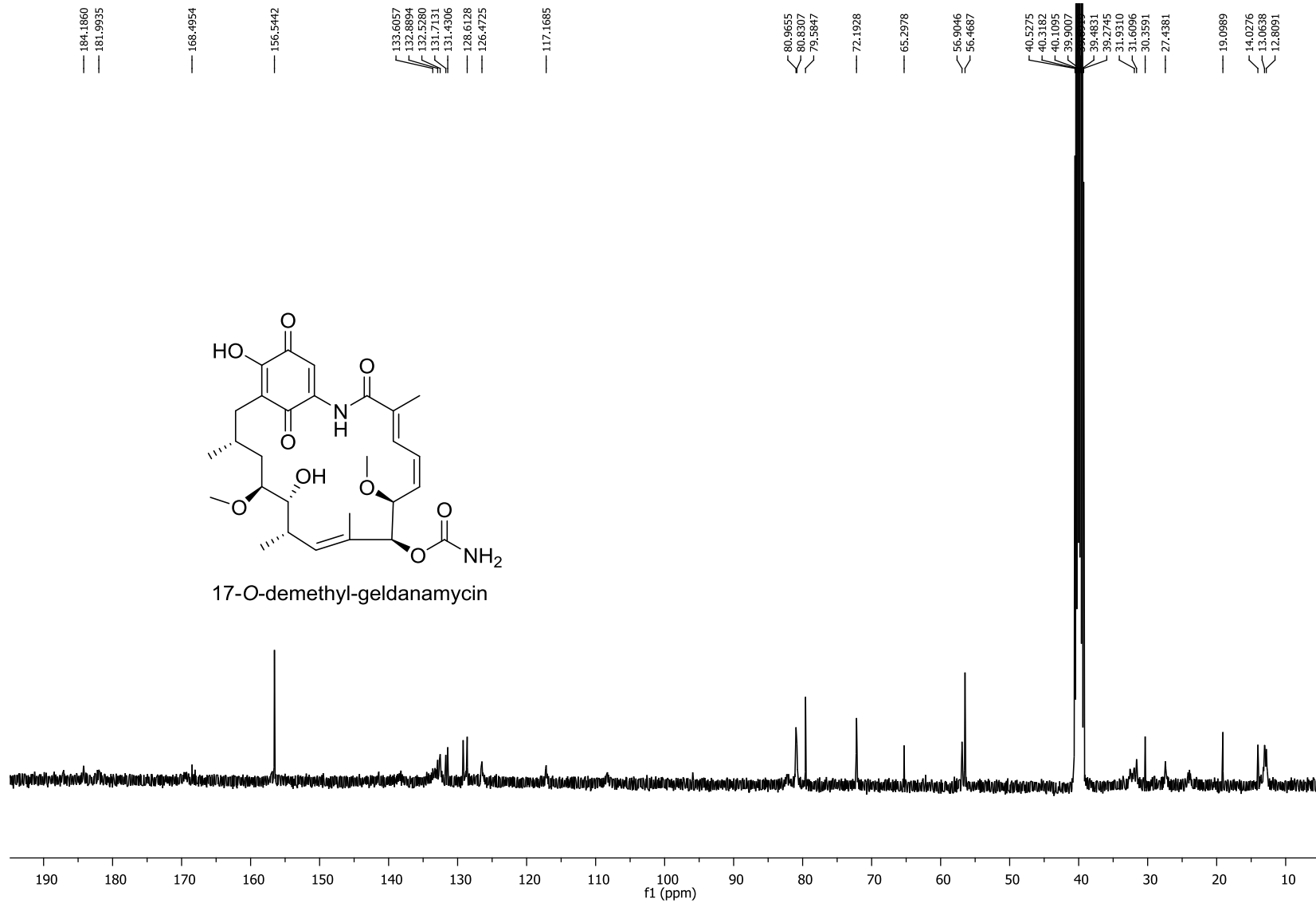


Figure S57. ¹³C NMR spectrum (CDCl₃, 100 MHz) of 17-O-demethyl-geldanamycin.

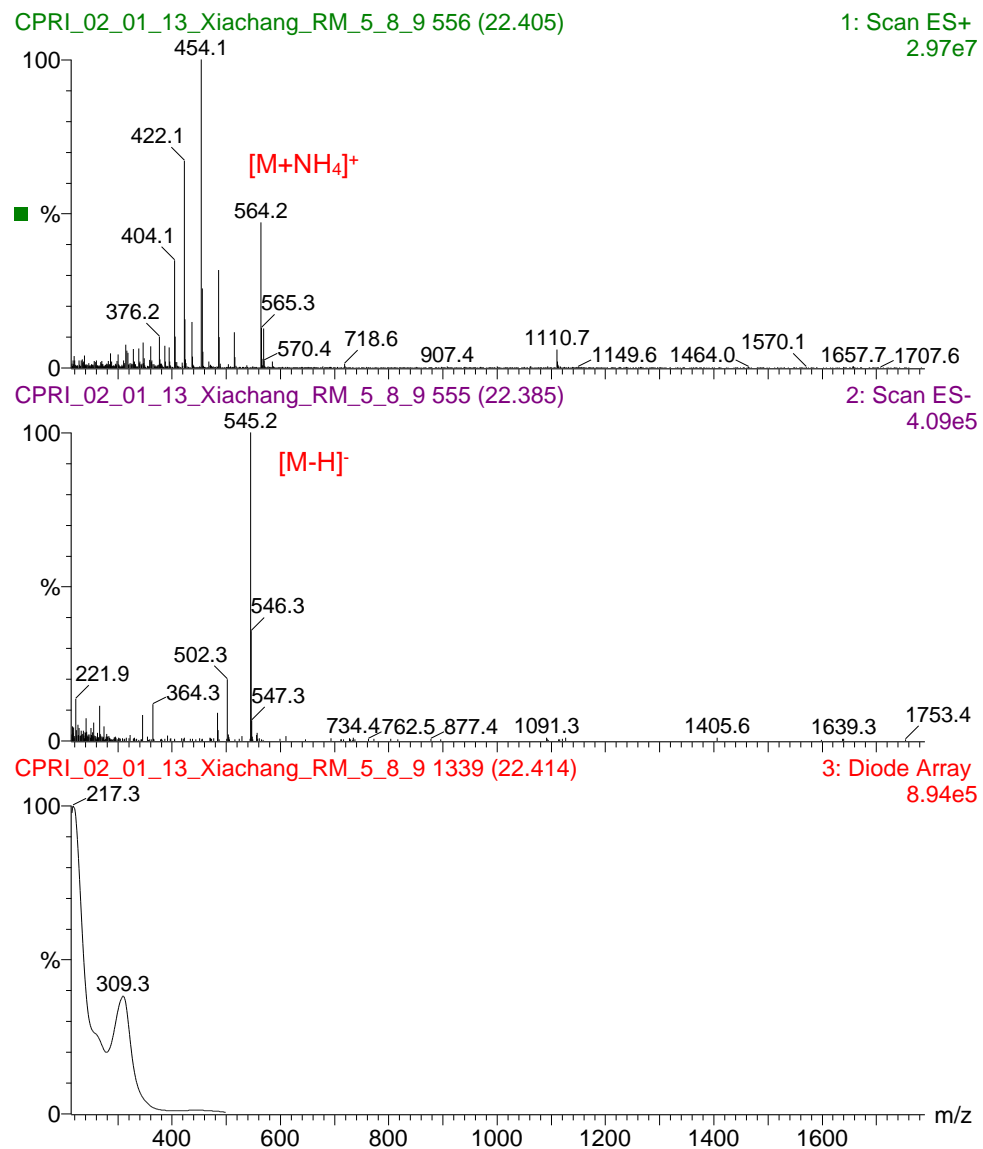


Figure S58. APCI-MS/UV of 17-O-demethyl-geldanamycin.



Figure S59. Photograph of *Streptomyces* sp. RM-5-8 (7 day growth on M₂-agar).